

THE UNIVERSITY OF CALGARY

EFFECTIVENESS OF AUXILIARY POSITIONING SYSTEMS
IN AERIAL PHOTOGRAMMETRY

by

NORMAN THYER

A THESIS

SUBMITTED TO THE FACULTY OF GRADUATE STUDIES
IN PARTIAL FULFILLMENT OF THE REQUIREMENTS FOR THE DEGREE OF
MASTER OF SCIENCE IN ENGINEERING

DEPARTMENT OF SURVEYING ENGINEERING

CALGARY, ALBERTA

JULY 1987

© Norman Thyer 1987

Permission has been granted to the National Library of Canada to microfilm this thesis and to lend or sell copies of the film.

The author (copyright owner) has reserved other publication rights, and neither the thesis nor extensive extracts from it may be printed or otherwise reproduced without his/her written permission.

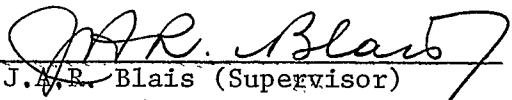
L'autorisation a été accordée à la Bibliothèque nationale du Canada de microfilmer cette thèse et de prêter ou de vendre des exemplaires du film.


L'auteur (titulaire du droit d'auteur) se réserve les autres droits de publication; ni la thèse ni de longs extraits de celle-ci ne doivent être imprimés ou autrement reproduits sans son autorisation écrite.


ISBN 0-315-38079-9

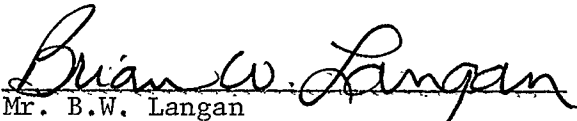
THE UNIVERSITY OF CALGARY
FACULTY OF GRADUATE STUDIES


The undersigned certify that they have read, and recommend to the Faculty of Graduate Studies for acceptance, a thesis entitled "Effectiveness of Auxiliary Positioning Systems in Aerial Photogrammetry", submitted by Norman Thyer in partial fulfillment of the requirements for the degree of Master of Science in Engineering.


Dr. J.A.R. Blais (Supervisor)
Department of Surveying Engineering


Mr. M.A. Chapman
Department of Surveying Engineering


Dr. K.P. Schwarz
Department of Surveying Engineering


Mr. B.W. Langan
Department of Civil Engineering


Dr. J.R. Gibson (External Reader)
Canada Centre for Remote Sensing

(DATE) 1987:10:01

ABSTRACT

In aerial photogrammetry, information on camera position and orientation from auxiliary systems can be used to supplement or replace ground control information when the latter is inadequate. Similar information is required when a laser profiler or multi-spectral scanner is used for terrain profiling or mapping. It is desirable to test the effectiveness of such auxiliary information in a real situation, by comparing it with a proved standard, such as aerial photogrammetry using ground survey control.

In 1983, high-altitude aerial photography was carried out over the Kananaskis area in the Rocky Mountains west of Calgary. Measurements of camera position and orientation were made simultaneously by an inertial system, and range to the ground by a laser profiler. The outputs of these measuring systems are here compared with the corresponding values derived from various photogrammetric adjustments based on ground control, with a view to evaluating their accuracy and their potential for inclusion in photogrammetric adjustments. Both sets of values are also compared with those from a photogrammetric bundle adjustment using both ground control and inertial data as input.

For the conditions of this experiment, it is found that the absolute position coordinates and orientation angles, as given by the inertial system without updates, are unsatisfactory. However, the changes in these quantities between consecutive stations agree with the photogrammetry to a degree at least as close as the reliability of the photogrammetry itself, and even better

agreement is obtained for rotation-invariant functions of these changes of position and orientation. Agreement also improves if one ignores those camera stations whose position coordinates give the greatest residuals in the photogrammetric adjustment, indicating that inclusion of auxiliary information should improve the quality of the contribution of those images to the adjustment.

Ranges from aircraft to ground by laser were initially found to differ considerably from their photogrammetric estimates, but the discrepancy was drastically reduced after a misalignment of the laser beam was detected, and appropriate corrections were applied. It follows that use of laser range in a photogrammetric adjustment requires accurate location of the laser beam's target on the photogrammetric image, and image measurements at that point.

Analysis of some laser profiles between camera stations shows that a combined laser and inertial system can give a terrain elevation profile with accuracy of a few decimetres or a few metres, depending on the terrain type, vegetation and slope, provided that the laser alignment is known and photogrammetry using ground control is used to update the inertial system at each end of the profile.

ACKNOWLEDGEMENTS

This thesis is really the outcome of a cooperative effort by a number of people.

In the first place, many thanks are due to my supervisor and advisor, Dr. J.A.R. Blais, for his guidance, suggestions and encouragement.

I am also much indebted to other people who have contributed in some way to the completion of this work. They include:

Mr. M.A. Chapman, Department of Surveying Engineering, University of Calgary, for his participation in numerous discussions,

Dr. J.R. Gibson, Canada Centre for Remote Sensing, for supplying data and other information, and discussing the progress of the project,

Mr. A.L. Kok for running the photogrammetric adjustment programs whose outputs were essential input to my analyses,

Mr. G. Wanamaker for his many hours spent in producing photogrammetric information,

Mr. R. Goss, of the Department of Surveying Engineering, J. Cluett, N. Barnecut, N. Mancell and D. Teale of Academic Computing Services, University of Calgary, for their help in enabling the computer processing to proceed.

As less direct contributions, I appreciate the opportunities for financial support through part-time work which were facilitated by Drs. J.A.R. Blais, C.S. Fraser, K.P. Schwarz, and W.F. Teskey of the Department of Surveying Engineering, by the Atmospheric Sciences Division of the Alberta Research Council, by Mr. E. Kennedy of the Canadian Institute of Surveying and Mapping, and by Mr. M.K. Singleton of Nelson, B.C.. Mr. Singleton also facilitated the thesis preparation by offering the use of office equipment.

Finally, I express my appreciation to my wife for running the household and raising and helping to support our family during my long absences, and to her and my children for tolerating these absences.

This study was partly funded by NSERC and the Canada Centre for Remote Sensing.

TABLE OF CONTENTS

	Page
ABSTRACT	iii
ACKNOWLEDGEMENTS	v
TABLE OF CONTENTS.	vii
LIST OF TABLES	ix
LIST OF FIGURES.	xi
GLOSSARY, ABBREVIATIONS AND SYMBOLS.	xiii
CHAPTER	
1. INTRODUCTION.	1
1.1 Auxiliary Systems as an Aid to Photogrammetry	1
1.2 Photogrammetry as an Aid to other Systems	4
1.3 Scope of Present Project	5
2. EXPERIMENTAL CONDITIONS AND DATA SOURCES	8
2.1 Experimental Conditions	8
2.2 Data Sets and Processing	12
3. ACCURACY OF PHOTOGRAMMETRIC ADJUSTMENTS	16
3.1 Perspective Centre Position Estimates from SPACE-M	18
3.2 Position Estimates from Bundle and SPACE-M Adjustments	24
4. POSITION DETERMINATION FOR PERSPECTIVE CENTRES.	29
4.1 Matching of Perspective Centres	29
4.2 Relation between Photogrammetric and Auxiliary Estimates of Position	35
4.3 Double Differences - Relation between Photogrammetric and Auxiliary Estimates of PC Position Increments.	39
4.4 Comparison of PC Coordinates as given by CCRS Bundle and SPACE-M Adjustments	44
5. CAMERA ORIENTATION AND LASER RANGE.	49
5.1 Computation of Orientation Angles from SPACE-M Output	49
5.2 Comparison of Roll, Pitch, Heading and Range Values from Different Photogrammetric Adjustments	54
5.3 Comparison of Photogrammetric and Auxiliary Estimates of Range and Orientation Angles	59
5.4 Comparison of Orientation Angles as given by CCRS Bundle and SPACE-M Adjustments	70

TABLE OF CONTENTS - continued

6.	COORDINATE-INDEPENDENT MEASURES OF ORIENTATION CHANGES.	74
6.1	Computation of Principal Axis Direction Change. . .	74
6.2	Comparison between Photogrammetric Determinations of Principal Axis Direction Change	76
6.3	Comparison of Photogrammetric and Auxiliary Determinations of Principal Axis Direction Change	76
6.4	Direction Change of the Longitudinal Axis	78
6.5	Comparison of Principal and Longitud. Axis Direction Changes from CCRS Bundle and SPACE-M Adjustments	82
6.6	Summary .	82
7.	FURTHER STUDY OF LASER RANGE DATA	85
7.1	Determination of Laser Beam Alignment	85
7.2	Detailed Laser Profiles over Water.	91
8.	LASER PROFILING OVER LAND	96
8.1	Method of Analysis	96
8.2	Analyses of Specific Profiles	101
9.	CONCLUSIONS AND RECOMMENDATIONS	109
9.1	Results Classified according to Type of Measurement	110
9.2	Results Classified according to Application	116
9.3	Recommendations	122
	REFERENCES	124

APPENDICES

A	Data on Individual Flight Lines.	126
B	Calculation of Convergence of Meridians.	132
C	Transformation between Ground-based and Camera-based Coord- inate Systems in terms of Roll, Pitch and Heading Angles	133
D	Determination of Range, Roll, Pitch and Heading from Photogrammetry via Orientation Angles ϕ , ω and κ . . .	136
E	Derivation of Principal Point Offset Compensation . . .	143
F	Suggested Procedures for Use of Laser Ranges with Photogrammetry	147
G	Tables of Profile Elevation Discrepancies	154
H	Detailed Comparison of Orientation Angles	165
I	Detailed Comparisons of Perspective Centre Positions . .	184
J	Graphs of Orientation Angles as Functions of Time . . .	208

LIST OF TABLES

TABLE	Page
3.1 - 3.3 Discrepancies between PC Position Estimates from SPACE-M	
3.1 RMS Values	20
3.2 Max. Values	21
3.3 Mean Values	22
4.1 - 4.2 Comparison of PC Position Increments from Auxiliary Systems and Photogrammetry	
4.1 RMS Values	41
4.2 Max. Values	42
4.3 Comparison of PC Positions from CCRS Bundle and SPACE-M Adjustments	45
4.4 - 4.5 Comparison of PC Position Increments from CCRS Bundle and SPACE-M Adjustments	
4.4 RMS Values	46
4.5 Max. Values	47
5.1 Double Differences of Orientation Parameters and Range: Photogrammetric minus Auxiliary	65
5.2 - 5.3 Comparison of Orientation Angles from Auxiliary Systems and Photogrammetry	
5.2 Single Differences	68
5.3 Double Differences	69
5.4 - 5.5 Comparison of Orientation Angles from CCRS Bundle and Other Photogrammetric Adjustments	
5.4 Single Differences	71
5.5 Double Differences	72
6.1 - 6.4 Comparison of Orientation Angle Changes	
6.1 Principal Axis - Aux. Systems and Photogrammetry	79
6.2 Longitudinal Axis - Aux. Systems and Photogrammetry	81
6.3 Principal Axis - CCRS Bundle and SPACE-M Adjustments	83
6.4 Longitud. Axis - CCRS Bundle and SPACE-M Adjustments	84
7.1 Laser Spot Coordinates on Photographic Image	90
8.1 Nine-point Scale for Terrain Cover Type	98
8.2 Characteristics of Terrain Profile Sections	101

LIST OF TABLES - continued

TABLE	Page
G.1 - G.5 Profile Elevation Discrepancies as Functions of Terrain Type and Slope Separately . .	155 - 159
G.6 - G.10 Profile Elevation Discrepancies as Functions of Terrain Type and Slope Jointly . . .	160 - 164
H.1 - H.10 Detailed Comparison of Orientation Angles from Auxiliary Systems and Photogrammetry	166 - 175
H.11 - H.18 Detailed Comparison of Orientation Angles from CCRS Bundle and SPACE-M Adjustments	176 - 183
I.1 - I.7 Detailed Comparison of PC Positions from Auxiliary Systems and Photogrammetry	185 - 191
I.8 - I.14 Detailed Comparison of PC Position Incre- ments from Aux. Systems and Photogrammetry	192 - 198
I.15 - I.17 Detailed Comparison of PC Positions from CCRS Bundle and SPACE-M Adjustments	199 - 201
I.18 - I.23 Detailed Comparison of PC Position Increments from CCRS Bundle and SPACE-M Adjustments	202 - 207

LIST OF FIGURES

FIGURE	Page
2.1 Approximate Map of Flight Path	10
2.2 Flight Lines in Relation to Ground Control	11
2.3 Original Data Sources and Data Sets for Analysis .	15
3.1 - 3.2 PC Position Plots from Different Photogrammetric Adjustments	25-26
4.1 N-S Flight Lines and Positions of Camera Stations .	31
4.2 Differences of PC Coordinate Estimates Plotted as Functions of Time	36
4.3 Data Sets Used in Analyses of Chapter 4	38
5.1 Relation between Inter-QNP Vectors in Images and on Ground	52
5.2 Data Sets Used in Analyses of Chapters 5 & 6 . .	55
5.3 - 5.4 QNP Position Plots from Different Photogrammetric Adjustments	56-57
5.5 - 5.6 Camera Orientation Plots from Different Photogrammetric Adjustments	60-61
6.1 Plots of Principal and Longitudinal Axis Direc- tion Changes from Different Adjustments	77
7.1 - 7.2 Laser Alignment Calibration Grid with Isopleths	88-89
7.3 - 7.5 Lake Surface Profiles by Laser	
7.3 with Laser Alignment	92
7.4 with Laser Alignment Corrected	94
7.5 Uncorrected and Corrected for Comparison . .	95
8.1 Range of Positions of Laser Spot with Laser Mounted separately from Camera	99
8.2 - 8.5 Characteristics of Terrain Profiles	
8.2 Section W	103
8.3 Section X	104
8.4 Section Y	106
8.5 Section Z	107

LIST OF FIGURES - continued

FIGURE	Page
E.1 Geometry for Principal Point Offset Compensation	143
F.1 Positions of Laser and Laser Spot in Profiling .	148
F.2 Positions of Laser Spots in Image, with Laser Attached to Camera or Mounted Separately . . .	152
J.1 - J.4 Orientation Angles as Functions of Time	209-212
J.5 - J.8 Orientation Angle Differences as Functions of Time	213-216
J.9 Heading Angle Differences as Functions of Time	217

GLOSSARY, ABBREVIATIONS AND SYMBOLS

Bundle adjustment	A photogrammetric adjustment which simultaneously integrates the information from a number of partially overlapping images into a single block
CCRS	Canada Centre for Remote Sensing - a branch of EMR
f	focal length of camera lens
EMR	Energy, Mines and Resources Canada (A Federal Government Department)
GPP	Ground Principal Point - see QNP
GPS	Global Positioning System - a system of positioning by satellite
h	Heading angle
Heading	A camera orientation angle, measured about a vertical axis
Independent model block adjustment	A photogrammetric adjustment in which individual stereomodels are integrated into a block
Laser spot	(a) The area where the beam of the laser profiler meets the ground (b) The centre point of that area
p	Pitch angle
PC	Perspective Centre

Pitch	A camera orientation angle - measured about a horizontal axis perpendicular to the heading direction
QNP	Quasi Nadir Point (or Ground Principal Point - GPP) - the point on the ground corresponding to the principal point of a photographic image
r	Roll angle
R	Range from PC to QNP
RMS	Root Mean Square quantity
Roll	A camera orientation angle - measured about the fore-aft axis (x-axis) of the camera
SPACE-M	Spatial Photogrammetric Adjustment for Control Extension using independent Models - an independent model block adjustment, developed by Blais (1979)
UTM	Universal Transverse Mercator projection
κ	A camera rotation angle - measured about the photogrammetric z-axis
ϕ	A camera rotation angle - measured about the photogrammetric y-axis
ω	A camera rotation angle - measured about the photogrammetric x-axis

Chapter 1

INTRODUCTION

1.1 Auxiliary Systems as an Aid to Photogrammetry

Photogrammetric triangulation and mapping involve the determination of coordinates of points in a ground coordinate system from the coordinates of corresponding points in photographic images. Usually the transformation from image to ground coordinates is determined by identifying and measuring certain image points which correspond to surveyed control points on the ground. A certain minimum number of control points is needed for the photogrammetric orientation, this number depending on whether one is analyzing a single model or a block of models.

If this ground control is inadequate, then to some extent it can be replaced by information on the camera's position and orientation. This information can be provided by auxiliary positioning systems. The use of such information was foreseen over a decade ago by Zarzycki (1972) and Blais (1976).

One such auxiliary system is an inertial navigation device, which gives both the position and the orientation of the camera. Others, such as satellite positioning systems, laser altimeters and statoscopes, give at least partial information on the camera position. The auxiliary information may consist of actual values of distances and angles, or of relative values in the form of the changes in these quantities from one camera position to another. In some cases, auxiliary data can be included in the relative or

absolute orientation process, depending on their nature and reliability, and photogrammetric adjustment programs can sometimes be modified to include such data.

One proposed procedure for coastal mapping involves the use of aerial photogrammetry over areas with little ground control. When a large portion of a stereomodel is occupied by water, there is a lack of tie points, and problems occur due to refraction at the water surface. To compensate for these deficiencies, inertial measurements give the camera position and orientation, and the inertial system is updated by photogrammetry over clusters of control points at the ends of the flight lines. Masry (1977) establishes the relations between errors in the inertial data and resultant errors in the coordinates of ground points, and concludes that for coastal mapping, the standard error for rotations should be 25 arc seconds or less.

In the context of more general photogrammetry, Goldfarb (1985), Goldfarb and Schwarz (1985), Schwarz, Fraser and Gustafson (1984) and Lucas (1987) describe computer simulations in which the auxiliary data, comprising the output of an inertial system updated by GPS (satellite positioning), are used to locate the perspective centres, and are incorporated into a bundle adjustment to determine coordinates of ground points; the third of these papers also considers an experimental terrestrial check on a combined inertial-GPS system, described in more detail by Wong et al. (1985).

Blais and Chapman (1984a) performed a computer simulation in which the perspective centre coordinates, their first-order differences (i.e. the stereomodel bases) and their second-order differences were used as input to a SPACE-M independent model block adjustment (Blais, 1979). The simulated perspective centre positions were derived from an earlier photogrammetric adjustment using ground control, and the terrain relief was fairly low. Blais and Chapman (1984b) also compared SPACE-M adjustments using ordinary ground control with similar adjustments which included independent control networks. The inclusion of the independent networks gave an improvement in accuracy, and although the networks were on the ground in this case, the same principle could be applied to an independent network of perspective centres. Later, Blais and Chapman (1985) incorporated first and second differences of perspective centre positions into a SPACE-M adjustment using the same observational data as this thesis.

Hence, when appropriate auxiliary data are available, aerial triangulation becomes feasible in situations where, due to lack of ground control, it would otherwise be impossible.

1.2 Photogrammetry as an Aid to Other Systems

The foregoing situation applies when photogrammetry is the main mapping tool, and auxiliary systems are used to support it. In some circumstances, photogrammetry may be unsuitable for mapping. This may be the case over areas which exhibit few distinctive features, such as snowfields, sand desert and grassland, where it is difficult to match uniquely pairs of points in the two images required to form the stereomodel. In these conditions, a laser profiler can function well. Essentially, it consists of a device in an aircraft which determines the distance (range) from itself to a point on the ground by measuring the time taken by a light pulse to travel from instrument to target and back. The coordinates of the point on the ground can be found if one knows the position and orientation of the instrument, plus the range that it measures. Position and orientation can be provided by an inertial positioning system, but such a system requires frequent updating.

Such mapping systems have already been used in certain situations. Jepsky (1986) describes typical laser profiler systems and their applications. Schreier et al. (1984) describe experiments in Ontario in which 95% of the laser elevations agree with those from conventional photogrammetry within 1.8m, using aircraft-mounted equipment at a flying height of 300m, while Moreau and Jeudy (1986) report acceptable results for a laser profiler survey by helicopter.

When the equipment is contained in a helicopter, the inertial systems can be updated frequently by landing. Hursh reports satisfactory results when the inertial measuring unit, mounted in an aircraft flying at 600-900m above ground, is updated by a laser tracker with retroreflectors on the ground.

Additionally, photogrammetry can be used to provide the updates if the nature of the terrain and availability of control points permit its use at some points on the flight line. In this situation, photogrammetry plays the auxiliary role in its integration with another system.

Similar information on the instrument's position and orientation is desirable for other airborne mapping systems such as multispectral scanners.

1.3 Scope of Present Project

Any auxiliary information must, of course, be of adequate quality if its use is to result in an improvement in the accuracy of photogrammetric mapping or triangulation. The purpose of this thesis is to evaluate the accuracy and precision of the outputs of some auxiliary systems by comparing these outputs, as determined experimentally, with the equivalent values computed by "traditional" photogrammetry using ground control, and also to evaluate the accuracy of the photogrammetric values by comparing these values as derived from different photogrammetric adjustments based on the same images.

Some evaluations have been made already, as mentioned in previous paragraphs. However, whereas most other experiments were performed using low-flying helicopters and over terrain of gentle relief, this thesis treats data obtained under the extreme conditions of a high-flying aircraft over very rugged terrain. Such conditions will generally maximize the effects of any errors that are present. Also emphasis is given to evaluation of the quantities measured by the auxiliary systems, rather than their eventual effect on the accuracy of triangulation and mapping .

To be more specific, comparisons are made between different estimates of the camera position coordinates and of the camera orientation angles, as made by different photogrammetric adjustments based on ground control only, and also between the estimates from photogrammetry and from an inertial navigation system. The same is done for the changes in these quantities between consecutive camera stations, and also for various functions of position coordinates and orientation angles that are independent of a coordinate system. When the agreement between auxiliary values and the more reliable of the photogrammetric values is better than that between some of the photogrammetric estimates, then one can conclude that the auxiliary data are of adequate quality for inclusion in an adjustment, unless ground check indicates otherwise. The results of the various comparisons may also indicate the best ways of including the auxiliary data from the point of view of accuracy, though not necessarily of convenience.

Corresponding comparisons are made between a bundle adjustment that uses inertial data as well as ground control for input, and independent model adjustments of the same block based on ground control only.

Essentially the same analysis is applied to the range measured by the laser profiler at the camera stations. In addition, a few detailed terrain elevation profiles between camera stations are examined, with a view to determining the equipment preparation and observational procedure that will give the highest accuracy.

Details of the general experimental conditions, and of the data sets available for this project, are given in Chapter 2. Chapter 3 covers evaluation of the accuracy of photogrammetry. In Chapters 4, 5 and 6 are discussed the quality of agreement of perspective centres, specific orientation angles and orientation angle changes, as determined by different methods. Chapters 7 and 8 discuss the laser ranger and its performance in terrain profiling, and finally Chapter 9 gives the general conclusions and recommendations.

Chapter 2

EXPERIMENTAL CONDITIONS AND DATA SOURCES

The purpose of this study is to evaluate the effectiveness of certain auxiliary positioning systems in aerial photogrammetry on the basis of field trials. Their outputs must be compared with some standard, and photogrammetry is used as that standard, since its reliability is well known after decades of use.

In this investigation, photogrammetry, using ground control, is used to estimate the values of quantities that are measured by the auxiliary systems. The photogrammetric estimates are compared with the actual measurements. If the discrepancies between them are less than the errors normally present in the photogrammetry, then it can be assumed that the auxiliary measurements will be acceptable as input to the photogrammetric adjustment.

2.1 Experimental Conditions

In the summer of 1983, aerial photography was carried out in the Kananaskis area west of Calgary, Alberta. This is an area of rugged terrain near the eastern edge of the Rocky Mountains, including peaks, valleys and lakes, in which there exists a ground control network of high quality. The project was a cooperative one, involving the University of Calgary, the Canada Centre for Remote Sensing (CCRS, a branch of Energy, Mines and Resources Canada (EMR)), the Directorate of Cartography (Department of National Defence) and the Surveys and Mapping Branch of EMR. Flying

height was about 9800m and terrain elevation was between 1300m and 3350m above sea level. Data were acquired by CCRS, using a Falcon 20 jet aircraft. A Wild RC-10 camera, with lens of focal length 153.30mm and image size 230 x 230mm, was used, and the flight pattern comprised 5 lines of length 70km oriented N-S, and 5 lines of length 25km oriented E-W, flown at 200m/s. Fig. 2.1 is an approximate map of the flight path, and the relation of the flight lines to ground control is shown in Fig. 2.2.

Endlap and sidelap were 80% and 60% respectively, giving a high redundancy of measurement from multiple overlap and a base-to-height ratio smaller than normal.

While the aerial photography was in progress, the camera position and orientation were recorded continuously by a combination of two inertial systems, a Litton LTN-051 navigation system of the local level type, mounted about 3m from the camera, and a Honeywell 478H inertial reference unit of the strapdown type, which was attached directly to the camera, not to the airframe. The Litton instrument was capable of measuring, and producing values of, latitude, longitude, horizontal velocity, and roll, pitch and yaw angles. According to manufacturer's specifications, it was subject to a drift of 0.5m/s, giving coordinate errors of 1-2km after 1 hour, and a Schuler oscillation of amplitude 200-300m. Angular resolution and accuracy were about 5" (0.001°) and 1-2' (0.02°) respectively. The Honeywell unit measured differential velocities and angles to a resolution of 14" (0.004°) and subject to a drift of several degrees per hour.

As the data acquisition system that recorded the LTN-051

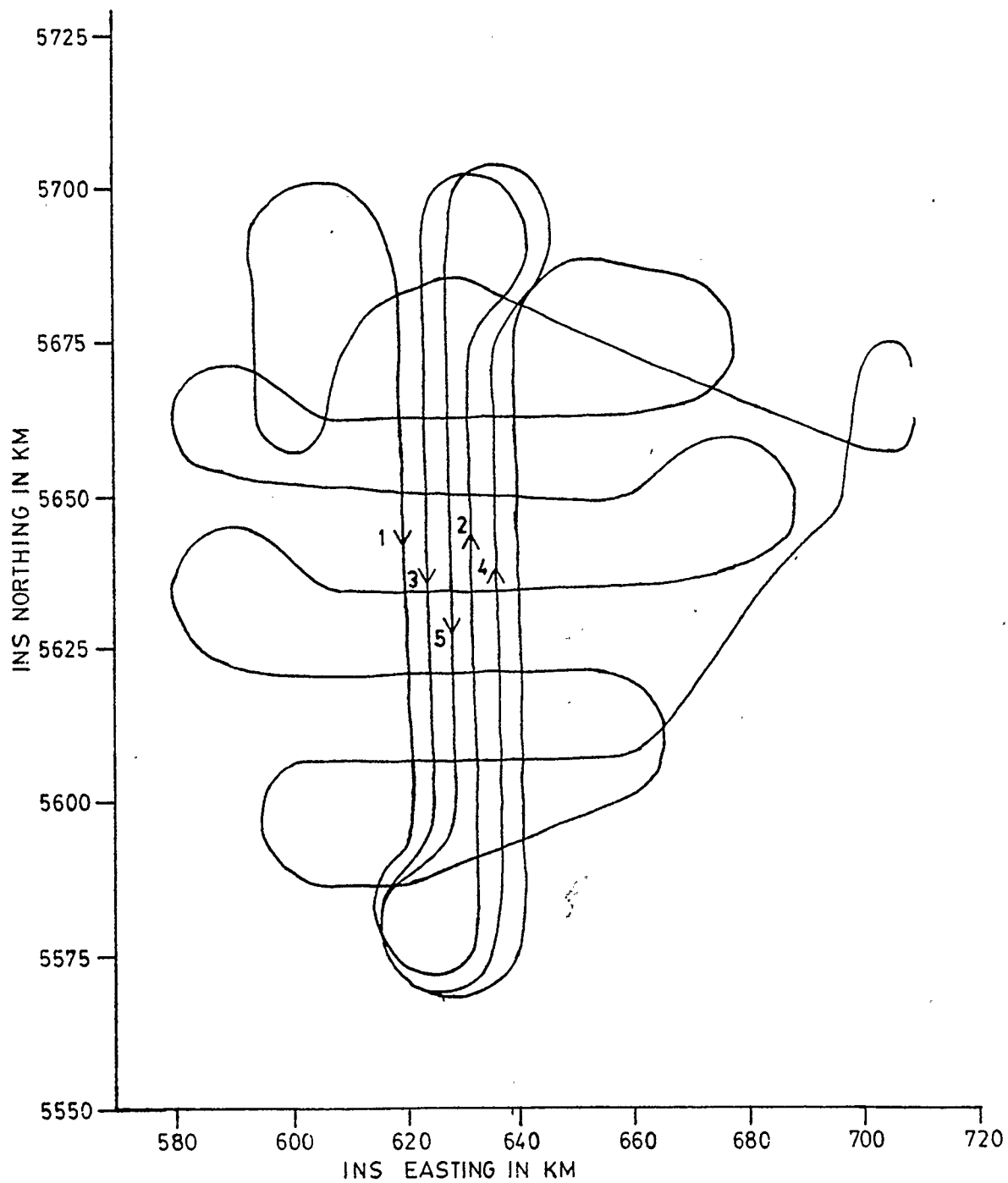


Fig. 2.1: Approximate Map of Flight Path

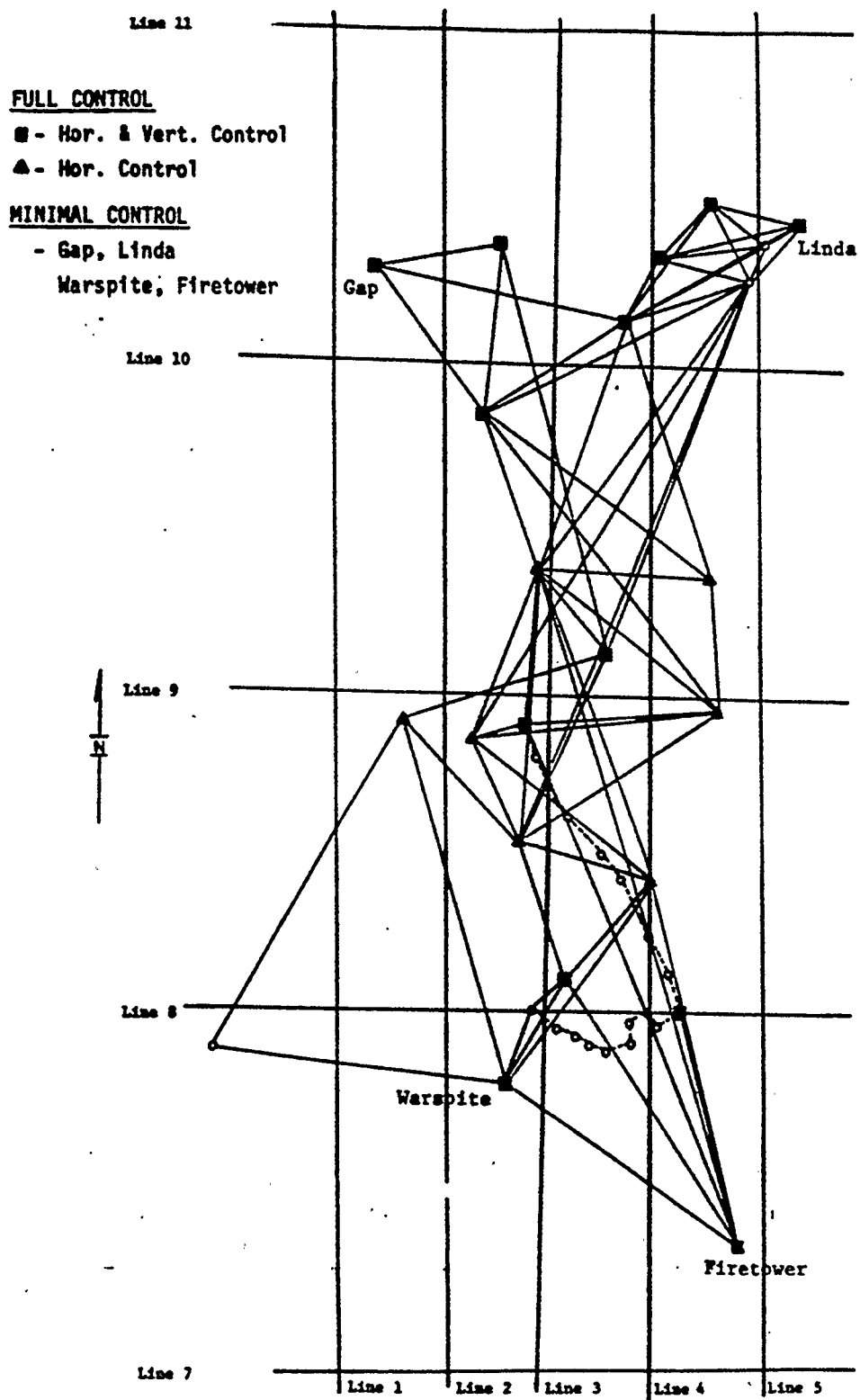


Fig. 2.2: Flight Lines in relation to Ground Control

data was not working properly, it had been necessary to combine the data from both of the inertial systems into a single set of estimates of position and orientation. Consequently it was not possible to obtain the accuracy referred to by Gibson (1984a), viz. that the LTN-51 system can achieve an accuracy of 1.0m and 30 arc-sec after correction for drift and Schuler oscillations. No updates were made during the mission. Neither was any model of anomalous gravity used. Instead, it was assumed that the mean vertical velocity was zero on each line.

Also, for much of the observation period, the aircraft's height above ground was recorded by a laser altimeter. The laser equipment was attached not to the camera but directly to the airframe, about 1m from the camera. It used a Neodymium-Yag laser of 100Mw peak power, with a pulse repetition rate of 20pps and a range greater than 10km [Gibson, 1986]. It had a resolution of 1 nanosecond in timing, equivalent to 15cm in range, and at the flying height typical for this experiment, the spread of the laser beam produced a circular spot of diameter 300 microns on the image, or 15m on the ground. The returning pulse was most typical of the best-reflecting part of the circle, generally around its centre, where it was brightest. That part of the pulse which corresponded to the first occurrence of half the maximum amplitude was used to compute the range.

2.2 Data Sets and Processing

The photogrammetric data were processed at the University of Calgary, with the help of Mr. J.-P. Agnard of Laval University. Image measurements were originally made in spring, 1985 on a Wild

STK-1 stereocomparator, but some measurements were repeated in autumn, 1985, in the hope that an improved data set would give smaller residuals in the adjustment. The SPACE-M method of independent model block adjustment (Blais, 1979) was applied, to both the set of 5 N-S lines and the set of 5 E-W lines, using ground control only.

The whole network of 5 N-S lines was also processed by a single bundle adjustment at CCRS in Ottawa which used both ground control and inertial data on camera position and orientation, described by Gibson (1984b). Both types of data were used simultaneously; it was assumed that, within each flight line, the inertially-derived values of the orientation angles had a constant bias, and the values of position had a bias with constant drift.

In addition, a small sub-block of 10 images was processed by a bundle adjustment at the University of Calgary, using ground control only.

For the purpose of this study, the relevant parts of the adjustment outputs were the coordinates of the perspective centres and of certain points on the ground, and, in the case of the bundle adjustment, the camera positions and orientation angles.

Processing of the auxiliary data, including determination of the camera positions and orientations from the inertial systems, was done by CCRS, who then forwarded the processed data to the University of Calgary.

Three separate data sets were received from CCRS. The first contained perspective centre coordinates, and camera orientation angles, determined from the bundle adjustment performed on the

first five flight lines at CCRS. The second comprised ten sections corresponding to the different flight lines, and included the time, the UTM x, y and z coordinates of the camera, plus the roll, pitch and heading angles, as determined by the inertial systems, and in most cases the laser range, for each camera station or perspective centre. The third set comprised detailed terrain profiles for the first five flight lines, as produced by the auxiliary systems. Gibson (1986) gives further details of the processing used in preparing these data sets. In the same paper, he refers to work that is described in this thesis.

The original data sources and the data sets that were available for analysis are summarized diagrammatically in Fig. 2.3.

In this study, to be described in the following chapters, the values of parameters such as perspective centre coordinates, as determined by the various photogrammetric adjustments, are compared, to give an indication of the reliability of the photogrammetry. Then each of the variables in the second data set is compared with the corresponding value computed from photogrammetry. This process is also performed for the changes in these variables between consecutive camera stations. Similar comparisons are made between the CCRS bundle adjustment using inertial data, and independent model block adjustments without inertial data. Finally, sample sections of the profiles in the third data set are compared with the equivalent values obtained from photogrammetry. From the results of this analysis, estimates can be made of the potential usefulness of the combination of auxiliary data with photogrammetry.

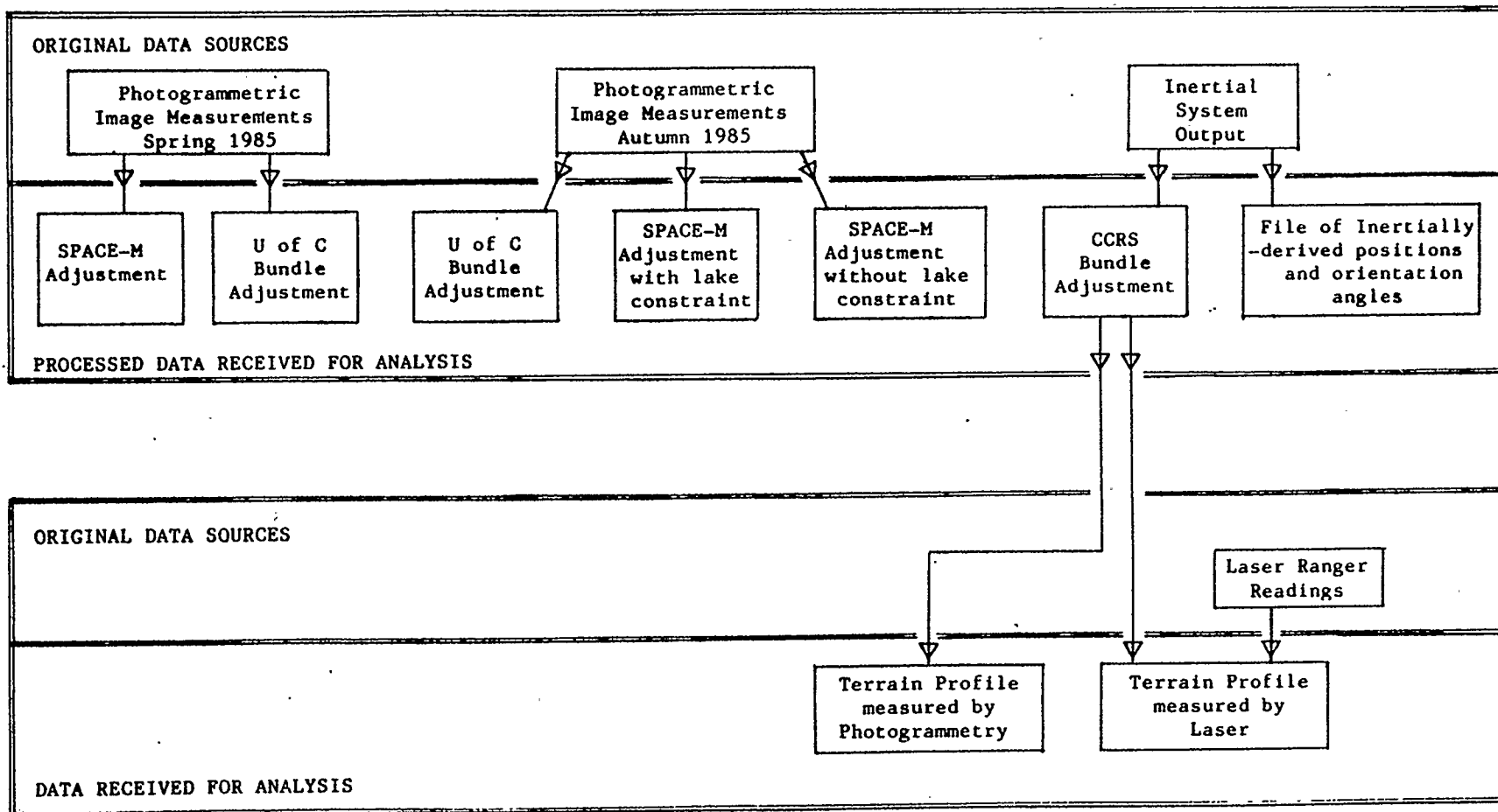


Fig. 2.3: Original data sources and data sets available for analysis

Chapter 3

ACCURACY OF PHOTOGRAMMETRIC ADJUSTMENTS

In this study, photogrammetry is used as a standard of comparison for the accuracy of the auxiliary data. One should therefore evaluate the accuracy and precision of the photogrammetry itself, and bear the results in mind when interpreting the analyses. In particular, a given set of photogrammetric data does not uniquely determine the coordinates of a set of points in object space. These coordinates depend also on factors such as the type of adjustment, amount and distribution of ground control, statistical weights, constraints that may be applied, and the size of the adjustment block. Therefore the values of coordinates from several different adjustments, and their mutual consistency, should be considered.

Most of the photogrammetric network was processed using the SPACE-M independent model block adjustment. Adjustments were made on two separate blocks, one using the first five flight lines (oriented N-S) and one using the last five flight lines (oriented E-W). As some of the auxiliary data were missing for the last five lines, most attention will be given to the first five.

For photogrammetric purposes, such as are considered in this chapter, the first five flight lines are numbered 1 to 5 from west to east, and the camera stations within them are numbered from north to south. Alternative numbering systems, such as are required for the auxiliary data, are discussed in Chapter 4.

The photography of the first five lines has 80% endlap and 60% sidelap, and the SPACE-M adjustment was made using all the images, apart from a few which lay outside the area covered by ground control. As endlap and sidelap are normally 60% and 20% respectively, the redundancy of data was higher than normal.

Several variations of the adjustment were performed, using photogrammetric data from an original set of measurements in spring, 1985, then using data revised by the remeasurement of some of the images in autumn, 1985. Two adjustments were made using this later data set: including and excluding the constraint that waterline points on a lakeshore should be at the same height.

After processing, the RMS residuals in the positions of ground points proved to be much greater than expected. Indeed, they were two or three times as great as those produced by a block adjustment using the same method and software, and at the same photo scale, for a large area near Hudson Bay, as described by Blais (1979). The Hudson Bay adjustment was made under operational conditions typical for production of 1:50000 topographic maps, without any special provisions for high accuracy. The reason for the large residuals in the present case has not yet been determined, but it may be related to photogrammetric measurements, or the high redundancy, or the small base-to-height ratio that corresponds to the large overlap. The terrain relief was also considerably higher in Kananaskis than near Hudson Bay. Further, while vertical distances were measured in metres, horizontal distances were measured in UTM plane, with a scale factor

of 0.9998. This discrepancy in units amounts to an apparent difference of 0.4m over the 2000m range of terrain elevations in the study area, and 1.7m in the 8500m flying height above ground, and could therefore result in a deformation of this magnitude.

The auxiliary measurements that are being considered are particularly related to two sets of points in the output of the SPACE-M adjustment. One set consists of the perspective centres (PC s), whose positions are also measured by the inertial system. The other set comprises the points on the ground corresponding to the principal points of the images. The length of the line from such a point to its PC should correspond to the range measured by the laser, and its direction is related to the orientation angles measured by the inertial system.

3.1 Perspective Centre Position Estimates from SPACE-M

The SPACE-M adjustment is primarily intended for topographic mapping at the best possible accuracy, and for such applications the PC s are of secondary importance. Though they are normally used in the adjustment process, some of them may be rejected from this process if they are associated with large residuals and if their rejection improves the fit of points on the ground. Nevertheless, estimates of their positions are still printed in the output. For this project, one had the option of working with the PC s of all images, for completeness, or with only those that were not rejected from the adjustment, for accuracy.

Apart from points at the ends of a flight line, the SPACE-M output gives two estimates of the position of each PC, one from

each of the two models in which it appears, and if each model is given equal weighting, the "best estimate" of the PC's position is the mean of these two estimates.

A basic statistical analysis was made on the difference between the two estimates of position, to give an indication of their reliability. The distance between the two estimated positions was calculated, together with its horizontal, vertical, x and y components, and for each of these quantities the RMS, maximum and mean values on each flight line were computed. This was done for three adjustments: one using "old" measurements from spring, 1985, and two using "new" measurements from autumn, 1985, with and without use of lake-level constraint. For each of these adjustments, the analysis was applied to data sets including and excluding points that were rejected from the adjustment. The results are shown in Tables 3.1 to 3.3.

The discrepancy between the two PC position estimates was always more pronounced (usually by a factor of 5 or more) in the horizontal than in the vertical, but there was not a noticeable difference between the x-direction (easterly, perpendicular to the flight line) and the y-direction (northerly, parallel to the flight line). The use of new (autumn, 1985) data did not cause a significant change from the use of old (spring, 1985) data. Exclusion of points that had been rejected in the adjustment did cause a great improvement, as these points included those perspective centres for which the discrepancies, and consequently residuals, were greatest.

An indication of magnitude of discrepancies can be given

Table 3.1

Discrepancies Between PC Position Estimates from SPACE-M

RMS Values (Metres)

All Points					Excluding Rejected Points		
Spatial Line	Old Data	New data w/lakes no lakes		Old Data	New data w/lakes no lakes		
X-Compt.							
1	11.1	11.7	7.9	4.0	5.1	4.6	
2	4.1	4.8	4.8	4.2	5.0	4.9	
3	5.1	5.0	4.9	3.4	3.5	3.7	
4	9.6	15.4	11.4	3.9	4.0	3.9	
5	4.4	4.7	4.2	3.8	4.2	4.1	
All	7.5	9.7	7.3	3.8	4.3	4.2	
Y-Compt.							
1	6.8	6.7	6.3	3.3	3.9	3.7	
2	4.5	4.1	4.2	3.2	3.1	3.3	
3	6.9	6.1	5.2	3.8	4.0	3.7	
4	8.4	10.9	7.5	5.0	4.9	2.7	
5	6.9	5.9	4.0	3.9	3.8	2.6	
All	6.8	7.2	5.6	4.0	4.1	3.2	
Z-Compt.							
1	3.0	2.6	2.1	0.9	0.8	0.7	
2	0.7	0.6	0.6	0.7	0.7	0.7	
3	1.0	0.8	0.8	0.7	0.5	0.5	
4	2.4	2.9	2.3	0.9	1.0	0.7	
5	1.6	1.4	1.0	1.0	0.9	0.7	
All	2.0	1.9	1.6	0.9	0.8	0.7	
Horiz.							
1	13.1	13.5	10.1	5.2	6.4	5.9	
2	6.1	6.4	6.4	5.3	5.9	6.0	
3	8.6	7.9	7.1	5.1	5.3	5.2	
4	12.8	18.9	13.6	6.3	6.3	4.8	
5	8.2	7.6	5.8	5.4	5.6	4.8	
All	10.2	12.1	9.2	5.5	5.9	5.3	
Total							
1	13.4	13.8	10.3	5.2	6.5	6.0	
2	6.1	6.4	6.4	5.3	5.9	6.0	
3	8.6	7.9	7.2	5.2	5.3	5.2	
4	13.0	19.1	13.8	6.4	6.4	4.8	
5	8.4	7.7	5.9	5.5	5.7	4.9	
All	10.4	12.3	9.4	5.6	6.0	5.3	

Table 3.2

Discrepancies Between PC Position Estimates from SPACE-M

Max. Values (metres)

All Points				Excluding Rejected Points			
Spatial Line	Old Data	New data w/lakes no lakes		Old Data	New data w/lakes no lakes		
X-Compt.							
1	37.0	37.7	24.2	9.8	11.0	9.5	
2	8.6	9.9	9.9	8.6	9.9	9.9	
3	16.3	14.0	12.3	6.4	7.8	7.9	
4	30.5	53.7	38.9	7.9	8.4	9.1	
5	12.1	12.9	9.3	7.8	10.0	9.3	
All	37.0	53.7	38.9	9.8	11.0	9.9	
Y-Compt.							
1	14.7	14.2	14.5	7.7	6.5	5.9	
2	11.2	11.0	11.2	6.5	6.3	6.8	
3	17.1	15.5	12.2	8.3	9.2	9.1	
4	19.1	35.8	25.5	11.7	11.9	5.3	
5	17.3	16.0	9.6	9.9	9.8	5.3	
All	19.1	35.8	25.5	11.7	11.9	9.1	
Z-Compt.							
1	9.9	8.7	7.0	2.0	1.2	1.2	
2	1.7	1.3	1.3	1.7	1.3	1.3	
3	3.2	2.0	2.8	2.0	1.2	1.1	
4	8.7	13.5	10.6	2.0	2.1	1.7	
5	5.2	4.4	2.7	2.3	2.3	1.3	
All	9.9	13.5	10.6	2.3	2.3	1.7	
Horiz.							
1	37.4	38.2	26.1	10.1	11.6	10.9	
2	11.4	11.1	11.3	10.8	10.8	10.9	
3	17.5	15.5	14.2	10.1	12.1	12.0	
4	36.0	64.5	46.6	14.1	13.6	10.3	
5	17.9	16.2	10.2	11.1	11.8	9.5	
All	37.4	64.5	46.6	14.1	13.6	12.0	
Total							
1	38.7	39.2	27.0	10.3	11.6	10.9	
2	11.4	11.1	11.3	10.8	10.8	10.9	
3	17.5	15.5	14.5	10.1	12.1	12.0	
4	37.0	65.9	47.8	14.1	13.6	10.3	
5	17.9	16.3	10.2	11.2	11.8	9.6	
All	38.7	65.9	47.8	14.1	13.6	12.0	

Table 3.3
Discrepancies Between PC Position Estimates from SPACE-M

Mean Absolute Values (metres)							
All Points				Excluding Rejected Points			
Spatial Line	Old Data	New data		Old Data	New data		
		w/lakes	no lakes		w/lakes	no lakes	
X-Compt.							
1	7.2	8.3	6.1	2.9	4.3	4.0	
2	3.5	4.0	3.9	3.6	4.0	3.9	
3	3.7	3.6	3.7	2.8	2.8	3.0	
4	6.4	8.0	6.2	3.4	3.4	3.1	
5	3.5	3.6	3.4	3.0	3.3	3.2	
All	4.9	5.6	4.7	3.1	3.5	3.4	
Y-Compt.							
1	5.1	5.5	5.1	2.5	3.5	3.4	
2	3.5	3.1	3.2	2.6	2.5	2.7	
3	5.1	4.5	4.0	3.2	3.1	2.8	
4	6.2	7.0	4.6	3.9	3.8	2.0	
5	5.0	4.5	3.0	3.0	3.1	2.2	
All	5.0	5.0	4.0	3.1	3.3	2.6	
Z-Compt.							
1	1.9	1.6	1.3	0.7	0.7	0.7	
2	0.6	0.5	0.5	0.6	0.5	0.5	
3	0.7	0.5	0.5	0.5	0.4	0.4	
4	1.4	1.4	1.1	0.7	0.8	0.6	
5	1.0	0.9	0.7	0.7	0.7	0.5	
All	1.1	1.0	0.8	0.6	0.6	0.5	
Horiz.							
1	9.6	10.7	8.4	4.4	5.9	5.5	
2	5.4	5.5	5.6	4.7	5.0	5.1	
3	7.1	6.6	6.1	4.6	4.7	4.5	
4	9.9	11.5	8.3	5.7	5.6	4.1	
5	6.6	6.2	5.1	4.6	4.8	4.3	
All	7.8	8.2	6.7	4.9	5.2	4.6	
Total							
1	9.9	10.8	8.6	4.5	6.0	5.6	
2	5.4	5.6	5.6	4.8	5.1	5.2	
3	7.1	6.7	6.1	4.7	4.7	4.6	
4	10.0	11.6	8.4	5.7	5.7	4.2	
5	6.7	6.4	5.2	4.7	4.9	4.3	
All	7.9	8.3	6.8	4.9	5.3	4.7	

here. When rejected points were excluded, the discrepancy was typically 5m in the horizontal and 1m in the vertical, but occasionally two or three times as great. These values are consistent with the generally accepted height accuracy expected from photogrammetry, namely 0.01-0.03% of flying height. Inclusion of rejected points roughly doubled these values.

When the lake-level constraint was used, the discrepancies between PC positions were greater than when it was not used. Probably this happened because inclusion of the lake-level constraint gave more weight to the ground-level points in the adjustment, and a smaller share of the weight to camera-level points. In other words, a strengthening of the adjustment at ground level produced a relative weakening at camera level.

The role of PC's in an adjustment is to control "hinging" between adjacent models in a line. The lake-level constraint does likewise, but at a different level in the model. A discrepancy between the effects of these two methods of "hinge control" could be due to incorrect correction for earth curvature; over a distance of 2.5km (the length of base between consecutive perspective centres) the height correction for earth curvature amounts to about 0.5m. The discrepancy could also be due to deformation within the models.

Flight line no.2 proved to be an exception to the general rule. In this line, the changes resulting from use of the lake-level constraint and exclusion of the rejected points were negligible, and sometimes even the reverse of those in the other lines. This line did not cross any lakes directly, but lakes did

appear near the edges of some of the images.

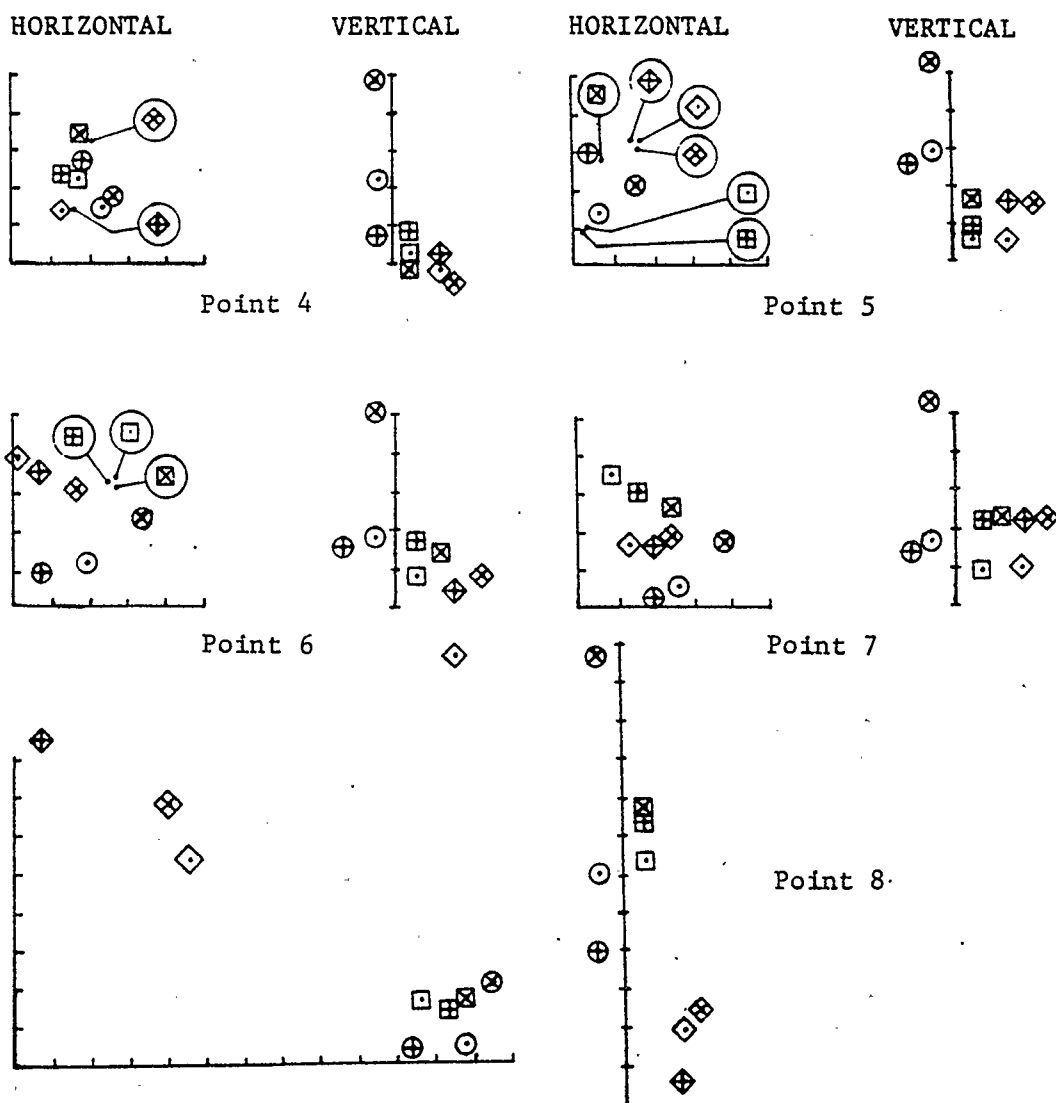
3.2 Position Estimates from Bundle and SPACE-M Adjustments

The foregoing analysis was concerned only with estimates of PC positions from SPACE-M adjustments. As mentioned in Chapter 2, some bundle adjustments were made too, using the same image data, and including PC coordinates in their output. To illustrate the dependence of PC position estimates on the method of adjustment, a comparison of these estimates from the different adjustments is now presented.

The bundle adjustment done at the University of Calgary was a simultaneous bundle adjustment based on collinearity equations, using ground control, and treating orientation parameters and object space point coordinates as unknowns. It used 10 images, those numbered 4 to 8 in flight lines 4 and 5, and it was performed on both the "old" and the "new" data.

Figs. 3.1-3.2 show the relative locations of the estimated PC positions, both in a horizontal plane and on a vertical scale, as determined by the 3 bundle and 6 SPACE-M adjustments. A separate symbol on the diagram is used for each adjustment. In the horizontal diagrams, if two positions are too close together for the symbols to be plotted directly, the symbol is enclosed in a circle which is joined by a line to the correct position.

Between the bundle adjustments, the discrepancies are around 10m in the horizontal and 6m in the vertical. The vertical coordinates from the two University of Calgary bundle adjustments never differ by more than 4m. The CCRS adjustment consistently

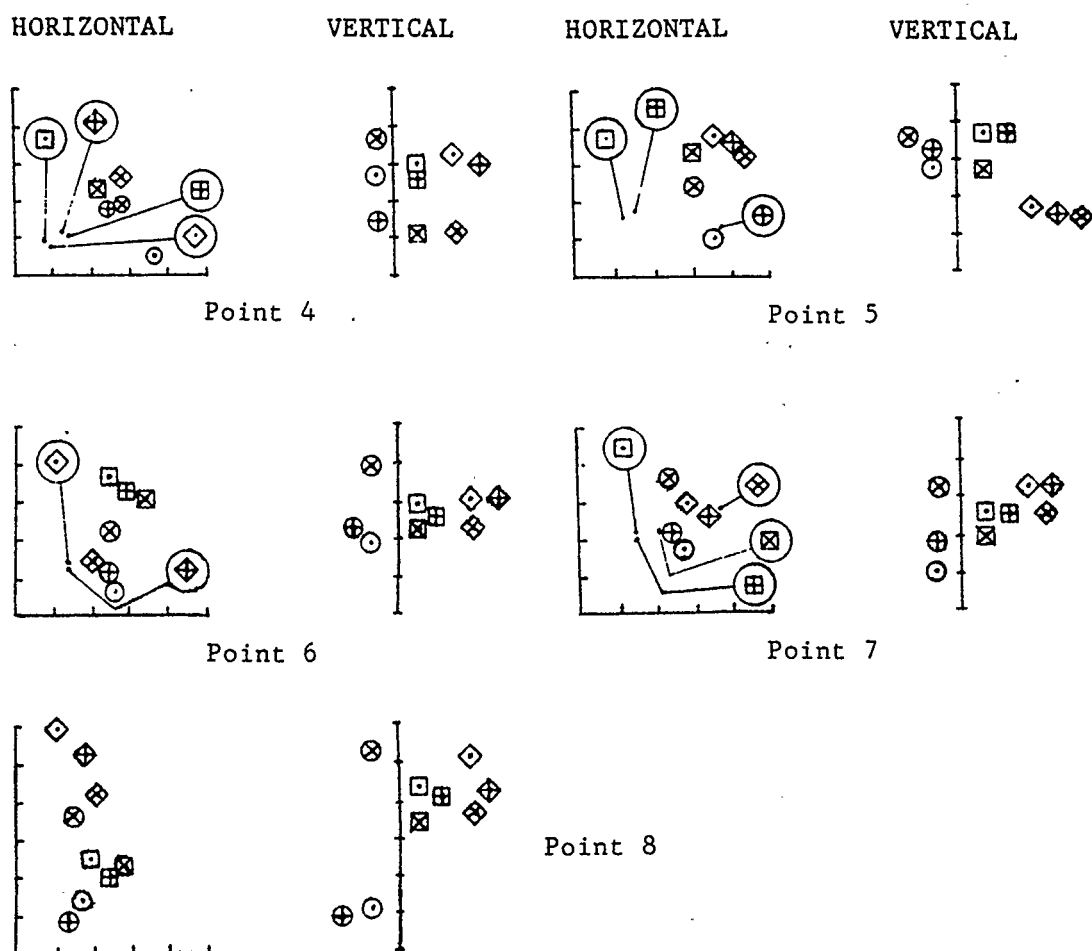


	BUNDLE	SPACE-M	
		Model 1	Model 2
OLD DATA	⊙	□	◇
NEW DATA	⊕	⊞	◆
		⊠	◇
CCRS	⊗		

With Lakes
Without Lakes

Horizontal: Scale marks every 5m Vertical: Scale marks every 2m

Fig. 3.1: Plots of Perspective Centre Position Estimates from Different Photogrammetric Adjustments:
Spatial Flight Line 4



	BUNDLE	SPACE-M	
		Model 1	Model 2
OLD DATA	⊙	□	◇
NEW DATA	⊕	⊞	⊞
		⊞	⊞
CCRS	⊗		

With Lakes
Without Lakes

Horizontal: Scale marks every 5m

Vertical: Scale marks every 2m

Fig. 3.2: Plots of Perspective Centre Position Estimates from Different Photogrammetric Adjustments: Spatial Flight Line 5

gives a height that is greater than those given by the University of Calgary adjustments, sometimes by about 1m and sometimes by as much as 8m. This difference could be attributed to use of different camera lens focal lengths in the two adjustments.

For the positions estimated by SPACE-M, the variation in the horizontal is usually greater than that for the bundle adjustments, and is of a magnitude around 10-20m. In the vertical, it is generally around 3m or 4m, and less than the discrepancy between the University of Calgary and CCRS bundle adjustments.

In some instances, notably point 8 in line 4, the variation between the SPACE-M estimates is exceptionally great, of the order of 60m in the horizontal. This, and also four others of the ten points, is one of the PC's that was rejected from the SPACE-M adjustment.

In summary, then, while the best estimates of PC positions from SPACE-M are reliable to about 5m, all estimates, on the whole, are reliable only to about 10m, and in extreme cases only to about 40m.

In retrospect, it appears that the SPACE-M adjustment did not prove to be a satisfactory standard on this occasion. Unfortunately, a bundle adjustment, based on ground control only and covering the complete block, was not available for comparison.

The data sets used in the analyses of this chapter are depicted diagrammatically in Fig. 3.3.

Since the reliability of photogrammetric estimates of PC coordinates has now been evaluated, the investigation can proceed to comparison of them with values derived from auxiliary systems.

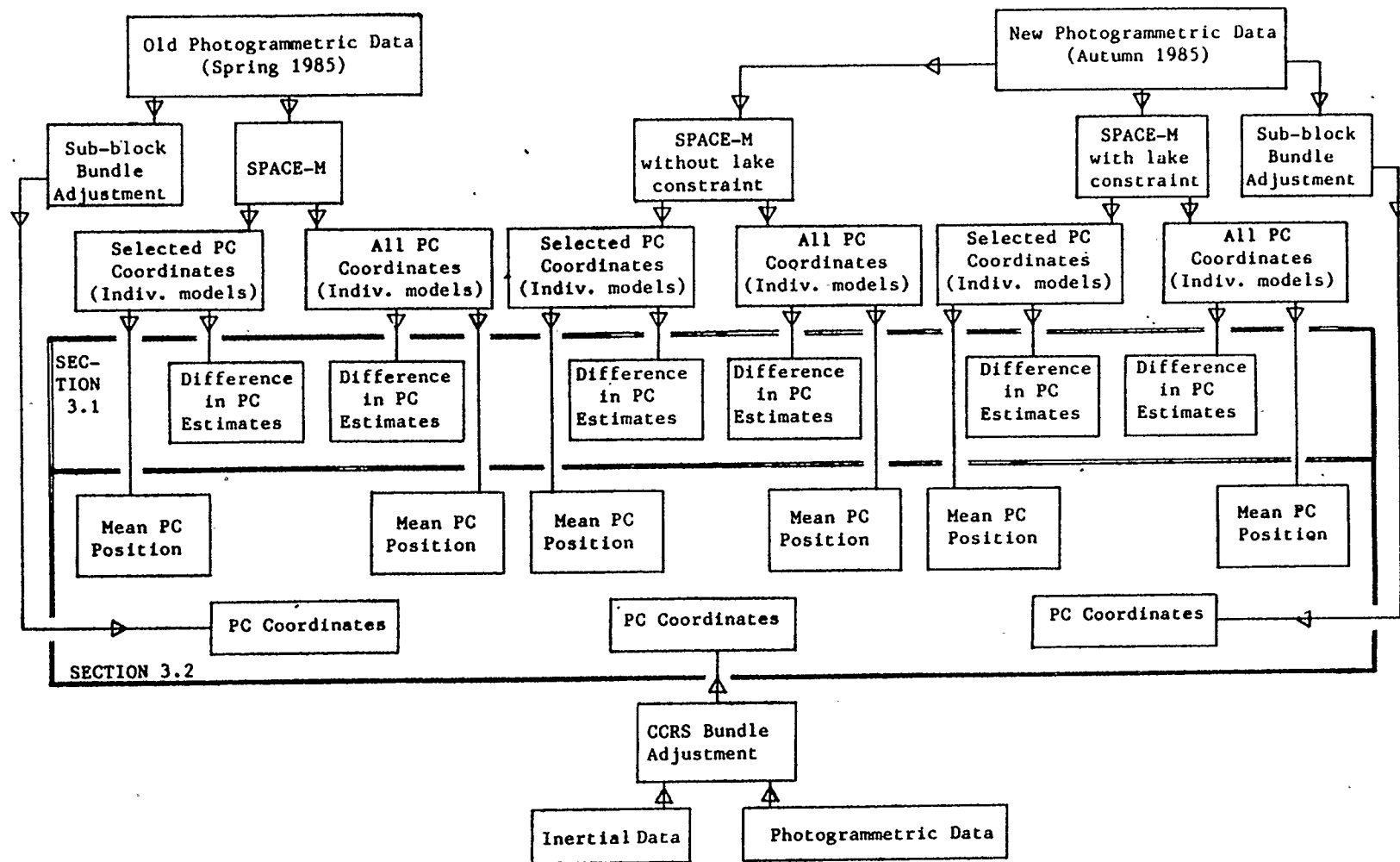


Fig. 3.3: Data sets used in analyses of Chapter 3

Chapter 4

POSITION DETERMINATION FOR PERSPECTIVE CENTRES

The reliability of the appropriate photogrammetry output having been evaluated, the investigation can now proceed to a comparison of the positions of perspective centres, as determined by photogrammetry and as given by the inertial data provided by CCRS. Any comparison of two time-dependent quantities requires correct synchronization, and time tagging of photogrammetric data was absent. In the present context, then, it is first necessary to ensure that any pair of coordinate values, as obtained from the two sources, refers to the same camera station. Once this is established, then the differences between the coordinate values can be analyzed.

4.1 Matching of Perspective Centres

In any comparison between photogrammetric and auxiliary data, one must match each auxiliary record correctly with the corresponding photogrammetric point. This matching was achieved by comparing coordinates of the perspective centre positions.

Each perspective centre can be identified by two numbers, of which one indicates the flight line in which it lies, and the other its position in the flight line. Unfortunately, it was not practical to assign a unique pair of numbers to each PC. The lines in the flight pattern were flown in alternating directions, and in a sequence different from their spatial arrangement. For the photogrammetrist, it was most convenient to number the lines

1 to 5 from west to east, and the perspective centres within them from north to south in the case of the first five lines, and to number the lines 7 to 11 from south to north, and the points within them from west to east in the case of the last five lines. (Evidently a line no. 6 was flown but not used.) However, the second auxiliary data set was arranged in chronological order, so that the ordering of both the lines and of the points within them was different. For some purposes, such as studying drift of the inertial system as a function of time, a chronological ordering was preferable to a spatial ordering. Further, the photogrammetric adjustments did not use all of the images, some of those at the ends of the lines being omitted because they covered terrain outside the ground control area. After the auxiliary records that did not correspond to any photogrammetric points had been rejected, there resulted a second chronological numbering of the points within each line.

As the first step in the matching process, the "best estimate" of the PC positions from photogrammetry was made by taking the mean of the two estimates from a SPACE-M adjustment. A graphical plot of the PC positions in the horizontal plane was then made. The positions of flight lines 1 to 5, which are aligned N-S and each contain over twenty points, are shown in Fig. 4.1, as given by photogrammetric and auxiliary systems. Since the lines from the two systems do not coincide, it is evident that there is a discrepancy between the x-coordinates given by the two methods, which is sometimes as great as 700m. The data files also indicated that there was a discrepancy of

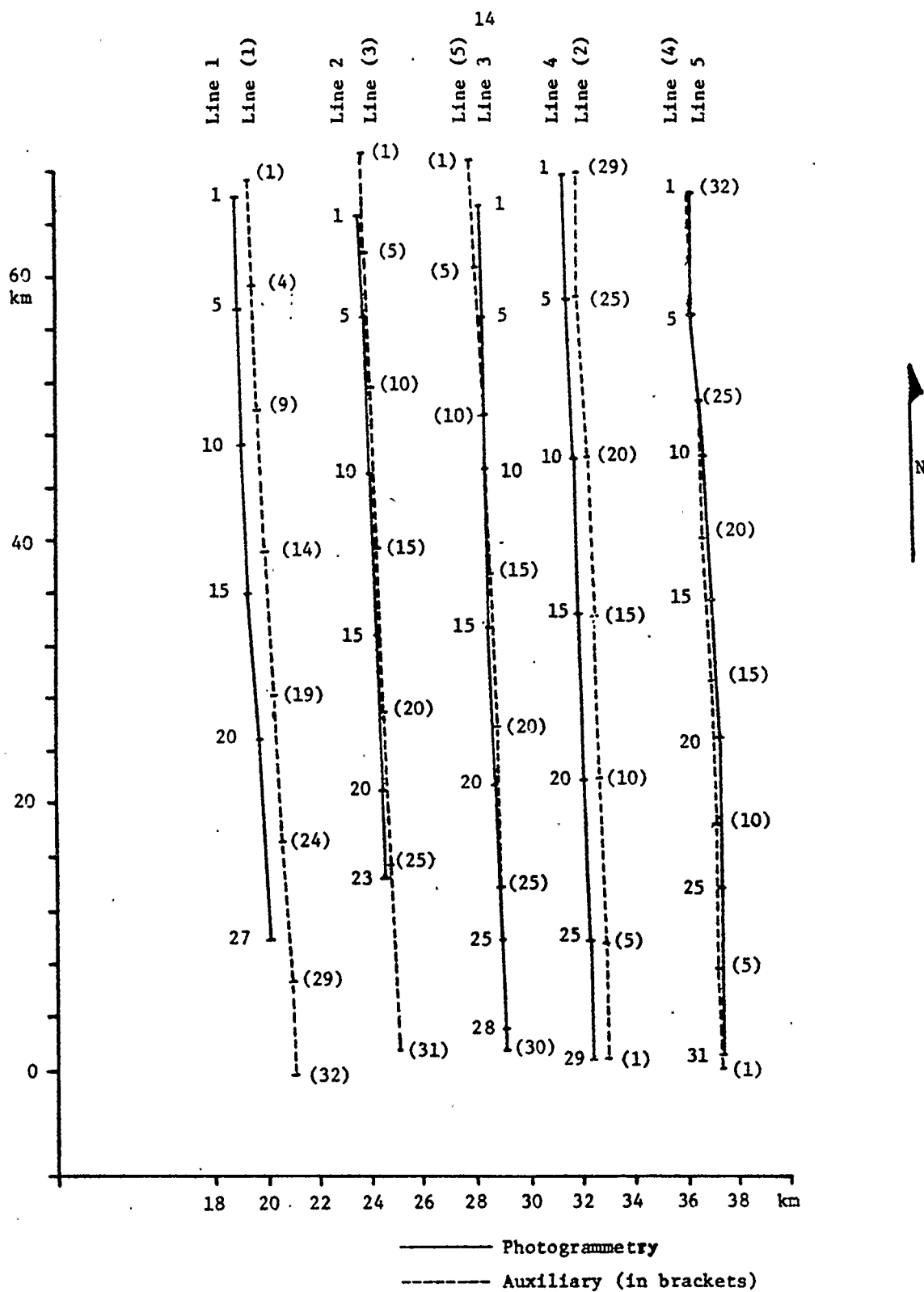


Fig. 4.1: Relative Locations of Flight Lines and Points thereon as given by Photogrammetry and Auxiliary Systems. (Lines 1 to 5)

200-300m in the z (vertical) direction.

To match corresponding points within a line, the first approach was to find "closest neighbours". I.e. for each photogrammetric position, the closest auxiliary position would be taken as the corresponding one. This method might work if one could be sure that the discrepancy between the two positions was less than half the spacing between stations. In this case, it did not work, for it was found that both points 5 and 6 of photogrammetric line 1 had point 6 of the auxiliary line as their closest neighbours. This result indicated that the position discrepancy was sometimes more than half of the spacing between stations. Therefore the "nearest neighbour" method was inapplicable.

An alternative method was therefore needed, and the approaches used will be described in terms of line 1, on which there are 27 perspective centres used in photogrammetry and 32 points given by the auxiliary system.

First, a method using correlation coefficients was tried.

Points 1 to 27 of the photogrammetric set were paired with points 1 to 27 of the auxiliary set. The correlation coefficients were then found between the photogrammetric and auxiliary values for the x, y and z coordinates.

Next, points 1 to 27 of the photogrammetric set were paired with points 2 to 28 of the auxiliary set. This involved a shift of one place in the auxiliary data set. The correlation coefficient was found as before for x, y and z coordinates.

This procedure was repeated, pairing points 1 to 27 of the

photogrammetric set with points 3 to 29 of the auxiliary set, corresponding to a shift of two places in the auxiliary data set, and so on for as many shifts as were possible.

Now the correlation coefficients corresponding to different shifts were compared. Presumably the shift giving the greatest correlation coefficient would be the one corresponding to the correct matching of points.

This procedure was also carried out using the coordinate differences between successive points along the line, rather than the actual coordinates themselves.

The outcome of this test was not as decisive as had been hoped. In the correlation of coordinates, in every case it was found that the best correlation occurred for a shift of zero. In the correlation of coordinate differences, the best correlations sometimes occurred for shifts different from zero, but the shift giving the best correlation for one coordinate (e.g. x) was not always the same as the shift giving the best correlation for another coordinate (e.g. y).

On the whole, this approach using correlations proved to be inconclusive.

Second, a method of "double differencing" was tried. Here, "double difference" means the coordinate difference between adjacent stations from photogrammetry minus the corresponding difference from auxiliary systems.

If (x_{p1}, y_{p1}, z_{p1}) and (x_{p2}, y_{p2}, z_{p2}) are the estimates of two PC positions from photogrammetry, and (x_{a1}, y_{a1}, z_{a1}) and (x_{a2}, y_{a2}, z_{a2}) are the estimates of the same PC positions from the auxiliary systems, then $dx_p = (x_{p2} - x_{p1})$ and $dx_a = (x_{a2} - x_{a1})$ are the single differences in the photogrammetric and auxiliary cases respectively, and $dx_a - dx_p$ is the double difference for the x-component, and similarly for the y and z components.

Further, if $dh_p = [(x_{p2} - x_{p1})^2 + (y_{p2} - y_{p1})^2]^{1/2}$ and dh_a is defined similarly, then $dh_a - dh_p$ is the double difference in the horizontal component, and if $ds_p = [dh_p^2 + (z_{p2} - z_{p1})^2]^{1/2}$ and ds_a is defined similarly, then $ds_a - ds_p$ is the double difference in the total, or three-dimensional, distance.

The sum of squares of these double differences was then computed for each of the x, y and z coordinates, as well as the sum of squares of the three-dimensional distances between perspective centres. This was performed for shifts of 0, 1, 2, places as appropriate for each line. One should note that in every case the number of terms in the sum of squares is the same, viz. the number of perspective centres used in the photogrammetry for that line.

The outcome of this test was clear. In every case, there was a definite shift for which the sum of squares was least for all three coordinates and the three-dimensional distance. It was concluded that this shift corresponded to the correct matching.

With the matching complete, the positions of the camera stations could be entered on Fig 4.1. Also the difference between photogrammetric and auxiliary values of the coordinates, and the double differences, could be studied.

Since further details of the numbering systems for lines and points would be of interest only to people wishing to use the same data, they are given in Appendix A.

4.2 Relation between Photogrammetric and Auxiliary Estimates of Position

Plots were made of the difference between auxiliary and photogrammetric position estimates as functions of time, and they are shown in Fig. 4.2 for all ten flight lines, the first five being in northerly-southerly directions and the last five in easterly-westerly directions.

The graph for the x-coordinate shows a sinusoidal pattern with a period of about 70 minutes in the first five lines; this could be a Schuler oscillation. The graph for the y-coordinate shows a fairly steady drift in the last five lines. However, the graphs for the x-coordinate for the last five lines, and the y-coordinate for the first five lines, show violent oscillations with amplitude of hundreds of metres which appear to be connected with the direction of flight, e.g. whether the aircraft was flying from south to north or north to south. These oscillations probably indicate an error in one accelerometer in the strapdown system. The graph for the z-coordinate shows a fairly constant difference.

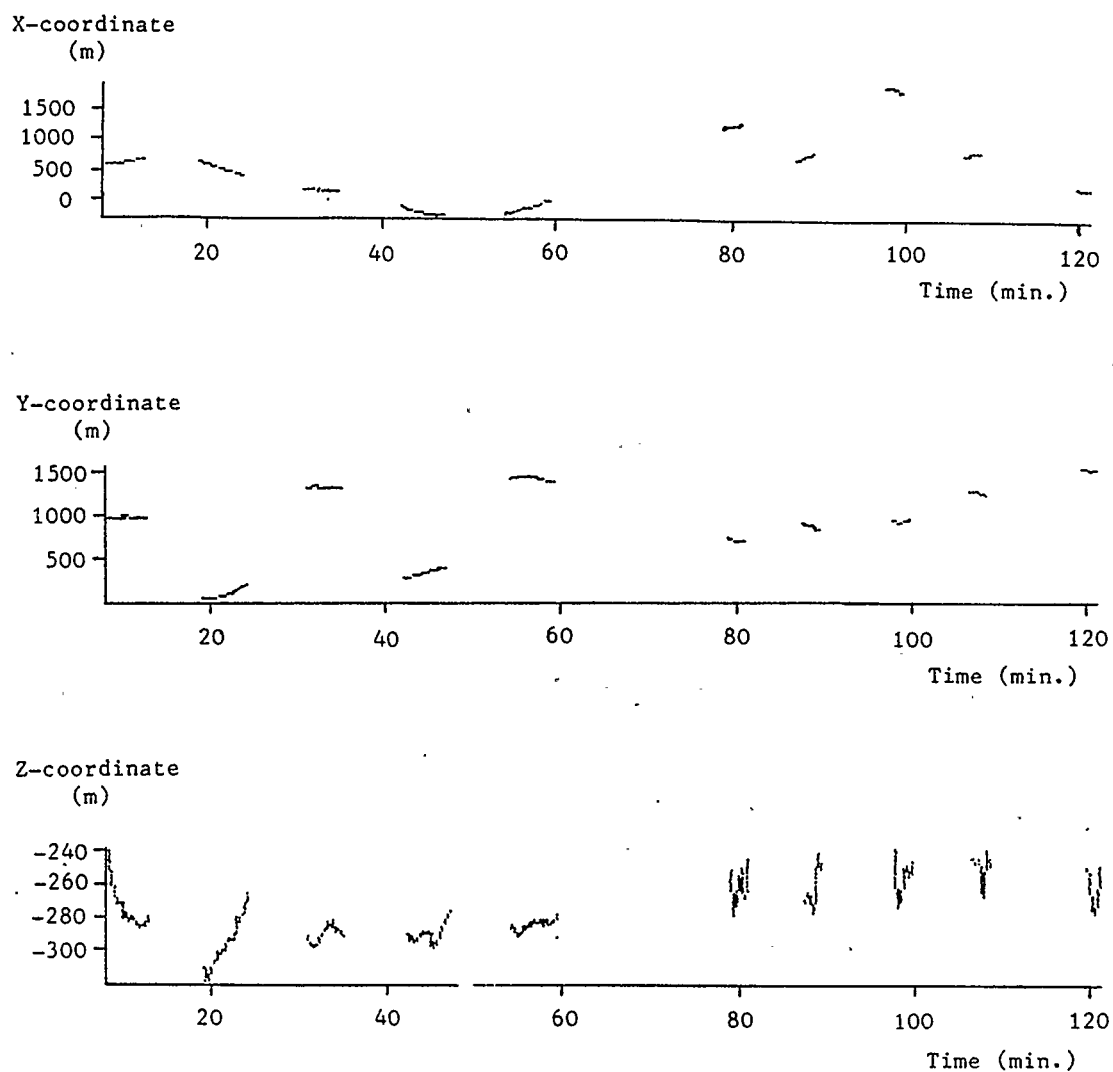


Fig. 4.2: Graphs of Differences between Auxiliary and Photogrammetric Estimates of PC Coordinates as Functions of Time.

The graphs just discussed were based on the output of the first SPACE-M adjustment. Subsequent analyses involved outputs of various adjustments. The relations between these adjustments and the various quantities being compared are summarized diagrammatically in Fig. 4.3.

Results of a statistical analysis of the discrepancies are shown in Tables I.1-I.7 in Appendix I. This analysis was performed on the outputs of all three SPACE-M adjustments, both including and excluding points that had been rejected, plus the bundle adjustment from CCRS, and it considered the discrepancies, on a given flight line, to be functions of time. It determined the regression line of the discrepancy, or a component thereof, (in metres) on time (in minutes). Such a regression line passes through the mean values of the time and of the dependent variable, which are specified in the tables. Also given are the slope of each regression line, the correlation coefficient, and the RMS deviation of the discrepancy from the regression line.

If the discrepancy were due to a linear drift of the inertial system with very little noise, one would expect the correlation coefficient to be close to 1 or -1, and the RMS deviation to be small. In fact, the correlation coefficients are close to zero, suggesting that effects of drift within a flight line are negligible compared to the noise. The only hint of a systematic variation occurs in the analysis for the y-coordinate. Noting that the flight lines are numbered chronologically and that they were flown in alternating directions, there is then an alternation in the sign of the regression line slope and

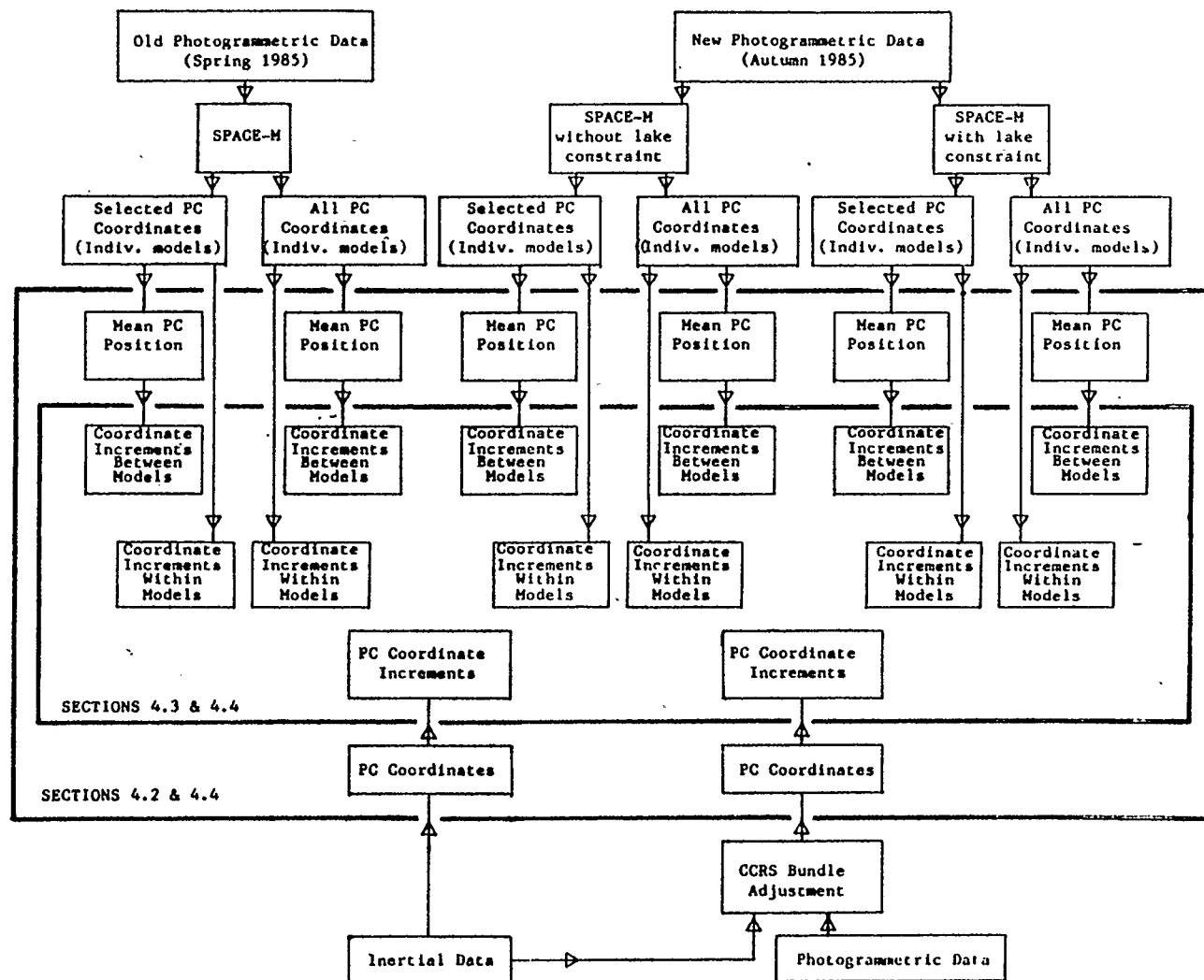


Fig. 4.3: Data sets used in analyses of Chapter 4

correlation coefficient which is consistent with the alternation of flight direction. As this alternation is evident only in the y-component, it is probably related to the aforementioned possible error in an accelerometer.

The differences between the values in the seven different tables are negligible. However, it is evident that the measured values of position coordinates from the inertial system, without updates, are unacceptable as indicators of the camera position. The values in the columns for "Mean Dependent Variable", which give typical values of the discrepancies, are far greater than any of the uncertainties of PC position that were discussed in Chapter 3.

4.3 Double Differences - Relation between Photogrammetric and Auxiliary Estimates of PC Position Increments

The effect of bias in the inertially-derived position coordinates can be eliminated by comparing the position increments, or displacements between successive PC's, as measured by the two systems. The difference between the increments as measured by the two systems is called a "double difference".

Since SPACE-M gives two different estimates of each PC position, two different methods are possible for calculating the displacement between adjacent PC's. One method uses those two estimates that resulted from the same model, giving a within-model estimate. The other method involves finding the mean estimate of each position and computing the displacement between two adjacent mean positions, giving a between-model estimate.

As each double difference corresponds to a time interval, not a time point, the double difference cannot be treated as a function of time. However, a statistical survey of the values of the double differences was made. It resulted in Tables I.8 to I.14 of Appendix I, corresponding to the various adjustments, encompassing in the case of SPACE-M alternatives such as inclusion or exclusion of points rejected during the adjustment and the method of calculating the displacement. These tables give the RMS and maximum values for the double differences in x , y and z coordinates and also in the horizontal component and spatial distance. Summary tables, without reference to individual flight lines, are presented in Tables 4.1 and 4.2.

In examining these values, it may seem surprising at first that in many cases they are greater for the individual components than for the total distance. This is an effect of orientation errors in one or both systems. Referring to the notation of Section 4.1, the values of dx_p , dy_p , dx_a and dy_a depend on the orientation of the x and y axes. However, dx_p and dy_p are components of a displacement vector in the photogrammetric coordinate system, whereas dx_a and dy_a are components in the auxiliary coordinate system. Therefore the photogrammetric and auxiliary components will not be equal if the systems are mutually inclined, even though they refer to the same vector. Inter-coordinate correlations could occur; for example, a y -displacement detected by the auxiliary system could correspond partly to an x -displacement measured by the photogrammetry. The total displacement, ds_p or

Table 4.1

Comparison of PC Position Increments by
Auxiliary and Photogrammetric Systems

RMS Discrepancies (metres)

SPACE-M including rejected points

Case	No. of Points	X-compt.	Y-compt.	Z-compt.	Horiz. Dist	Total Dist.
(a)	133	6.39	4.21	2.93	4.25	4.25
(b)	133	6.41	4.15	2.92	4.19	4.18
(c)	133	6.41	4.15	2.96	4.19	4.18
(d)	133	7.13	5.85	2.98	5.89	5.89
(e)	133	7.54	5.76	2.87	5.80	5.80
(f)	133	7.11	5.35	2.89	5.40	5.39

SPACE-M excluding rejected points

Case	No. of Points	X-compt.	Y-compt.	Z-compt.	Horiz. Dist	Total Dist.
(a)	64	6.02	3.57	2.34	3.59	3.58
(b)	73	5.96	3.48	2.21	3.50	3.49
(c)	73	5.97	3.49	2.45	3.50	3.50
(d)	64	6.27	4.25	2.35	4.26	4.26
(e)	73	6.35	4.38	2.14	4.41	4.41
(f)	73	6.33	4.31	2.39	4.34	4.34

CCRS Bundle Adjustment

133	5.93	4.54	1.18	4.60	4.60
-----	------	------	------	------	------

Key to cases:

Increments within models:

- (a) Old (spring, 1985) data
- (b) New (autumn, 1985) data with lake level constraint
- (c) New (autumn, 1985) data without lake level constraint

Increments between models:

- (d) Old (spring, 1985) data
- (e) New (autumn, 1985) data with lake level constraint
- (f) New (autumn, 1985) data without lake level constraint

Table 4.2

Comparison of PC Position Increments by
Auxiliary and Photogrammetric Systems

Maximum Discrepancies (metres)

SPACE-M including rejected points

Case	No. of Points	X-compt.	Y-compt.	Z-compt.	Horiz. Dist	Total Dist.
(a)	133	15.53	14.26	8.43	14.28	14.28
(b)	133	15.49	13.92	12.78	13.94	13.94
(c)	133	15.55	13.96	10.22	13.98	13.98
(d)	133	17.97	17.39	9.98	17.60	17.60
(e)	133	29.04	22.04	9.81	22.45	22.44
(f)	133	22.87	18.87	10.63	19.23	19.22

SPACE-M excluding rejected points

Case	No. of Points	X-compt.	Y-compt.	Z-compt.	Horiz. Dist	Total Dist.
(a)	64	12.31	9.50	6.71	9.46	9.44
(b)	73	12.32	9.62	6.15	9.58	9.56
(c)	73	12.32	9.59	7.64	9.55	9.53
(d)	64	13.13	12.73	7.38	12.71	12.69
(e)	73	13.34	12.39	5.96	12.36	12.34
(f)	73	13.52	13.00	7.42	12.96	12.94

CCRS Bundle Adjustment

133	8.52	12.43	2.71	12.45	12.45
-----	------	-------	------	-------	-------

Key to cases:

Increments within models:

- (a) Old (spring, 1985) data
- (b) New (autumn, 1985) data with lake level constraint
- (c) New (autumn, 1985) data without lake level constraint

Increments between models:

- (d) Old (spring, 1985) data
- (e) New (autumn, 1985) data with lake level constraint
- (f) New (autumn, 1985) data without lake level constraint

ds_a , however, is invariant with respect to rotation.

Illustrating with an example, if $(dx_p, dy_p, dz_p) = (3, 4, 0)$ and $(dx_a, dy_a, dz_a) = (4, 3, 0)$, then the double differences in x and y are 1 and -1 respectively, whereas the double difference in total displacement is zero.

The important features of the double-difference analysis, as they apply to the SPACE-M adjustments, are now summarized. In almost every case the double difference is smaller for increments within models than between mean PC's. Also, as one might expect, the double difference is in most cases smaller when one considers the more "reliable" points, which were not rejected from the adjustment, than when one considers all points. Inclusion or exclusion of the lake-level constraint makes little difference, with one exception: when the rejected points are excluded, the use of the lake-level constraint gives a slight improvement in the value for the vertical component.

Values of double differences resulting from the CCRS bundle adjustment are also included in Tables 4.1 and 4.2, and in more detail in Table I.14 of Appendix I, and they are generally about the same as for the SPACE-M adjustments. However, they are smaller for the vertical (z) component.

Combining this analysis with that of Chapter 3, the RMS value of the double difference is generally smaller than the RMS discrepancy between the PC position estimates from SPACE-M, when one considers the total distance. With the individual components, this is not so often the case, and for the vertical (z) component, indeed, the reverse is usually true.

Generally, then, it appears that the length of the displacement vector between adjacent PC's, as determined from the inertial system, is at least as reliable as the determination of the PC position from SPACE-M, especially when one considers the increments within models.

4.4 Comparison of P.C.Coordinates as given by CCRS

Bundle Adjustment and SPACE-M Adjustments

Tables I.15 to I.17 of Appendix I give statistics on the difference between PC coordinate estimates from the CCRS Bundle Adjustment and the SPACE-M Adjustments, and Tables I.18 to I.23 give corresponding information on the double differences. The main features of these tables, summarized for all flight lines, are given in Tables 4.3 to 4.5.

For the actual positions (single differences), there is generally better agreement in the horizontal than in the vertical. The discrepancy between estimates is of the order 5-10m in the horizontal, with extremes of 20-30m, and this is somewhat greater than the uncertainty in PC position as found in Chapter 3. However, the vertical discrepancy is generally about 9m, with extreme values 3 times greater, which is several times greater than the uncertainty given in Chapter 3.

Table 4.3

Comparison of PC Positions by
CCRS Bundle and SPACE-M Adjustments

RMS Discrepancies (metres)

SPACE-M including rejected points

Case	No. of Points	X-compt.	Y-compt.	Z-compt.	Horiz. Dist	Total Dist.
(a)	138	8.85	6.71	9.44	11.11	14.57
(b)	138	8.50	6.68	9.01	10.81	14.07
(c)	138	7.41	7.23	9.74	10.35	14.21

SPACE-M excluding rejected points

Case	No. of Points	X-compt.	Y-compt.	Z-compt.	Horiz. Dist	Total Dist.
(a)	93	8.36	5.98	8.70	10.27	13.47
(b)	98	7.38	5.70	8.49	9.33	12.61
(c)	98	6.73	6.24	9.17	9.18	12.97

Maximum Discrepancies (metres)

SPACE-M including rejected points

Case	No. of Points	X-compt.	Y-compt.	Z-compt.	Horiz. Dist	Total Dist.
(a)	138	26.21	21.50	26.78	28.43	36.48
(b)	138	33.19	19.49	26.19	37.71	39.01
(c)	138	23.57	21.92	28.85	26.97	39.28

SPACE-M excluding rejected points

Case	No. of Points	X-compt.	Y-compt.	Z-compt.	Horiz. Dist	Total Dist.
(a)	93	19.85	21.50	22.33	24.60	27.40
(b)	98	18.15	19.49	21.64	23.14	31.68
(c)	98	17.09	18.34	23.43	24.64	34.00

Key to cases:

- (a) Old (spring, 1985) data
- (b) New (autumn, 1985) data with lake level constraint
- (c) New (autumn, 1985) data without lake level constraint

Table 4.4

Comparison of PC Position Increments by
CCRS Bundle and SPACE-M Adjustments

RMS Discrepancies (metres)

SPACE-M including rejected points

Case	No. of Points	X-compt.	Y-compt.	Z-compt.	Horiz. Dist	Total Dist.
(a)	133	2.23	2.72	2.55	2.72	2.72
(b)	133	2.26	2.76	2.54	2.76	2.76
(c)	133	2.26	2.75	2.51	2.76	2.76
(d)	133	4.12	4.31	2.65	4.32	4.31
(e)	133	4.81	4.12	2.53	4.14	4.14
(f)	133	4.04	3.73	2.48	3.75	3.75

SPACE-M excluding rejected points

Case	No. of Points	X-compt.	Y-compt.	Z-compt.	Horiz. Dist	Total Dist.
(a)	64	2.27	2.82	2.01	2.83	2.82
(b)	73	2.26	2.85	1.91	2.85	2.85
(c)	73	2.26	2.85	2.11	2.85	2.85
(d)	64	3.30	3.64	2.02	3.64	3.64
(e)	73	3.27	3.28	1.86	3.29	3.28
(f)	73	3.20	3.13	2.07	3.13	3.13

Key to cases:

Increments within models:

- (a) Old (spring, 1985) data
- (b) New (autumn, 1985) data with lake level constraint
- (c) New (autumn, 1985) data without lake level constraint

Increments between models:

- (d) Old (spring, 1985) data
- (e) New (autumn, 1985) data with lake level constraint
- (f) New (autumn, 1985) data without lake level constraint

Table 4.5

Comparison of PC Position Increments by
CCRS Bundle and SPACE-M Adjustments

Maximum Discrepancies (metres)

SPACE-M including rejected points

Case	No. of Points	X-compt.	Y-compt.	Z-compt.	Horiz. Dist	Total Dist.
(a)	133	7.39	7.13	6.55	7.32	7.31
(b)	133	7.34	7.25	10.94	7.31	7.29
(c)	133	7.41	7.22	8.38	7.28	7.26
(d)	133	16.16	11.57	8.56	11.49	11.50
(e)	133	28.54	13.32	8.78	13.85	13.86
(f)	133	21.01	10.64	8.13	10.70	10.67

SPACE-M excluding rejected points

Case	No. of Points	X-compt.	Y-compt.	Z-compt.	Horiz. Dist	Total Dist.
(a)	64	5.33	7.32	4.65	7.32	7.31
(b)	73	5.53	7.25	4.44	7.31	7.29
(c)	73	5.47	7.22	5.51	7.28	7.26
(d)	64	7.85	10.35	5.25	10.44	10.42
(e)	73	7.73	10.01	4.09	10.09	10.07
(f)	73	7.51	10.63	5.29	10.70	10.67

Key to cases:

Increments within models:

- (a) Old (spring, 1985) data
- (b) New (autumn, 1985) data with lake level constraint
- (c) New (autumn, 1985) data without lake level constraint

Increments between models:

- (d) Old (spring, 1985) data
- (e) New (autumn, 1985) data with lake level constraint
- (f) New (autumn, 1985) data without lake level constraint

For the double differences, agreement is considerably better, and the discrepancy is of about the same magnitude as the uncertainty given in Chapter 3, though it is still somewhat larger in the z-component. Two points are noteworthy; agreement is much better for within-model than for between-model increments from SPACE-M, and the inclusion or exclusion of points rejected in the SPACE-M adjustments makes only a marginal difference to the values. The tables in Appendix I do not indicate any systematic dependence on the flight line.

Consequently, if one accepts the SPACE-M adjustments as standards, the PC position estimates from the CCRS Bundle Adjustment are liable to be in error by 5-10m in the horizontal and 8m in the vertical, quantities which are greater than the uncertainty of the standard. However, the double differences agree to within the reliability of the standard.

Chapter 5

CAMERA ORIENTATION AND LASER RANGE

The x, y and z coordinates of the PC's having been analyzed, the remaining items in the auxiliary data file are the roll, pitch and heading angles of the camera and the laser range. Heading angle is measured about a vertical axis (clockwise from true north), pitch is measured about an axis perpendicular to the vertical plane containing the camera fore-aft (x) axis (positive when aircraft is climbing), and roll is measured about the camera x-axis (positive clockwise when looking forward). They are therefore different from the angles kappa, omega and phi. The laser altimeter was fixed to the aircraft about 1m from the camera, and its beam was supposedly aligned parallel to the principal axis of the camera.

5.1 Computation of Orientation Angles from SPACE-M Output

The output of the SPACE-M adjustment included the coordinates of the ground point corresponding to the principal point of the image. This point can be referred to as the quasi nadir point (QNP) or the ground principal point (GPP); it corresponds to the nadir point if the principal axis is perfectly vertical. As the SPACE-M output also gave the coordinates of the perspective centre (PC), it provided all information required to determine the length and direction of the vector from the PC to the QNP. This length should be equal to the range measured by the laser.

The length is computed by taking the mean perspective centre coordinates (x_p, y_p, z_p) and the QNP coordinates (x_c, y_c, z_c) . Putting $\Delta x = x_p - x_c$, $\Delta y = y_p - y_c$, $\Delta z = z_p - z_c$, then the length = $(\Delta x^2 + \Delta y^2 + \Delta z^2)^{1/2}$.

Although the aforementioned coordinates can determine the direction of the line from PC to QNP, they are not enough to determine the heading, roll and pitch angles because they give no information on rotation of the camera about that line (the kappa angle). So further data are needed, namely certain image coordinates.

For most photographs, the image coordinates that are recorded include those of the QNP corresponding to the current PC (their values are close to zero) and also those of QNP's corresponding to up to four neighbouring PC's. Since the coordinates of the QNP's are known in both a ground-based system (from SPACE-M) and a camera-based system (x & y coordinates only, from the image coordinates), the ground-based coordinates of the PC's are known (from SPACE-M), and the transformation between the two systems is expressible in terms of orientation angles, it follows that there is enough information to determine these angles, plus laser range, from the photogrammetry alone.

As the photogrammetry is computed in UTM coordinates, but the heading given by the inertial system is relative to true north, the convergence of meridians must be considered. The computation of this convergence is described in Appendix B.

A transformation of coordinates between ground-based and camera-based systems can be expressed directly in terms of roll,

pitch and heading angles. This transformation is derived in Appendix C. The transformation can then be applied to specific vectors. One such vector is the one joining the perspective centre to the corresponding QNP. This vector has components $(0,0,R)$ in the camera-based system, where R is the laser range. Its components in the ground-based system are obtained from the SPACE-M output. Other such vectors are those joining the current QNP to neighbouring QNP's. Components of these inter-QNP vectors in the ground-based system are obtained from the SPACE-M output, and can be transformed into the camera-based system. One can note that, in the camera coordinate system, the image vector is a perspective projection on to the x - y plane of a vector on the ground. Therefore the ratio between x and y components is the same for both ground and image vectors. (See Fig. 5.1)

In principle, one inter-QNP vector plus the vector from PC to QNP are enough to give the range and all orientation angles. In practice, more than one inter-QNP vector is available, giving a redundancy of data, so an optimization process is required.

A parametric least-squares process was formulated to perform the optimization, but first attempts with this least-squares approach were not successful. The process was non-linear, and so needed iterations, and also there were problems with convergence. At this point, another approach was tried, and found to work successfully.

Using the second approach, if the orientation is expressed in terms of the angles ϕ , ω and κ , instead of roll, pitch and heading, then it is found that ϕ and ω , plus range, can be

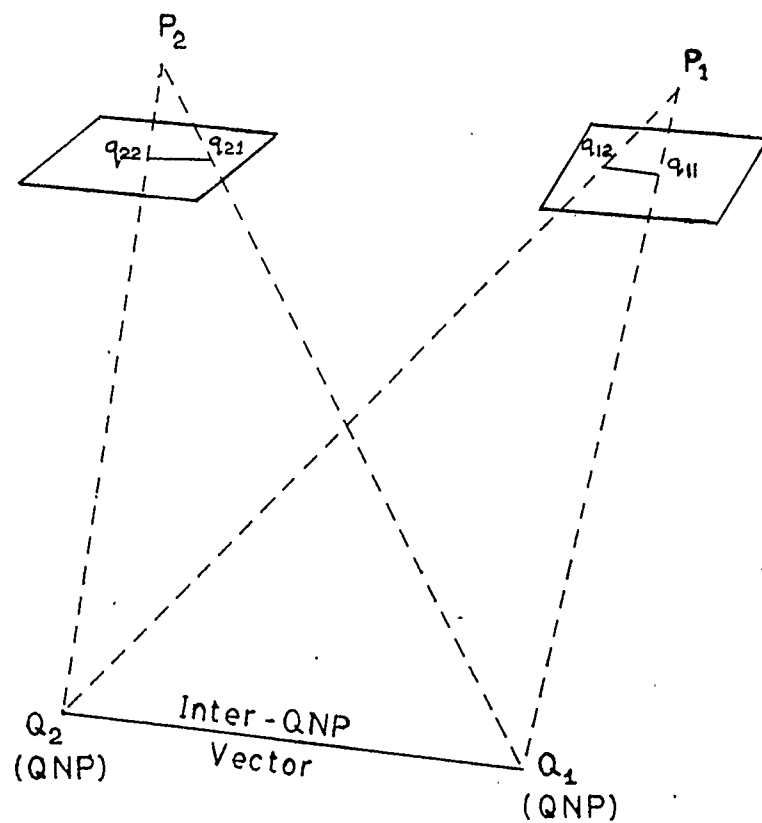


Fig. 5.1: Relation between Inter-QNP Vectors in Images
 $(q_{11} - q_{12}$ and $q_{21} - q_{22})$ and on ground $(Q_1 - Q_2)$

determined entirely from the vector from PC to QNP. Inter-QNP vectors are then required to determine κ subsequently. A separate estimate of κ is available from each inter-QNP vector, and so a "best estimate" of κ can be found from a weighted mean of these estimates. Roll, pitch and heading angles can then be found from ϕ , ω and κ . The mathematics of this process are given in Appendix D.

When there are three or more estimates of κ , it sometimes happens that most of these estimates are very close together, but one or more may differ significantly from the majority. One then has the option of rejecting such "outliers". In this analysis, results were considered both including and rejecting the outliers. In the latter case, an estimate was rejected if it differed from the mean value by more than 1.5 times the standard deviation of the set of estimates. The critical value of 1.5 standard deviations was chosen because it is large enough to avoid rejection in the case where there are only two estimates, and in practice was found to result in rejection of about 13% of the readings (65 out of 488).

The greatest change in estimate of h , the heading angle, due to outlier rejection was 0.7° ; the median value of the change was 0.008° and the mean 0.042° . Effects on roll and pitch were still smaller; the change in roll was generally about one hundredth, and in p around one fiftieth, of the change in h .

The determination of orientation angles so far described assumed that the QNP corresponded exactly to the principal point of the image. In practice, the image measurements were often made at

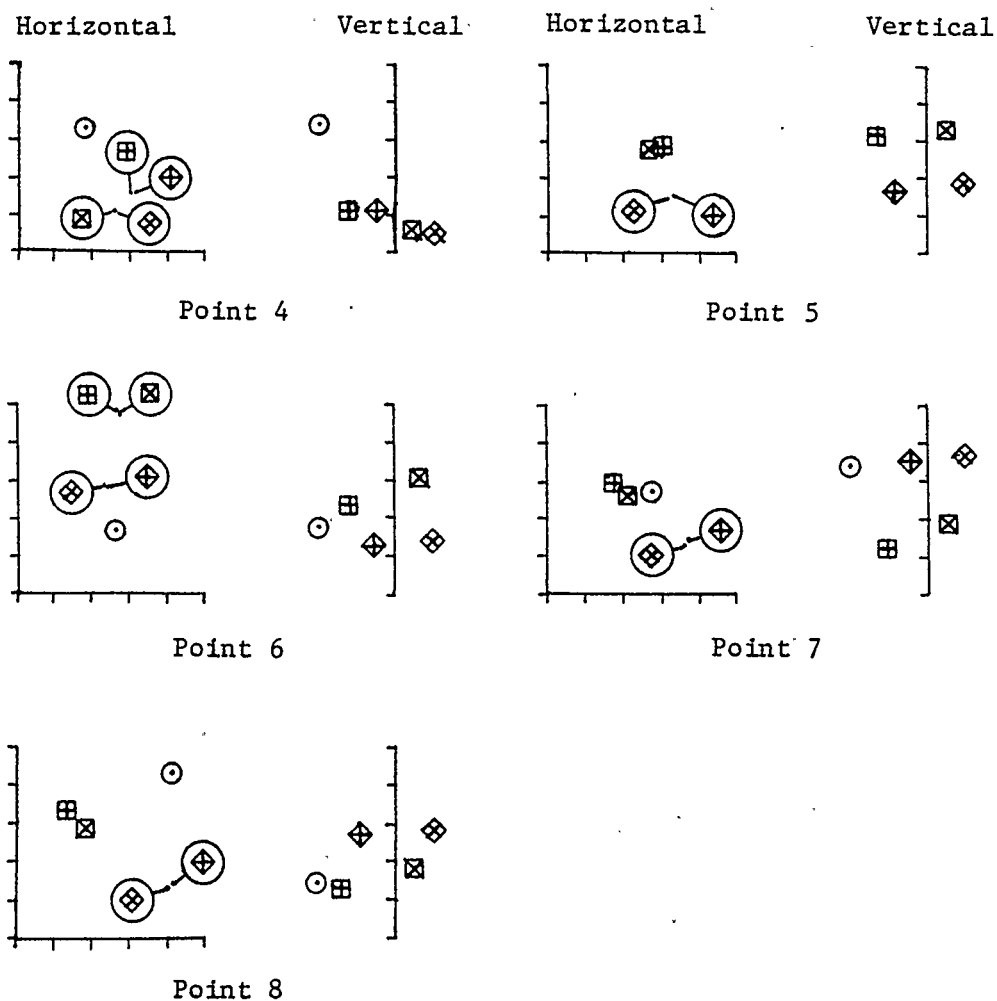
a point close to, but not exactly at, the principal point. The displacement of this image point from the principal point had RMS and maximum values of 0.0004mm and 0.18mm, corresponding to angular errors of 0.00015° and 0.067° . Compensation for these errors can be applied; it will be referred to as compensation for principal point offset. The mathematics of this process are described in Appendix E.

5.2 Comparison of Roll, Pitch, Heading and Range Values from Different Photogrammetric Adjustments.

Before the auxiliary and photogrammetric estimates of PC positions were compared in Chapter 4, the consistency of various photogrammetric estimates of these quantities was examined in Chapter 3. It is now appropriate to compare various photogrammetric estimates of the orientation angles, and of the positions of, and range to, the QNP, for the same sample of 10 points. The quantities to be compared in this chapter are summarized diagrammatically in Fig. 5.2.

QNP coordinates were obtained as output from all the four SPACE-M adjustments that used the new (autumn, 1985) data, but from only one of the bundle adjustments, viz. the University of Calgary one using the old data. The relative positions of the QNP estimates are plotted in Figs. 5.3 and 5.4 in the same way as the PC position estimates were displayed in Figs. 3.1 and 3.2.

The closeness of the various QNP position estimates contrasts strongly with that of the PC estimates in two ways. In the horizontal, the spread between position estimates is much



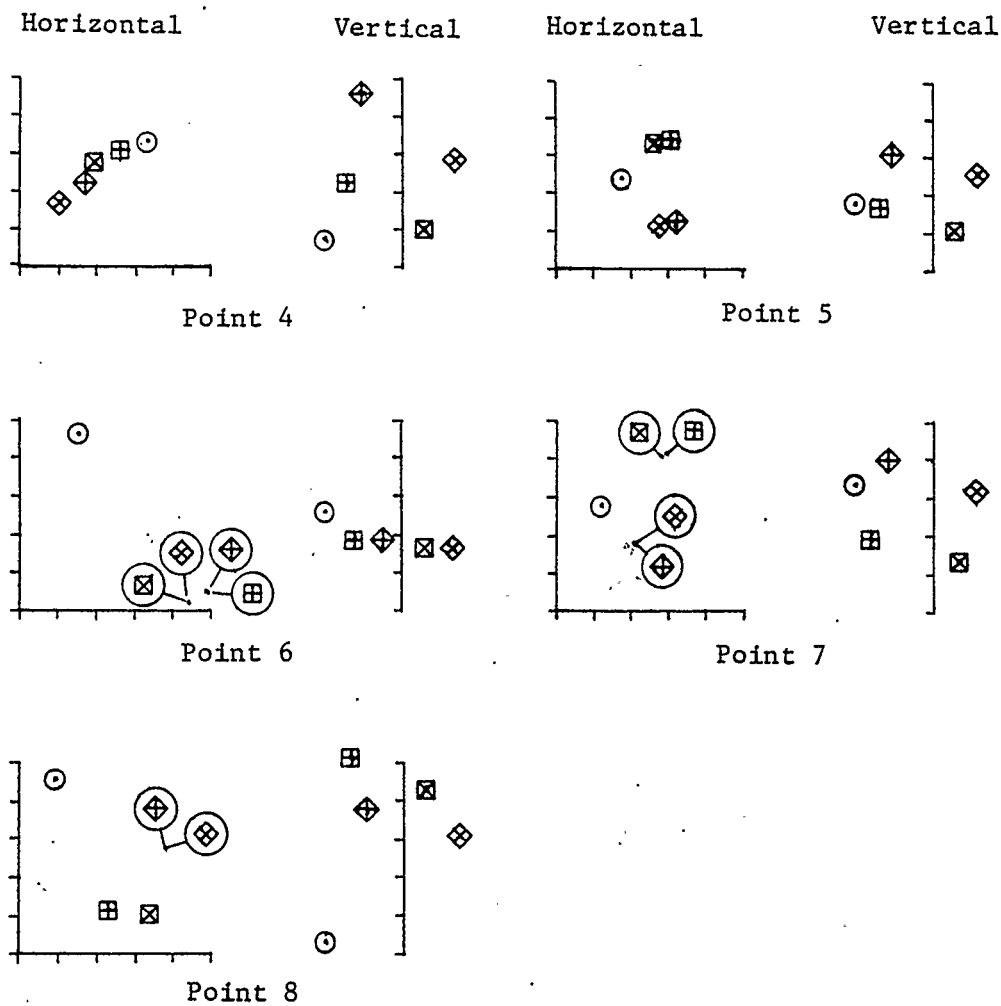
Horizontal: Scale marks every 0.5m

Vertical: Scale marks every 2m

	BUNDLE	SPACE-M		
		RPI	RPE	
OLD DATA	⊙			
NEW DATA		⊞	⊞	With Lakes
		⊞	⊞	Without Lakes

RPI/RPE - Rejected Points Included/Excluded

Fig. 5.3: Spatial Line 4 - QNP Position Estimates from Different Photogrammetric Adjustments



Horizontal: Scale marks every 0.5m

Vertical: Scale marks every 2m

	BUNDLE	SPACE-M		
		RPI	RPE	
OLD DATA	⊙			
NEW DATA		⊠	⊞	With Lakes
		⊡	⊞	Without Lakes

RPI/RPE - Rejected Points Included/Excluded

Fig. 5.4: Spatial Line 5 - QNP Position Estimates from Different Photogrammetric Adjustments

smaller, by a factor of about 10; all estimates lie within 6m of each other. In the vertical, the spread is about 10m, which is smaller than that for the PC's by a factor of about 2. Thus, whereas there is more spread in the horizontal than the vertical for the PC's, the opposite is true for the QNP's. In the case of the estimates from SPACE-M, it appears that inclusion or exclusion of the lake-level restraint has less effect than the inclusion or exclusion of points that were rejected during the adjustment.

Proceeding now to discuss the orientation angles and range from PC to QNP, in the case of SPACE-M adjustments these quantities were obtained from the ground-based coordinates of the PC and QNP, plus the image coordinates, as described in Section 5.1. This analysis was performed only for adjustments using the lake-level constraint, but with the following variations:

- (a) including points rejected in the adjustment,
without kappa outlier rejection,
- (b) including points rejected in the adjustment,
with kappa outlier rejection,
- (c) excluding points rejected in the adjustment,
with kappa outlier rejection,
- (d) as for (c), with compensation for principal point offset.

In the case of the bundle adjustments, the orientation angles formed a standard part of the output; in the University of Calgary bundle adjustment, they were in terms of ϕ , ω and κ , and these were converted to roll, pitch and heading angles by the process described in Appendix D, whereas they were given directly

as roll, pitch and heading angles in the data file for the CCRS adjustment.

The variation between these values is illustrated in Figs. 5.5 and 5.6. It is generally about 0.05° , sometimes 0.1° . This spread is notably exceeded at point 8 in line 4, where there was also a large spread in the PC position estimates. The original large spread in heading angle estimates at point 7 of line 4 (point 23 of line 2 chronologically) was eliminated by the refinements introduced later, as described in Section 5.1. Range measurements, from PC to QNP, have a spread which is typically about 4m.

5.3 Comparison of Photogrammetric and Auxiliary Estimates of Range and Orientation Angles

At this point, there exist both photogrammetric and auxiliary estimates of roll, pitch and heading angles, and of range to the ground, as functions of time. Photogrammetric estimates from SPACE-M correspond to the cases (a) to (d) mentioned in Section 5.2. The following discussion will refer initially to cases (a) and (b), and subsequently to cases (c) and (d). Estimates from the CCRS bundle adjustment will also be considered. Variations of these four measured quantities with time, and of the discrepancies between the photogrammetric and auxiliary estimates, are best understood by means of graphs. Henceforth flight lines will be numbered chronologically.

First, the graphs of each of the four parameters, determined by the two different methods, are considered, plotted as

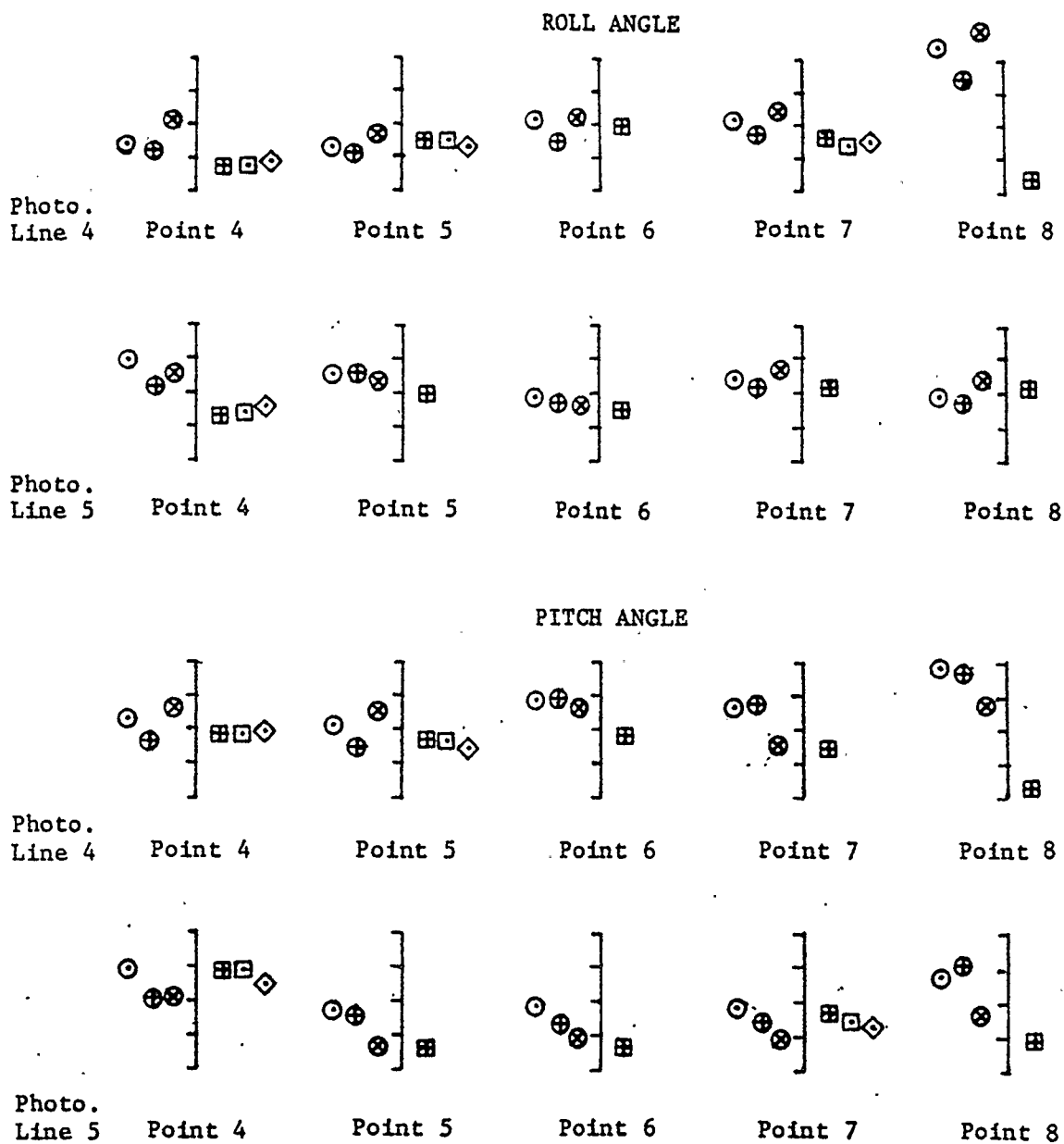
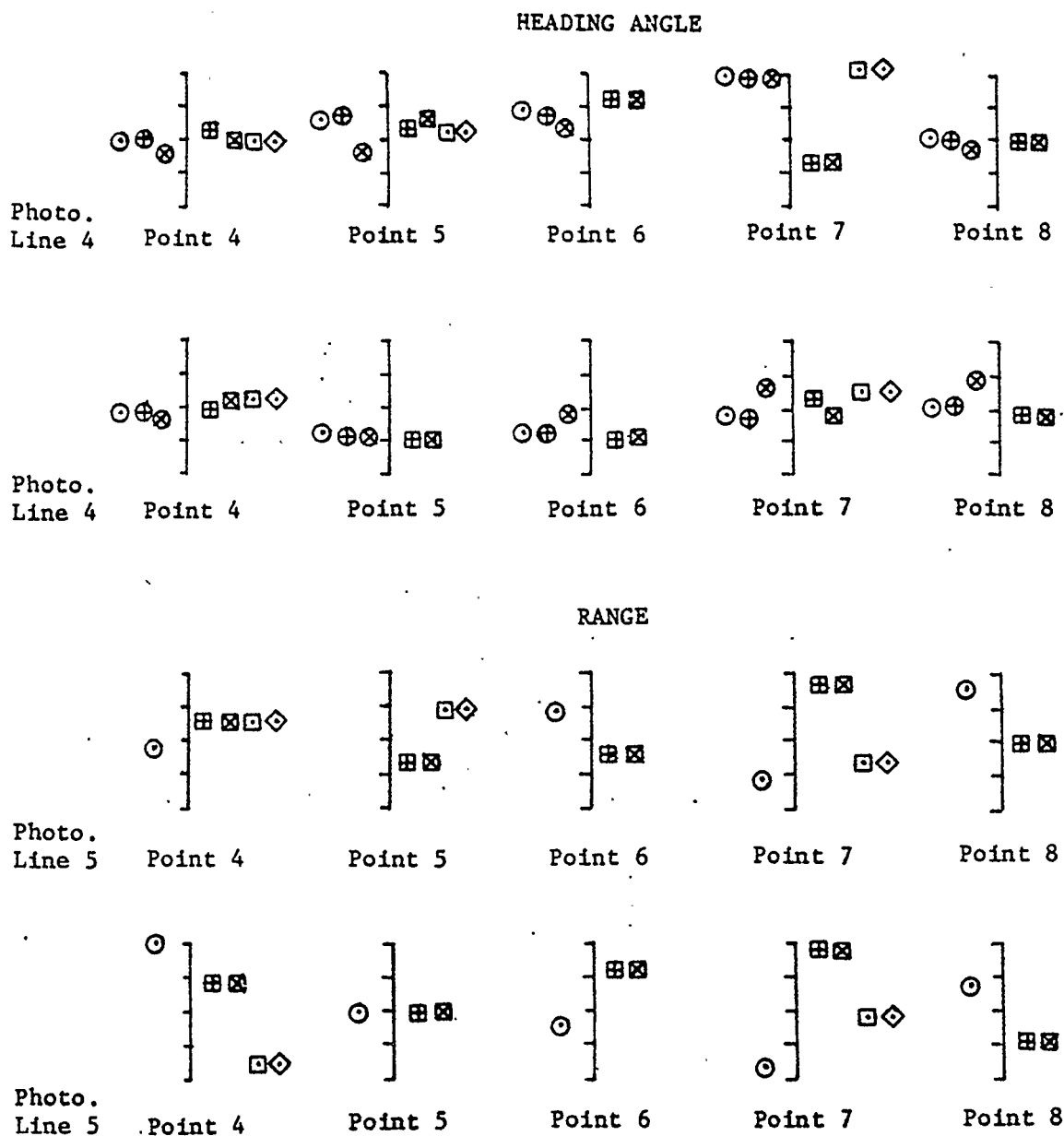


Fig. 5.5

Plots of Camera Orientation Estimates from
Different Photogrammetric Adjustments



Angle: Scale marks every 0.05 deg

Range: Scale marks every 2m

	BUNDLE	SPACE-M	
OLD DATA	⊙	⊞	Case (a)
NEW DATA	⊕	⊠	Case (b)
		⊡	Case (c)
CCRS	⊗	⊢	Case (d)

Fig. 5.6
Plots of Camera Orientation Estimates from
Different Photogrammetric Adjustments

functions of time. Samples of these graphs appear in Figs. J.1 to J.4 of Appendix J.

For all parameters, the values from both photogrammetric and auxiliary data undergo essentially the same changes with time. In the cases of the roll, pitch and heading angles, there is a definite bias of auxiliary values relative to photogrammetric ones. The values of this bias change from one flight line to another. In the case of roll, the bias changes fairly steadily from 2° in (chronological) flight line no. 1 to 1.4° in flight line no. 5. In the case of pitch, it alternates between about -1° for odd-numbered flight lines (N to S) and -2° for even-numbered flight lines (S to N). In the case of heading, it alternates between positive for odd-numbered lines (N to S) and negative for even-numbered lines (S to N); the bias has a magnitude of 1.5° - 2° for the first two lines, but its magnitude decreases to less than 0.2° at the last (fifth) line.

There is no evident bias in range values.

Because of these biases, the direct use of auxiliary values of these angles in a photogrammetric adjustment is not recommended, unless the values of the biases can be determined adequately, as by updates of the inertial system, for example.

One interesting feature is a regular oscillation, of period slightly over one minute, in the pitch angle in all flight lines. It occurs in both photogrammetric and auxiliary graphs, and is therefore probably a physical reality in the flight of the aircraft, most likely a feature of the aircraft control system.

Second, the graphs which show the difference between

photogrammetric and auxiliary values as functions of time are considered. Samples are shown in Figs. J.5 to J.8. Regression lines are plotted on the same axes, to represent any general bias and drift which may be present. The effect of the rejection of kappa outliers is illustrated in Fig. J.9.

In the case of range, the bias and its drift are both very small compared to random fluctuations. The residual random deviations from the regression lines are between 65m and 90m on the five lines. Since this is much greater than the error that normally occurs in photogrammetry, it appears at this point that the laser range values are of no help in a photogrammetric adjustment.

For the heading angle, in some flight lines (1 and 2) there appears to be a drift of about $0.03^{\circ}/\text{min}$, while in others (3, 4 and 5) it is less than $0.01^{\circ}/\text{min}$. The larger values in lines 1 and 2 each appear to be due to two anomalous values which were not eliminated by outlier rejection because of insufficient redundancy. These anomalous values are at points 3 & 15 in (chronological) flight line no.1, and points 1 & 23 in flight line no.2. The ranges in photogrammetric estimates of at these four points are 1.189° , 0.896° , 1.328° and 0.454° respectively. As the graphs of heading against time are smoother for auxiliary than photogrammetric values, it is probably the photogrammetric estimates which are faulty. For lines 3, 4 and 5, the RMS (random) deviation from the regression line is about 0.03° .

In the case of roll and pitch angles, within each flight line there appears to be a slight drift towards a positive bias

of the auxiliary value; this drift has a value of about 0.03° /min for pitch and 0.008° /min for roll. RMS random deviations from the regression line are around 0.05° or less.

Third, one can consider the changes (increments) in the values of the parameters between one perspective centre and the next. These quantities cannot be expressed so specifically as functions of time, as they are each linked to a time interval. Correlation coefficients between photogrammetric and auxiliary estimates were calculated. Here, the roll angle gives the best result, with correlation coefficients of 0.999 on three flight lines, 0.998 on another and on all lines combined, and 0.992 in the remaining case. For pitch, correlation coefficients vary from 0.949 to 0.995, and for heading from 0.845 to 0.996 (though 0.985 is the lowest value that occurs in lines 3 to 5).

From another point of view, one can consider the differences in the inter-station increments, i.e. the photogrammetric minus the auxiliary value. In Table 5.1 are summarized the statistical parameters describing these "double differences", namely the mean, standard deviation and root mean square value, for each flight line and for all flight lines together. Note that a non-zero mean value for any of these increments is equivalent to a drift in the original measurement.

Drawing attention to the important features of this table, it appears that the laser ranges are unreliable by something of the order of 100m. This matter will be discussed further in Chapter 7.

On the whole, the double differences in all three angles are

TABLE 5.1

DOUBLE DIFFERENCES OF ORIENTATION PARAMETERS AND RANGE
PHOTOGRAMMETRIC MINUS AUXILIARY: Case (b)

RANGE (metres)

Flight Line		Mean	S.D.	RMS Value	Abs. Max.	No. of Points
Chr.	Spat.					
1	1	-14.0	124.9	125.6	270.6	22
2	4	-10.9	101.2	101.8	238.7	26
3	2	9.9	141.4	141.8	289.1	22
4	5	-1.1	121.8	121.8	345.4	30
5	3	-0.9	84.0	84.0	192.1	27
All		-3.4	115.5	115.5	345.4	127

ROLL (degrees)

Flight Line		Mean	S.D.	RMS Value	Abs. Max.	No. of Points
Chr.	Spat.					
1	1	-0.0034	0.0344	0.0345	0.0871	22
2	4	0.0004	0.0569	0.0569	0.1827	26
3	2	-0.0042	0.0279	0.0282	0.0590	22
4	5	-0.0002	0.0226	0.0226	0.0556	30
5	3	-0.0050	0.0270	0.0275	0.0770	27
All		-0.0023	0.0358	0.0359	0.1827	127

PITCH (degrees)

Flight Line		Mean	S.D.	RMS Value	Abs. Max.	No. of Points
Chr.	Spat.					
1	1	-0.0050	0.0411	0.0414	0.0948	22
2	4	-0.0074	0.0398	0.0405	0.1135	26
3	2	-0.0096	0.0310	0.0325	0.0731	22
4	5	-0.0054	0.0403	0.0407	0.0750	30
5	3	-0.0078	0.0405	0.0413	0.0821	27
All		-0.0070	0.0390	0.0396	0.1135	127

HEADING (degrees)

Flight Line		Mean	S.D.	RMS Value	Abs. Max.	No. of Points
Chr.	Spat.					
1	1	-0.0201	0.1323	0.1338	0.4950	22
2	4	-0.0159	0.1087	0.1099	0.4955	26
3	2	0.0017	0.0379	0.0379	0.0850	22
4	5	0.0006	0.0294	0.0294	0.0588	30
5	3	0.0042	0.0297	0.0300	0.0585	27
All		-0.0054	0.0787	0.0789	0.4955	127

less than 0.04° in their RMS values. The main exceptions are the heading angles in (chronological/auxiliary) flight lines 1 & 2, which are probably due to the anomalous values mentioned earlier. (Chronological) flight line 2 also has an exceptionally high RMS value for roll. Since this line has the greatest "maximum" value for all three angles, it is probable that the results are affected by a significant outlier value.

Recalling the evaluation of accuracy of the photogrammetry in Chapter 3, it was seen there that at some points in (chronological) line 2, the two estimates of the positions of the PC's differ by more than 60m. These estimates differ by about 53m in the x-direction and 30m in the y-direction, and at a flying height of about 8000m above ground, such uncertainties in position could produce corresponding uncertainties of 0.4° and 0.2° in the roll and pitch angles respectively.

Ignoring the flight lines that have these anomalous values, the RMS values of differences in the two PC positions given by SPACE-M are of the order of 5m, corresponding to uncertainties of 0.04° in the roll and pitch angles. Thus it appears that the double differences of orientation angles are no greater than the effect of uncertainty in the photogrammetry that is used as the standard of comparison.

Cases (c) and (d), as defined in Section 5.2, can now be considered, with respect to the orientation angles only. For comparison, the main statistics for cases (a) and (b) are presented in Tables H.1 to H.4, and the corresponding ones for cases (c) and (d) in Tables H.5 to H.8 of Appendix H; the main features,

regardless of flight line, are summarized in Tables 5.2 and 5.3.

In case (c), one immediate effect of the exclusion of the "rejected" points is the exclusion of three of the four large values of kappa discrepancy mentioned earlier. This fact supports the hypothesis that four large discrepancies were due to errors in the photogrammetry, rather than in the auxiliary systems. The remaining large discrepancy was at point 1 in flight line no. 2. Here, the estimate of κ that differed by about 0.5° from the auxiliary value was now arbitrarily rejected on the basis of inspection.

The improvement in the heading discrepancy in the double differences is immediately obvious from a comparison of Tables H.2 and H.6, or cases (b) and (c) of Table 5.3. The greatest (absolute) value of heading discrepancy was reduced from about 0.5° to less than 0.09° , and the RMS discrepancy for all 5 lines from 0.08° to 0.03° . Improvements of a lesser degree were evident in the double differences for pitch and roll angles too. Changes in the values for single differences were not so evident, because they were dominated by the biases.

The effect of principal point offset compensation (applied in case (d)) can be seen by comparing Tables H.6 and H.8, or cases (c) and (d) of Table 5.3. The effect on heading is negligible. There is some improvement in the mean and RMS values of roll and pitch, but this improvement is only about one tenth of the magnitude of the remaining "noise" which is indicated by the significant excess of RMS over mean values.

The CCRS Bundle Adjustment gives even better agreement than

Table 5.2

Single Differences of Orientation Angles (deg)
All flight lines combined

Auxiliary Systems and Photogrammetric Adjustments

Roll

Case	Pts.	Mean	RMS	Max.	Min.
(a)	135	-1.729	1.740	-1.414	-2.098
(b)	135	-1.729	1.740	-1.414	-2.098
(c)	93	-1.719	1.728	-1.415	-2.091
(d)	93	-1.721	1.731	-1.423	-2.096
(e)	138	-1.712	1.722	-1.446	-2.022

Pitch

Case	Pts.	Mean	RMS	Max.	Min.
(a)	135	1.537	1.609	2.268	0.849
(b)	135	1.536	1.609	2.268	0.849
(c)	93	1.549	1.624	2.260	0.850
(d)	93	1.549	1.623	2.268	0.867
(e)	138	1.538	1.612	2.134	0.911

Heading

Case	Pts.	Mean	RMS	Max.	Min.
(a)	135	0.097	1.245	2.620	-1.999
(b)	135	0.087	1.247	2.620	-1.999
(c)	93	0.111	1.217	2.217	-1.560
(d)	93	0.111	1.217	2.217	-1.559
(e)	138	0.074	1.249	2.154	-1.505

Key to cases: (a) SPACE-M including rejected points,
without kappa outlier rejection
(b) SPACE-M including rejected points,
with kappa outlier rejection
(c) SPACE-M excluding rejected points,
with kappa outlier rejection
(d) As for (c) with principal point offset
compensation
(e) CCRS Bundle Adjustment

Table 5.3

Double Differences of Orientation Angles (deg)
All flight lines combined

Auxiliary Systems and Photogrammetric Adjustments

Roll

Case	Pts.	Mean	RMS	Max.	Min.
(a)	127	-0.002	0.036	0.183	-0.181
(b)	127	-0.002	0.036	0.183	-0.181
(c)	59	-0.004	0.024	0.074	-0.059
(d)	59	-0.002	0.022	0.078	-0.046
(e)	133	-0.001	0.008	0.018	-0.024

Pitch

Case	Pts.	Mean	RMS	Max.	Min.
(a)	127	-0.007	0.040	0.113	-0.102
(b)	127	-0.007	0.039	0.113	-0.102
(c)	59	-0.008	0.028	0.094	-0.054
(d)	59	-0.005	0.025	0.102	-0.059
(e)	133	-0.001	0.007	0.016	-0.019

Heading

Case	Pts.	Mean	RMS	Max.	Min.
(a)	127	-0.006	0.130	0.743	-0.699
(b)	127	-0.005	0.079	0.270	-0.496
(c)	59	0.001	0.032	0.089	-0.061
(d)	59	0.001	0.032	0.090	-0.061
(e)	133	0.000	0.007	0.021	-0.020

Key to cases: (a) SPACE-M including rejected points,
without kappa outlier rejection
(b) SPACE-M including rejected points,
with kappa outlier rejection
(c) SPACE-M excluding rejected points,
with kappa outlier rejection
(d) As for (c) with principal point offset
compensation
(e) CCRS Bundle Adjustment

SPACE-M with the auxiliary values. This is not surprising, as this adjustment used inertial data in its input; evidently they were very constraining. Table H.9 (single differences) still shows discrepancies due to biases in the auxiliary system, but Table H.10 (double differences) shows even better agreement than case (d) of SPACE-M, with RMS discrepancies generally less than 0.01° , and an occasional discrepancy of 0.02° , indicated by the "Max." and "Min." columns.

Comparing the contents of Tables H.1 to H.10 with those of Figs. 5.2 to 5.5, then, it appears that the double differences, indicating changes in orientation angles between successive camera stations, are of about half the size of the uncertainties in these angles as indicated by the discrepancies between different adjustments. Therefore these double differences are of sufficient accuracy to be used as auxiliary input to an adjustment. The inertial results may indeed be better than the photogrammetry.

This is not true of the laser ranges hitherto obtained, however, and the ranges will be examined in more detail in Chapter 7.

5.4 Comparison of Orientation Angles as given by

CCRS Bundle and SPACE-M Adjustments

Tables H.11 to H.18 of Appendix H give details of the discrepancies between orientation angle estimates from the CCRS Bundle Adjustment and SPACE-M, and they are summarized, irrespective of flight lines, in Tables 5.4 and 5.5.

Lines (e) of Table 5.3, together with lines (a), (b) and (c) of Table 5.5, indicate that the orientation angles in the CCRS

Table 5.4

Single Differences of Orientation Angles (deg)
All flight lines combined

CCRS Bundle and other Photogrammetric Adjustments

Roll

Case	Pts.	Mean	RMS	Max.	Min.
(a)	135	-0.022	0.052	0.081	-0.234
(b)	135	-0.022	0.052	0.081	-0.234
(c)	93	-0.020	0.045	0.071	-0.121
(d)	93	-0.022	0.046	0.069	-0.121

Pitch

Case	Pts.	Mean	RMS	Max.	Min.
(a)	135	-0.003	0.050	0.149	-0.157
(b)	135	-0.003	0.050	0.149	-0.157
(c)	93	-0.001	0.051	0.148	-0.157
(d)	93	-0.001	0.052	0.145	-0.158

Heading

Case	Pts.	Mean	RMS	Max.	Min.
(a)	135	0.015	0.104	0.737	-0.520
(b)	135	0.005	0.071	0.470	-0.520
(c)	93	0.004	0.028	0.078	-0.055
(d)	93	0.004	0.028	0.078	-0.054

Key to cases: (a) SPACE-M including rejected points,
without kappa outlier rejection
(b) SPACE-M including rejected points,
with kappa outlier rejection
(c) SPACE-M excluding rejected points,
with kappa outlier rejection
(d) As for (c) with principal point offset
compensation

Table 5.5

Double Differences of Orientation Angles (deg)
All flight lines combined

CCRS Bundle and other Photogrammetric Adjustments

Roll

Case	Pts.	Mean	RMS	Max.	Min.
(a)	127	-0.002	0.037	0.182	-0.170
(b)	127	-0.002	0.037	0.182	-0.170
(c)	59	-0.003	0.027	0.081	-0.056
(d)	59	-0.001	0.026	0.085	-0.053

Pitch

Case	Pts.	Mean	RMS	Max.	Min.
(a)	127	-0.006	0.039	0.115	-0.092
(b)	127	-0.006	0.039	0.115	-0.091
(c)	59	-0.007	0.029	0.097	-0.064
(d)	59	-0.004	0.027	0.106	-0.067

Heading

Case	Pts.	Mean	RMS	Max.	Min.
(a)	127	-0.006	0.131	0.754	-0.698
(b)	127	-0.006	0.081	0.264	-0.516
(c)	59	0.002	0.034	0.090	-0.068
(d)	59	0.002	0.034	0.091	-0.068

Key to cases: (a) SPACE-M including rejected points,
without kappa outlier rejection
(b) SPACE-M including rejected points,
with kappa outlier rejection
(c) SPACE-M excluding rejected points,
with kappa outlier rejection
(d) As for (c) with principal point offset
compensation

Bundle Adjustment are much closer to the inertial values (with bias removed) than to the photogrammetric values from SPACE-M, and this suggests that inertial orientation angles carried a significant weight in the bundle adjustment.

The values in the tables show that, for the best photogrammetric data (cases (c) and (d)), the two sets of values agree within about 0.003° , or 10 arc seconds, except in the absolute values of roll angle. This accuracy is roughly equal to the variability that is evident in Figs. 5.4 and 5.5, and satisfies the requirements mentioned by Masry (1977).

The larger difference in the absolute values of roll angle could be a consequence of different methods that were used to link the strips in the two types of adjustment.

Chapter 6

COORDINATE-INDEPENDENT MEASURES OF ORIENTATION CHANGES

In Chapter 5, the orientation angles that were considered were all dependent on a certain coordinate system. Moreover, as there were biases in the orientation angles, it is probable that the cartesian coordinate axes used by the auxiliary and photogrammetric systems were not exactly parallel. In such a case, the roll, pitch and heading angles measured in the two systems would not correspond exactly (though the errors in double differences resulting from a constant misalignment of less than 2° would be insignificant).

This problem can be avoided by considering orientation parameters that are invariant with respect to rotation of coordinate axes. One such parameter is the angle between principal axes of the camera at two consecutive camera stations. As this angle is unrelated to any coordinate system, only its magnitude is relevant, and it would be meaningless to give it a sign.

6.1 Computation of Principal Axis Direction Change

To determine this angle, the principal axes are considered as unit vectors. The cosine of the desired angle is given by the scalar (dot) product of the two vectors, while the sine is given by the magnitude of the vector (cross) product. As the angle between the vectors is normally less than 3° , it can be determined more accurately from its sine than its cosine.

If, in equation (C1) of Appendix C, $[x_1 \ y_1 \ z_1]^T$ is replaced by $[0 \ 0 \ 1]^T$, a unit vector parallel to the principal axis, then it follows that

$$x_1 = \sin r \cos h - \cos r \sin p \sin h$$

$$y_1 = -\sin r \sin h - \cos r \sin p \cos h$$

$$z_1 = \cos r \cos p$$

One can compute the components of this vector $[x_1 \ y_1 \ z_1]^T$ at one camera station, and the corresponding vector $[x_2 \ y_2 \ z_2]^T$ at the next camera station.

The three components of their cross product are then

$$x_3 = y_1 z_2 - z_1 y_2$$

$$y_3 = z_1 x_2 - x_1 z_2$$

$$z_3 = x_1 y_2 - y_1 x_2$$

and the magnitude of this cross-product vector is

$$(x_3^2 + y_3^2 + z_3^2)^{1/2},$$

which is the sine of the angle between the vectors.

There are alternative methods of computation for situations where roll, pitch and heading values are not directly available.

For a bundle adjustment, x_1 , y_1 and z_1 can be calculated from ϕ , ω and κ , using equation (D2) of Appendix D. In this case,

$$x_1 = \sin \phi$$

$$y_1 = -\sin \omega \cos \phi$$

$$z_1 = \cos \omega \cos \phi$$

In terms of the coordinates of the PC and the QNP, as provided by a SPACE-M adjustment,

$$x_1 = \Delta x/R$$

$$y_1 = \Delta y/R$$

$$z_1 = \Delta z/R,$$

where $\Delta x = x_p - x_q$, x_p and x_q are the x-coordinates of the PC and QNP in a ground-based coordinate system, Δy and Δz are defined similarly, and $R = (\Delta x^2 + \Delta y^2 + \Delta z^2)^{1/2}$.

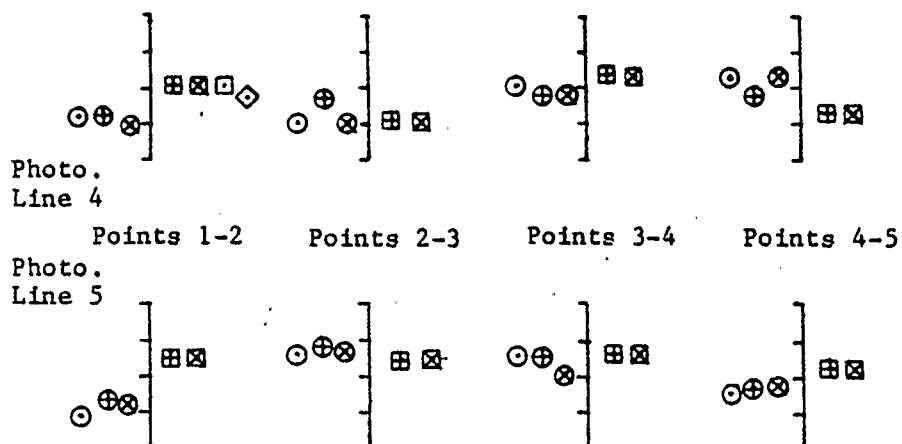
6.2 Comparison between Photogrammetric Determinations of Principal Axis Direction Change

For the region covered by the University of Calgary bundle adjustment, the changes in direction of the principal axis between consecutive camera stations were calculated for the four cases referred to as (a), (b), (c) and (d) in Section 5.2, plus the three bundle adjustments. There was only one value for cases (c) and (d), as only one pair of adjacent points was left after exclusion of points rejected in the adjustment. The relative values of the direction changes are illustrated in Fig. 6.1. Their agreement is approximately as good as was the case for the orientation angles discussed in Section 5.2.

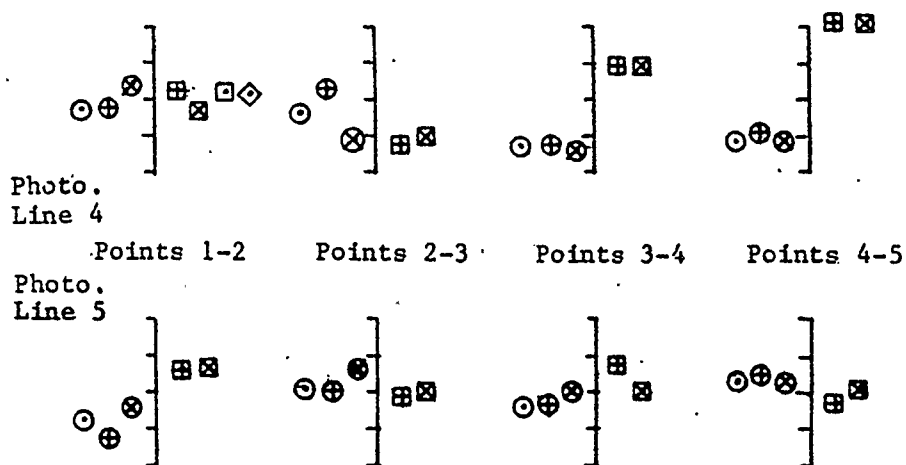
6.3 Comparison of Photogrammetric and Auxiliary Determinations of Principal Axis Direction Change

The changes in direction of the principal axis between consecutive camera stations were also calculated from the output of the inertial system. These changes were then compared with their counterparts from photogrammetry, and the discrepancies subjected to a simple statistical analysis. The results of this analysis

PRINCIPAL AXIS DIRECTION CHANGE



LONGITUDINAL AXIS DIRECTION CHANGE



Scale marks every 0.05 deg

	BUNDLE	SPACE-M	
OLD DATA	⊙	⊠	Case (a)
NEW DATA	⊕	⊡	Case (b)
		⊞	Case (c)
CCRS	⊗	◊	Case (d)

Fig 6.1

Plots of Camera Orientation Changes from
Different Photogrammetric Adjustments

are shown in Table 6.1.

The RMS values in this table are similar in magnitude to those in the corresponding tables for double differences mentioned in Section 5.3 (i.e. Tables H.2, H.4, H.6 and H.8).

Indeed, the formulas in Section 6.1 can be simplified for the case where r and p are small angles, using the approximations $r \approx \sin r$, $p \approx \sin p$, $\cos r \approx \cos p \approx 1$, neglecting products of sines of r and p , and assuming that h is the same at both camera stations. Under these conditions, the change of direction of the principal axis is approximately $((p_2 - p_1)^2 + (r_2 - r_1)^2)^{1/2}$, where r_1 , r_2 are the roll angles, and p_1 , p_2 are the pitch angles, at the two stations.

In the case of the CCRS Bundle Adjustment, which used inertial data as input, the agreement is really excellent, the RMS values of discrepancies being around 0.001° . As such values are what one would expect from computer round-off errors, it is clear that the inertial values played an important role in the adjustment.

6.4 Direction Change of the Longitudinal Axis

While the foregoing analysis treats the change of direction of a specific vector that is fixed with respect to the camera, it does not encompass all possible rotations of the camera, because it ignores rotations about that vector. Thus there remains one degree of rotational freedom that is undetected by that analysis, and so the change of direction of another vector can be considered independently. Such a vector could, for instance, be a unit

Table 6.1

Comparison of Changes in Principal Axis Direction (Deg.)

Auxiliary Systems and SPACE-M Variation (a)

Chr.Flight Line	No. of Points	Mean	RMS	Max.
1	22	0.027	0.038	0.103
2	26	0.030	0.047	0.181
3	22	0.021	0.029	0.074
4	30	0.029	0.035	0.068
5	27	0.019	0.029	0.085
All	127	0.026	0.036	0.181

Auxiliary Systems and SPACE-M Variation (b)

Chr.Flight Line	No. of Points	Mean	RMS	Max.
1	22	0.027	0.038	0.103
2	26	0.030	0.047	0.181
3	22	0.021	0.029	0.074
4	30	0.029	0.035	0.068
5	27	0.019	0.029	0.085
All	127	0.026	0.036	0.181

Auxiliary Systems and SPACE-M Variation (c)

Chr.Flight Line	No. of Points	Mean	RMS	Max.
1	10	0.020	0.030	0.079
2	11	0.018	0.023	0.051
3	10	0.025	0.032	0.068
4	17	0.024	0.030	0.059
5	11	0.020	0.025	0.050
All	59	0.022	0.028	0.079

Auxiliary Systems and SPACE-M Variation (d)

Chr.Flight Line	No. of Points	Mean	RMS	Max.
1	10	0.018	0.029	0.082
2	11	0.023	0.026	0.039
3	10	0.017	0.024	0.045
4	17	0.022	0.028	0.064
5	11	0.010	0.012	0.026
All	59	0.018	0.025	0.082

Auxiliary Systems and CCRS Bundle Adjustment

Chr.Flight Line	No. of Points	Mean	RMS	Max.
1	26	0.001	0.001	0.002
2	28	0.001	0.001	0.002
3	22	0.000	0.001	0.001
4	30	0.000	0.001	0.001
5	27	0.001	0.001	0.001
All	133	0.001	0.001	0.002

vector in the x-direction of the camera coordinate system. In this case, in Equation (C1), $[x_1 \ y_1 \ z_1]^T$ would be replaced by $[1 \ 0 \ 0]^T$, giving

$$x_1 = \cos p \sin h$$

$$y_1 = \cos p \cos h$$

$$z_1 = \sin p$$

in terms of pitch and heading, or

$$x_1 = \cos \phi \cos \kappa$$

$$y_1 = \cos \omega \sin \kappa + \sin \omega \sin \phi \cos \kappa$$

$$z_1 = \sin \omega \sin \kappa - \cos \omega \sin \phi \cos \kappa$$

in terms of ϕ , ω and κ .

The rest of the mathematics is identical to that described in Section 6.1.

Comparative photogrammetric estimates of the longitudinal axis direction change are also presented in Fig. 6.1. The discrepancies from the auxiliary estimates are shown in Table 6.2, and are generally similar in magnitude to, and slightly smaller than, those in Tables H.2, H.4, H.6 and H.8. Improvements in agreement are noticeable as one progresses from case (a) to case (b) etc.; these changes correspond to refinements such as rejection of outliers in the computation of kappa, and one can note here that when $r = p = 0$, or $\phi = \omega = 0$, then the direction change of the longitudinal axis is equal to the change in heading or kappa.

As was the case with the principal axis, there is excellent agreement in the case of the CCRS Bundle Adjustment.

Table 6.2

Comparison of Changes in Longitudinal Axis Direction (Deg.)

Auxiliary Systems and SPACE-M Variation (a)

Chr.Flight Line	No. of Points	Mean	RMS	Max.
1	22	0.056	0.102	0.369
2	26	0.043	0.085	0.363
3	22	0.043	0.067	0.199
4	30	0.041	0.065	0.246
5	27	0.059	0.127	0.611
A11	127	0.048	0.092	0.611

Auxiliary Systems and SPACE-M Variation (b)

Chr.Flight Line	No. of Points	Mean	RMS	Max.
1	22	0.058	0.108	0.369
2	26	0.045	0.085	0.363
3	22	0.025	0.032	0.082
4	30	0.026	0.033	0.080
5	27	0.030	0.036	0.068
A11	127	0.036	0.065	0.369

Auxiliary Systems and SPACE-M Variation (c)

Chr.Flight Line	No. of Points	Mean	RMS	Max.
1	10	0.022	0.032	0.084
2	11	0.020	0.025	0.049
3	10	0.027	0.038	0.089
4	17	0.020	0.025	0.045
5	11	0.028	0.034	0.056
A11	59	0.023	0.030	0.089

Auxiliary Systems and SPACE-M Variation (d)

Chr.Flight Line	No. of Points	Mean	RMS	Max.
1	10	0.024	0.035	0.093
2	11	0.019	0.022	0.038
3	10	0.028	0.037	0.091
4	17	0.019	0.023	0.045
5	11	0.024	0.030	0.056
A11	59	0.022	0.029	0.093

Auxiliary Systems and CCRS Bundle Adjustment

Chr.Flight Line	No. of Points	Mean	RMS	Max.
1	26	0.001	0.001	0.002
2	28	0.000	0.001	0.001
3	22	0.000	0.001	0.002
4	30	0.000	0.001	0.001
5	27	0.001	0.001	0.001
A11	133	0.000	0.001	0.002

6.5 Comparison of Principal and Longitudinal Axis Direction Changes from CCRS Bundle and SPACE-M Adjustments

Tables 6.3 and 6.4 show that the discrepancies between CCRS Bundle and SPACE-M values are almost identical to those between auxiliary and SPACE-M values. This is to be expected, in view of the near-equality of auxiliary and CCRS values.

6.6 Summary

To summarize this chapter, it appears that rotation-invariant parameters of orientation change from a SPACE-M adjustment differ from their inertially-derived equivalents by about as much as specific orientation angles do when any misalignment of coordinate axes is not more than 2 or 3 degrees; they would probably be more reliable in a case of large misalignment. For the CCRS bundle adjustment, the rotation-invariant parameters are far superior to the specific orientation angles in their agreement with the auxiliary data, probably because the bias and drift in the orientation angles were removed in that adjustment.

Table 6.3

Comparison of Changes in Principal Axis Direction (Degrees)

CCRS Bundle Adj. and SPACE-M Variation (a)

Chr.Flight Line	No. of Points	Mean	RMS	Max.
1	22	0.027	0.038	0.104
2	26	0.030	0.047	0.181
3	22	0.021	0.029	0.073
4	30	0.029	0.035	0.068
5	27	0.020	0.029	0.085
All	127	0.026	0.036	0.181

CCRS Bundle Adj. and SPACE-M Variation (b)

Chr.Flight Line	No. of Points	Mean	RMS	Max.
1	22	0.027	0.038	0.104
2	26	0.030	0.047	0.181
3	22	0.021	0.029	0.073
4	30	0.029	0.035	0.068
5	27	0.020	0.029	0.085
All	127	0.026	0.036	0.181

CCRS Bundle Adj. and SPACE-M Variation (c)

Chr.Flight Line	No. of Points	Mean	RMS	Max.
1	10	0.021	0.030	0.080
2	11	0.018	0.024	0.051
3	10	0.024	0.032	0.067
4	17	0.024	0.030	0.059
5	11	0.020	0.025	0.049
All	59	0.022	0.028	0.080

CCRS Bundle Adj. and SPACE-M Variation (d)

Chr.Flight Line	No. of Points	Mean	RMS	Max.
1	10	0.018	0.029	0.083
2	11	0.023	0.026	0.038
3	10	0.017	0.024	0.044
4	17	0.022	0.028	0.064
5	11	0.010	0.011	0.025
All	59	0.018	0.025	0.083

Table 6.4

Comparison of Changes in Longitudinal Axis Direction (Degrees)

CCRS Bundle Adj. and SPACE-M Variation (a)

Chr.Flight Line	No. of Points	Mean	RMS	Max.
1	22	0.056	0.102	0.370
2	26	0.043	0.085	0.362
3	22	0.043	0.067	0.199
4	30	0.040	0.065	0.245
5	27	0.059	0.127	0.610
All	127	0.048	0.092	0.610

CCRS Bundle Adj. and SPACE-M Variation (b)

Chr.Flight Line	No. of Points	Mean	RMS	Max.
1	22	0.058	0.108	0.370
2	26	0.045	0.085	0.362
3	22	0.025	0.032	0.080
4	30	0.026	0.033	0.080
5	27	0.030	0.036	0.069
All	127	0.036	0.065	0.370

CCRS Bundle Adj. and SPACE-M Variation (c)

Chr.Flight Line	No. of Points	Mean	RMS	Max.
1	10	0.022	0.032	0.085
2	11	0.020	0.025	0.050
3	10	0.027	0.037	0.087
4	17	0.020	0.025	0.044
5	11	0.028	0.034	0.055
All	59	0.023	0.030	0.087

CCRS Bundle Adj. and SPACE-M Variation (d)

Chr.Flight Line	No. of Points	Mean	RMS	Max.
1	10	0.024	0.035	0.093
2	11	0.019	0.022	0.039
3	10	0.028	0.037	0.089
4	17	0.019	0.023	0.044
5	11	0.024	0.030	0.055
All	59	0.022	0.029	0.093

Chapter 7

FURTHER STUDY OF LASER RANGE DATA

It is clear that the discrepancy between photogrammetric and laser ranges to the QNP is greater than both what one would expect from the laser specifications and what is acceptable for use in an adjustment, but that its bias is small compared with its random variation. Possible reasons for this include the following:

- (a) the laser ranger is intrinsically subject to random errors,
- (b) the range is being deduced from the wrong part of the return pulse,
- (c) when the ground surface is very irregular, with obstacles such as trees and boulders present, it is possible that the laser gives the range to the treetops, and the photogrammetry the range to the ground, or vice-versa,
- (d) the laser reading is not correctly synchronized with the photography,
- (e) the laser is not correctly aligned with the camera, and therefore the two ranges are not being measured to the same ground point.

7.1 Determination of Laser Beam Alignment

Reason (e) can be checked by finding the photogrammetric range to other points in the neighbourhood of the QNP, and

comparing it with the laser range. This check was made on several images, chosen such that they and their neighbours gave large discrepancies of varying sign between photogrammetric and laser ranges. A preliminary empirical check showed that the two ranges tended to agree better for a point in the image at which $x \approx 1\text{mm}$, $y \approx 3\text{mm}$. To try to locate this point accurately, a square grid of 81 points (9x9) was set up on 12 images; the grid had a mesh of 0.5mm (corresponding to an angle of about 0.2°), and occupied the square with corners at (0,0), (4,0), (4,4) and (0,4)mm. The ground coordinates of each grid point were found by photogrammetry, and the range calculated, using the perspective centre coordinates determined from the SPACE-M adjustment.

On a single image, one would expect to find an infinite number of points which are at a given range from the camera, lying on a "contour line" on the ground. However, the location of this "contour line" in the image should vary from one image to another, especially if the direction of slope of the terrain is different in every image. With a large sample of images, however, having a random distribution of terrain slope near the image centre, one would expect to find one point in the image at which the discrepancy tends to be smallest, if, in fact, misalignment is present.

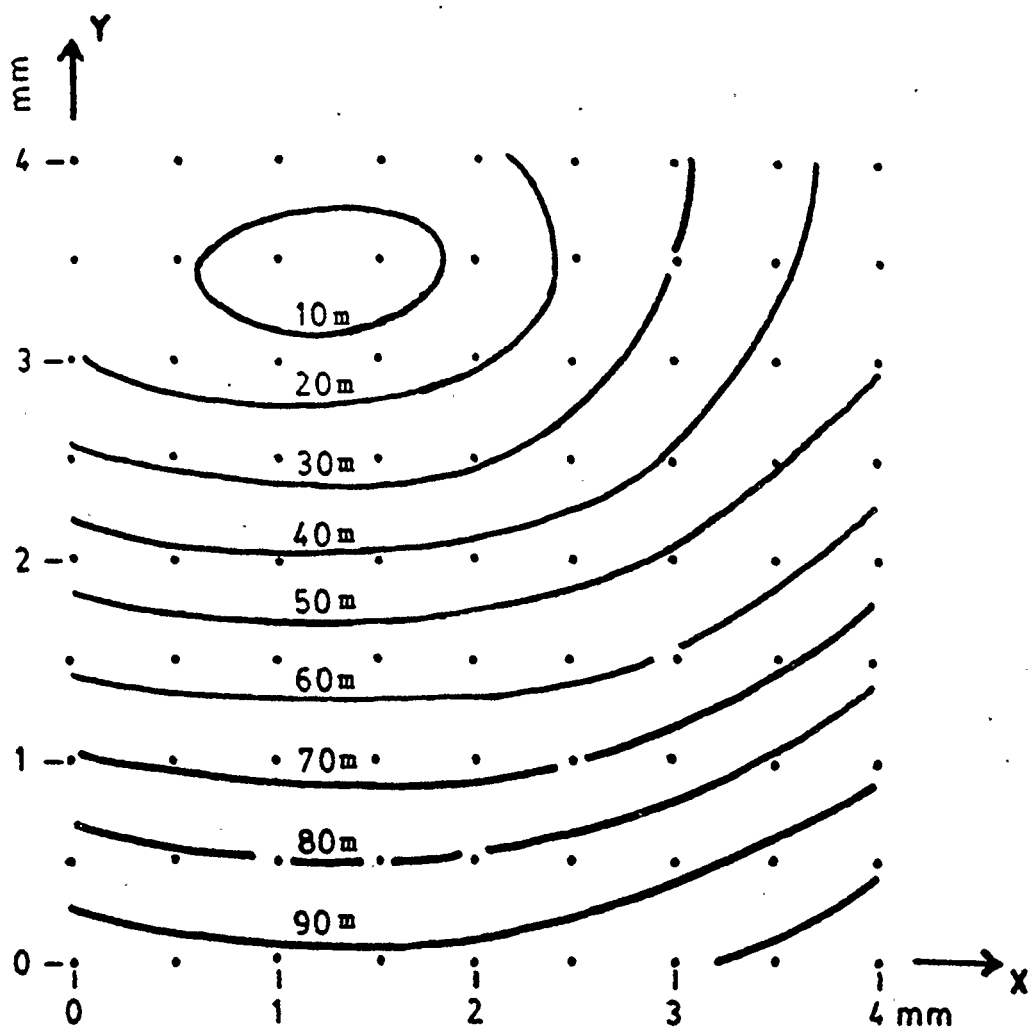
Therefore, for each of the 81 grid points, the root mean square discrepancy between photogrammetric and laser values was calculated for a set of images. Three different sets of images were considered: the set of all 12 images on which the grid measurements were made, the same set with two images rejected,

for which there were significant terrain irregularities, and the set of six images for which the photogrammetry was considered best.

When plots were made, showing the values of the r.m.s. discrepancy at all points in the grid, the smallest values (6.7m) were found to occur at the points (1.0, 3.5)mm and (1.5, 3.5)mm, indicating a minimum at $x=1.2\text{mm}$, $y=3.5\text{mm}$. This corresponds to a laser misalignment of about 1.4° . Isopleths of the root mean square values over the grid were plotted on diagrams such as Fig. 7.1 for each of the three data sets. The maximum value of the discrepancy at the point (1.0, 3.5)mm was 11.7m.

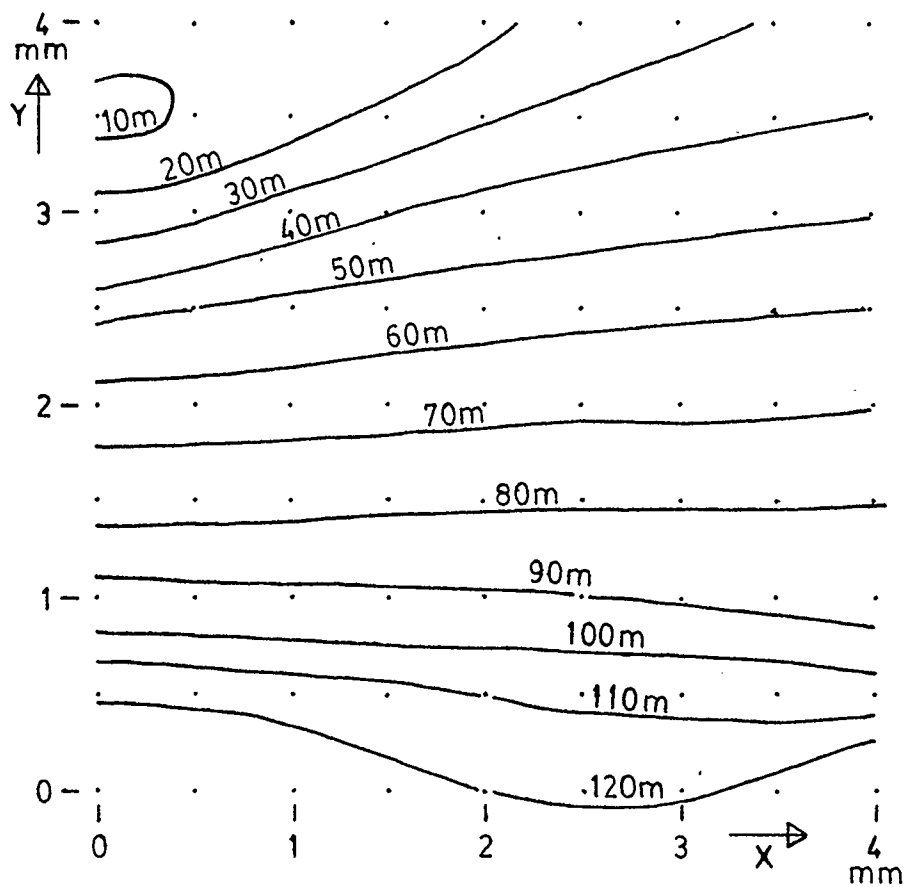
The elliptical shape of the isopleths in Fig. 7.1 is probably due to the nature of the topography, since the ridges and valleys were mainly parallel to the direction of flight (x-axis), and so the slope gradients were generally greater in the y-direction than the x-direction. If this test had been performed with a large sample of images over randomly-oriented topography, circular isopleths would have been expected.

So far, this analysis indicates that the laser was pointed in the direction corresponding to the coordinates (1.0, 3.5)mm in the photographic image. As the flight lines corresponding to the 12 images were both flown in the same direction, this result could include an effect of camera rotation to compensate for crabbing. So the test was repeated using data from two flight lines which were flown in the opposite direction, on which the crabbing effect would be the opposite. The resulting diagrams, such as Fig. 7.2, give a minimum discrepancy at about (0, 3.5)mm



Note: Values in mm are at image scale and
values in m are at ground scale.

Fig. 7.1: Sample of Isopleths of RMS Range Dis-
crepancy Values over the Measured Grid.



Note: Values in mm are at image scale and
values in m are at ground scale

Fig. 7.2: Sample of Isopleths of RMS Range Dis-
crepancy Values over the Measured Grid.

in the image. This point is at about the same distance from the image centre on the ground as the previously determined one. Hence, for zero rotation angle of the camera, the laser beam direction should correspond approximately to image coordinates (0.5, 3.5)mm.

An independent estimate of the laser beam misalignment was also made during a night flight over water. The camera shutter was held open, giving an image of a single spot corresponding to the ground or water point illuminated by the laser. Six photographs were taken in this way, the first at a flying height of 1500m and the rest at 450m above water. Table 7.1 gives the x and y coordinates of the spot on the image in mm.

Table 7.1

Coordinates (in mm) of laser spot on photographic image.
Night flight over water.

X	Y
0.7548	3.5736
0.5334	3.6101
0.5794	3.5892
0.5373	3.6037
0.5610	3.6083
0.5784	3.6078

It is evident that these values correspond closely to those obtained by the previous method. The "kappa" angle of the camera during this experiment is not known, but comparison with the previous values suggests that it is close to zero.

7.2 Detailed Laser Profiles over Water

Up to this point, the only laser data considered have been those readings corresponding to camera stations. During the experiment, the laser ranger was run continuously, taking about 20 readings per second. Results of these detailed measurements were received from CCRS in a more highly processed form; for each laser reading, the corresponding instrument position and orientation had been determined from the inertial system, with corrections for bias and drift based on photogrammetry. The data file received from CCRS then gave the times and the ground coordinates corresponding to the laser beam, rather than the range itself. Initially, however, a correction for the laser misalignment had not been made.

One test was made using this data file. Sections corresponding to flights over lakes were extracted, and the water height plotted as a function of time, as shown in Fig. 7.3. This height should, of course, be practically constant. These graphs appear as wavy curves with an amplitude of less than 1m, on which are superimposed noise with an amplitude of about 0.1m. The main "waves" in the curve are probably due to roll of the aircraft. Since the laser misalignment was not considered, the roll angle for the laser beam was probably in error by about 1.4° , and a tilt of this magnitude at the appropriate flying height would give a height error of around 1m. Assuming that the reason for the "waves" was this misalignment, it seemed that the laser range over water was accurate to within about 0.1m.

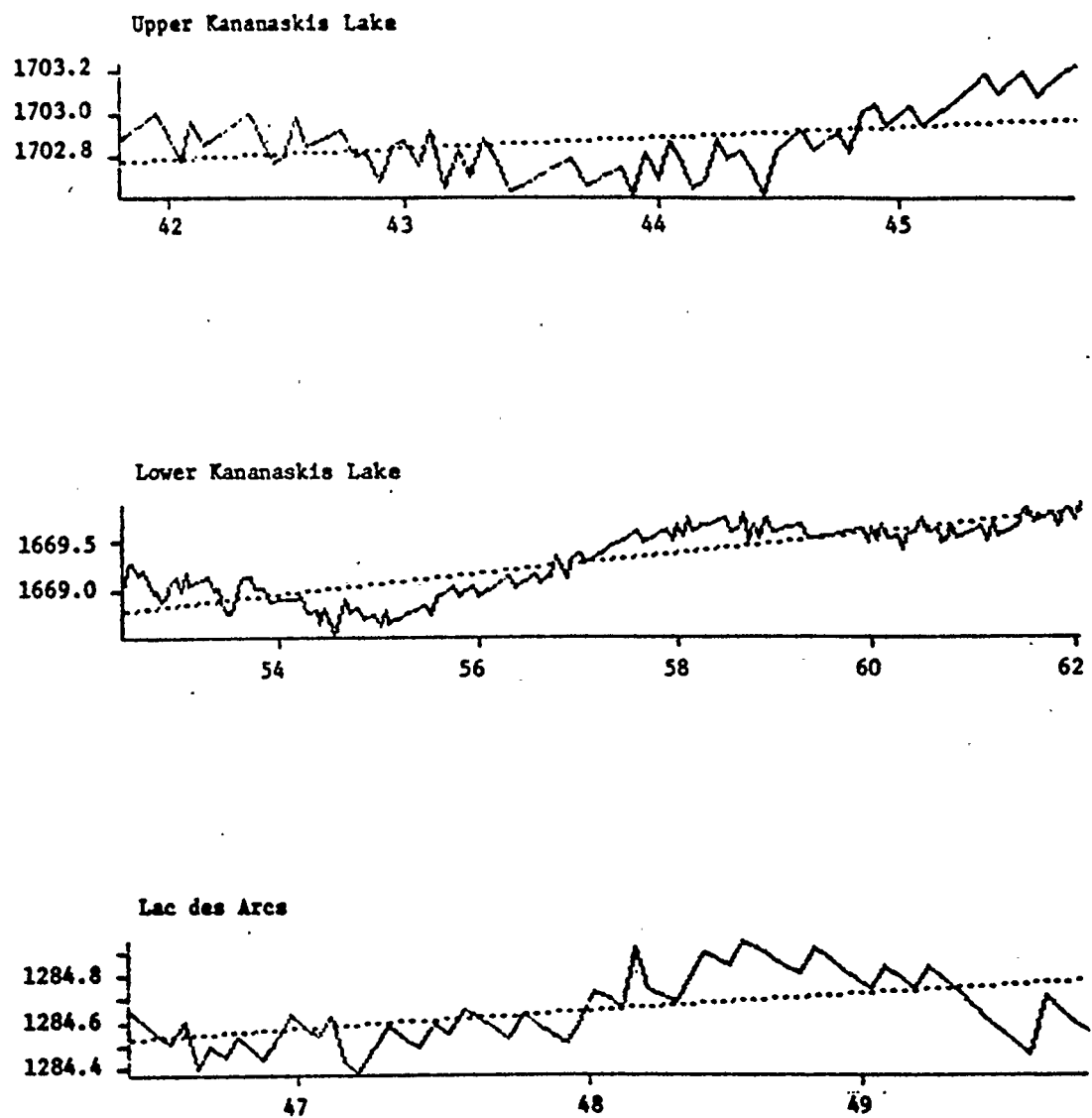


Fig. 7.3: Water Surface Profile from Uncorrected Laser over Lakes.
 Horizontal Axis is Time in Seconds.
 Vertical Axis is Elevation in Metres.
 Broken Line is Regression Line.

On receipt of a revised file of data from CCRS, for which the laser misalignment had been corrected, the graphs were re-plotted, as shown in Fig. 7.4. It is now clear that the waves have vanished, leaving essentially a straight line on which is superimposed noise having an RMS amplitude of about 0.1m.

Graphs from both uncorrected and corrected data are shown together in Fig. 7.5. They indicate that the main difference between the two data sets is a bias of about 1.8m.

Misalignment having been identified as a major cause of range error, and having been corrected for in the laser profile data file, the investigation can now proceed to laser profiles over land.

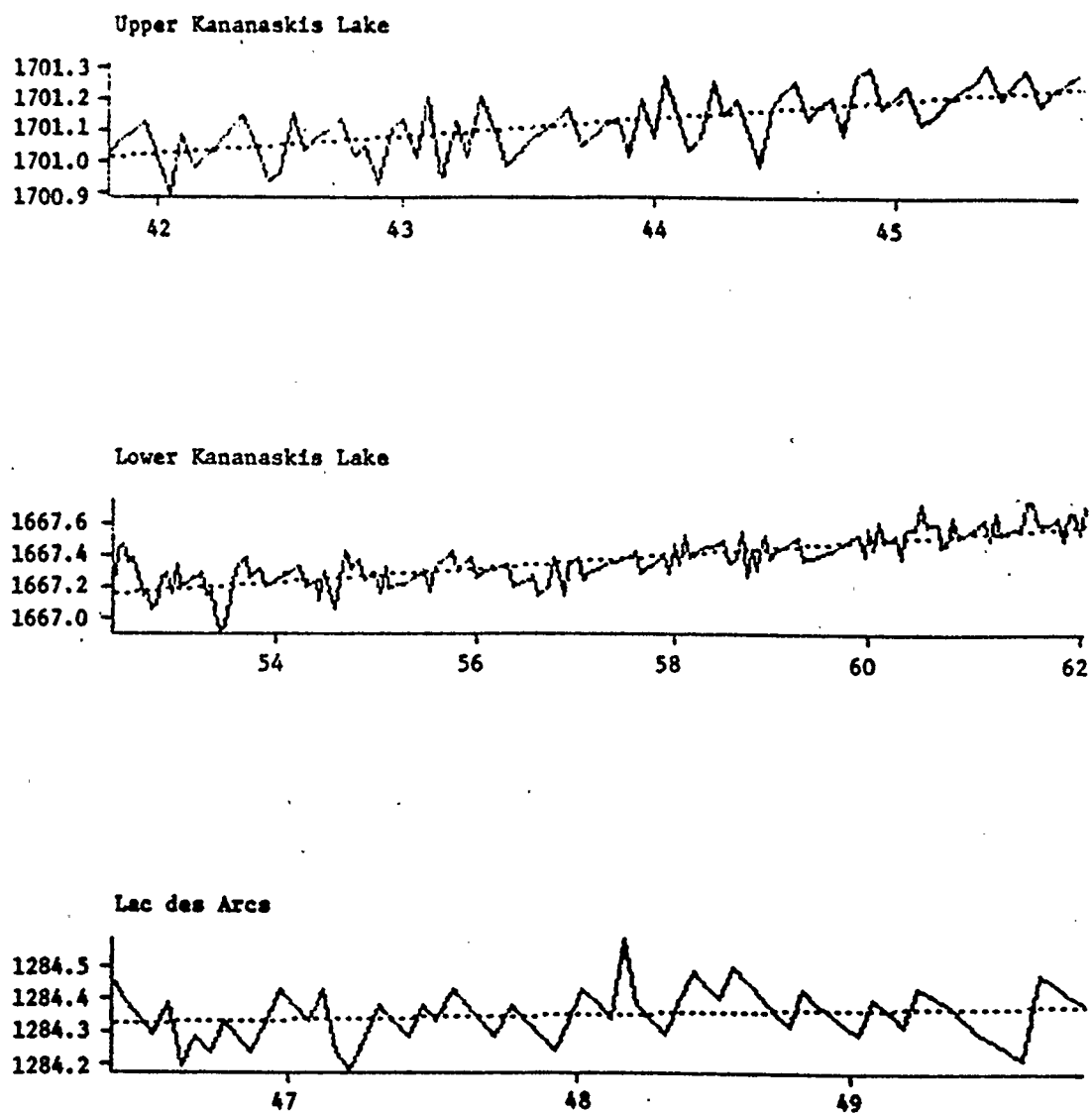


Fig. 7.4: Water Surface Profile from Corrected Laser over Lakes,
Horizontal Axis is Time in Seconds,
Vertical Axis is Elevation in Metres.
Broken Line is Regression Line.

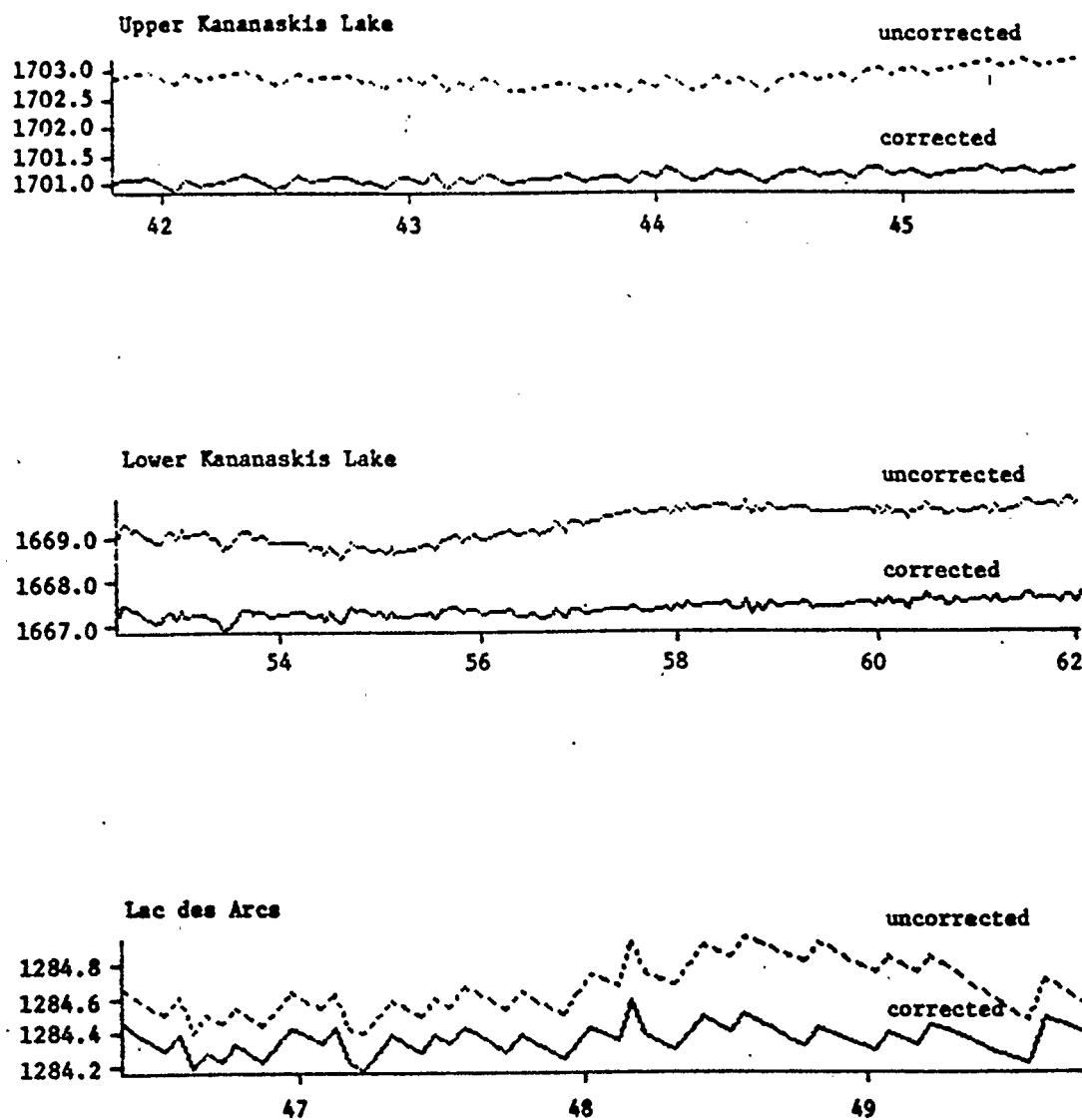


Fig. 7.5: Water Surface Profiles from Uncorrected and Corrected Laser Data.
Horizontal Axis is Time in Seconds.
Vertical Axis is Elevation in Metres.

Chapter 8

LASER PROFILING OVER LAND

8.1 Method of Analysis

After it was found that, over a water surface, the laser profiler gives elevations that agree with photogrammetric values within 0.8m, similar comparisons were made over land.

Greater discrepancies between laser and photogrammetric ranges should be expected over land for the following reasons:

- (a) Land surface is generally less smooth; the height of the ground, or of other objects intercepted by the laser beam, could vary considerably within the area of the laser spot. This is especially true in forest, where the laser echo could be partly from the treetops and partly from the ground, depending on the density of the forest, and where the photogrammetrist has the choice of measuring ground or treetop elevations. Indeed, Corten (1984) points out (p68) that a laser beam can penetrate between trees when there is up to 99% canopy, though the amount of penetration would depend on the width of the laser beam and the size of the openings. He also indicates (p55) that a laser airborne profile recorder can measure tree heights if it can distinguish the parts of the return pulse that are reflected from ground and treetops.
- (b) On sloping ground, different parts of the laser spot are at different elevations and therefore at different ranges.

Further, an error in the assumed alignment of the laser beam could mean that the laser beam is actually directed at a different point from what one expects, so that the laser measurement and photogrammetric measurement are actually being made at different ground points which have different elevations.

For this analysis, data were processed as described in Section 1(b) of Appendix F. The laser instrument's orientation and position, given by the inertial system updated by photogrammetry, were combined with the laser range to give the position of the laser spot on the ground. The laser misalignment, determined as described in Section 7.1, was taken into account. However, this misalignment was subject to some uncertainty, as its value depended on the crab-angle (κ); this angle may have changed from one flight line to another and its value had not been recorded.

A section of the whole laser profile was then selected at random, corresponding to the region between the two perspective centres of a photogrammetric model. This section contained 511 readings, spaced about 10m apart over a distance of about 5km. Using a Wild AC1 analytical stereo plotter, the photogrammetric model was set up using the control point coordinates from the same adjustment as was used to update the inertial system. (Use of values from a different adjustment might have resulted in the laser and photogrammetric measurements being made at different points.) Elevations were then measured at the x and y coordinates given in the laser profile. Besides this, elevations were measured along a straight line joining the two QNP's of the

model, and along two parallel lines, 12m to each side of it, to allow computation of terrain slope, defined as the tangent of the angle of slope. The type of terrain cover at each point in the profile was also noted and coded on a nine-point scale, as listed in Table 8.1.

Table 8.1

Nine-point Scale for Terrain Cover Type

1	Open	5	Open Timber
2	Rock	6	Medium Timber
3	Brush	7	Thicker Timber
4	Scattered Timber	8	Thick Timber
	9	Shade or Bad Photogrammetry	

A preliminary inspection showed that the variations in height along the profile, as determined from the photogrammetric and laser measurements, did not correspond exactly, but that they might match better if one profile was shifted by 3 data points relative to the other. This discrepancy could be explained by an error in the assumed laser misalignment value, resulting from ignorance of the crab-angle. Since the misalignment is mainly perpendicular to the flight line, a small change in crab-angle would move the laser spot, relative to the image, in a direction roughly parallel to the flight line. (See Fig. 8.1) For the flying height of this section, the shift of 3 places, or 30m, on the ground corresponded to an error of about a quarter of a degree in the laser misalignment, or of 10 deg in the assumed crab-angle.

The shift of 3 places was also checked analytically. The heights at points numbered 6 to 505 in this laser profile were matched with points 1 to 500 of the photogrammetric profile, and the RMS discrepancy computed. This computation was repeated, matching the same laser profile points with points 2 to 501, then points 3 to 502, etc.

of the photogrammetric profile. It was found that the smallest RMS discrepancy resulted by matching point 6 of the laser profile with point 9 of the photogrammetric profile.

The amount of shift was further checked by calculating the product-moment correlation coefficients between the two sets of heights instead of the RMS discrepancies. In this case, the best matches correspond to the greatest correlation coefficients, and they were found to occur for the same shifts as were determined from the least RMS discrepancies. In profiles with high relief, however, the value of the correlation coefficient is rather insensitive to the discrepancies that are being investigated, since the deviations of the height estimates from their mean values, having an amplitude of hundreds of metres over a typical horizontal distance of a few kilometres, are much greater in magnitude than the discrepancies in height estimates, and are therefore the dominating factor in the correlation coefficient.

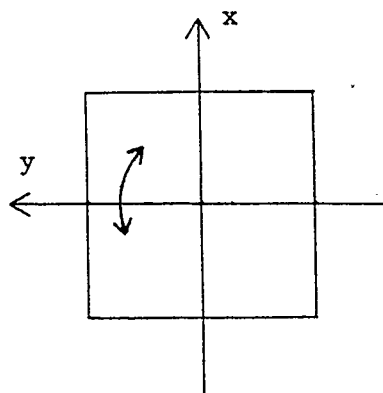


Fig. 8.1: Range of Positions of Laser Spot with Laser mounted separately from Camera.

Assuming that this shift of 3 points produced the correct matching, and that the shift was required for the reason given above, then the horizontal coordinates in the original laser profile were in error by about 30m, and those in the photogrammetric profile were comparatively reliable. Proceeding on this basis, data files were prepared comprising the number of each point in the profile, its distance from the end, the difference between the two height estimates (laser (shifted 3 points) minus photogrammetric), the slope of the terrain (x and y components, total slope and downslope direction, computed by finite differences) and terrain cover type.

It should be pointed out that the 3-point shift still may not produce a perfect match between the two profiles. A perfect match might require a shift corresponding to a non-integer number of points, which would involve interpolation in at least one of the profiles. Therefore, since the points are spaced 10m apart, there could still be a mismatch of up to 5m along the profile, as well as an unknown amount perpendicular to it.

One aim of this analysis was to determine whether the difference between the two height estimates depended on the terrain cover and slope, and if so, how. Both these factors varied considerably in the first profile studied.

The first stage of analysis determined the mean value, mean absolute value, RMS value, maximum, minimum and standard deviation of the difference between laser and photogrammetric heights, for each of the nine terrain types and also for the whole file. The second stage of analysis determined the same quantities, but

classified them according to nine ranges of terrain slope values instead of nine terrain cover types. The results of these two analyses are shown in Table G.1 of Appendix G.

8.2 Analyses of Specific Profiles

The foregoing profile sample will now be referred to as Section A. Generally, it is not wise to draw general conclusions from a single sample of data. Also Section A was complicated by the effects of both terrain cover and relief at the same time. Therefore four more profile samples were analyzed. They were selected such that two of them contained little relief, and two of them featured high relief with little vegetation, with the aim of separating the effects of these two causes. They were labelled as sections W, X, Y and Z, and their locations and main characteristics are given in Table 8.2.

Table 8.2

Profile Section	Characteristics	Flight Line (Spatial)	Approx. x-coord. (m)	Approx. y-coord. (m)
A	Varied relief and vegetation	1	18800	64000
W	Flat	5	36500	62000
X	Flat	4	32300	19500
Y	Rocky and very rugged	2	24400	30500
Z	Rocky - little vegetation	4	32100	27000

As these profiles appeared in different flight lines, in which the crab-angle may have differed, the process of matching laser and photogrammetric profiles, and performing the appropriate shift, had to be repeated. The determination of terrain slope was

simplified from the procedure used in Section A, in which the photogrammetric profile was measured along the straight line between the two QNP's and along two straight lines parallel to it. Instead, the photogrammetric profiles were measured along the laser-spot trajectory and two lines 12m to each side of it.

The discrepancies between photogrammetric and laser-derived terrain elevations can be analyzed in various ways. For various combinations of terrain cover and slope, including x and y slope components, one can consider the mean, with corresponding standard deviation, RMS, maximum and minimum values of the discrepancy, and also corresponding parameters for those cases where the discrepancy was positive or negative (as done by [Moreau and Jeudy, 1986]). An unmanageable proliferation of tables would be required to display all possible aspects of analysis. Therefore the counterparts to Table G.1, for the remaining sections, are presented in Tables G.2 to G.5, and the mean, standard deviation and RMS values of the discrepancies, categorized by terrain cover and total slope simultaneously, for all five sections, are given in Tables G.6 to G.10, and the most important features of the analysis are described in the following text.

Sections W and X cover mostly flat terrain, and are therefore suitable for studying the effect of terrain cover. Figs. 8.2 and 8.3 display graphs of terrain elevation difference (laser minus photogrammetric), terrain cover type, and terrain slope and its components as functions of the record number, which is an indicator of position along the profile, for Sections W and X respectively. In Section W, terrain slope effects evidently cannot

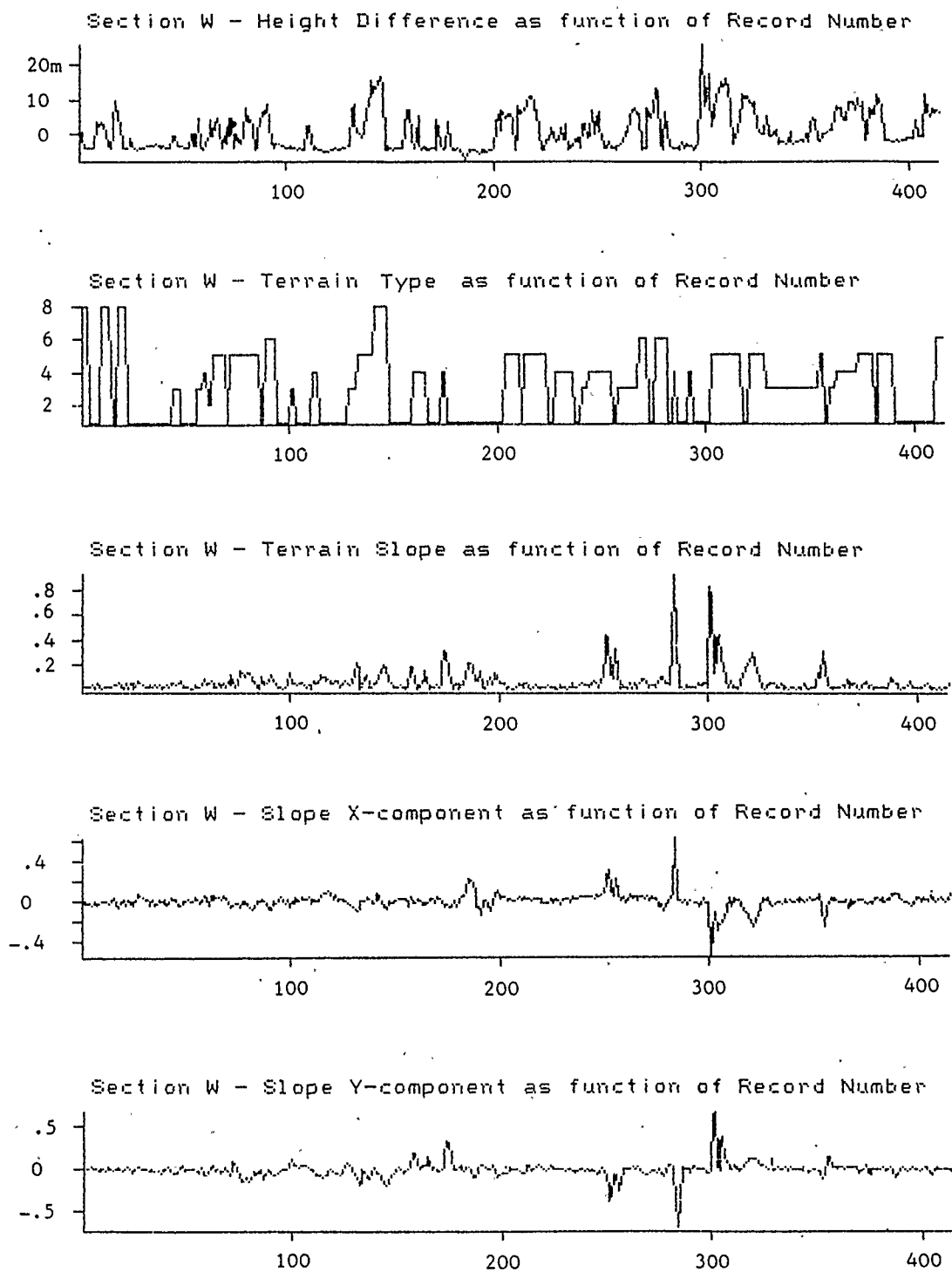


Fig. 8.2: Characteristics of Terrain Profile Section W

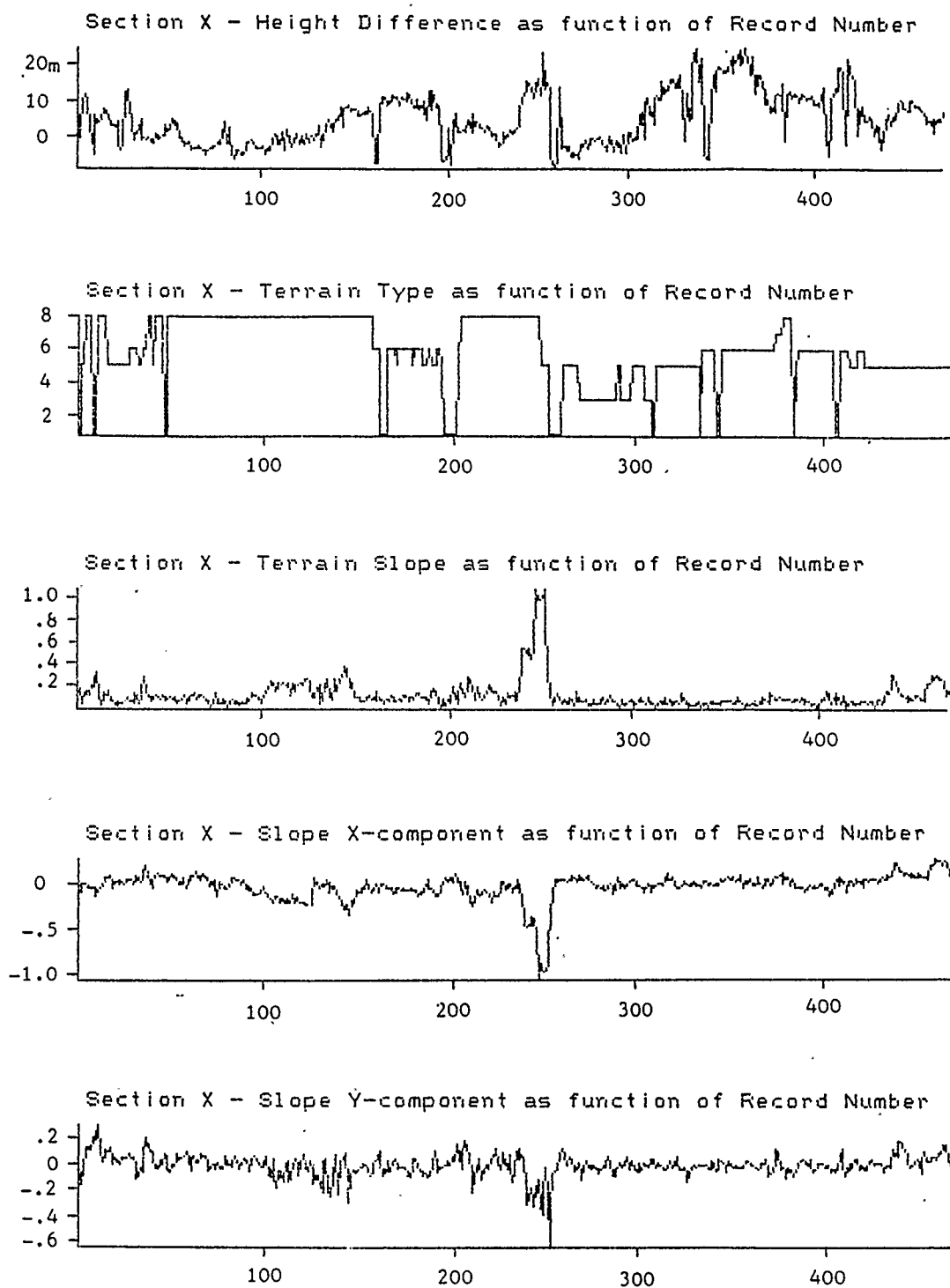


Fig. 8.3: Characteristics of Terrain Profile Section X

be ignored; the only difference greater than 20m clearly occurs at a point where there is a short, steep slope, with a negative x- and positive y-component. However, such a spike does not occur at another point of steep slope with a positive x- and negative y-component (See Fig. 8.2). This situation suggests that there could still be some laser alignment error. A short interval of steep slope in Section X also corresponds to a large difference.

Turning to terrain cover, Fig. 8.3 shows that there are several short intervals of open terrain, which in some cases correspond to roads through the forest. These often occur with negative values of the difference, whereas the neighbouring forest gives positive values. It can be seen from Tables G.7 and G.8 that, on the whole, there are negative differences for open terrain, but progressively higher differences for thicker forest. Indeed, for Section W, the correlation coefficient between elevation difference and terrain type number is equal to 0.528. This relation may be explained by the fact that the photogrammetric heights were estimates of the ground elevation, while the laser beam may have been partly reflected from the treetops.

Sections Y and Z cover terrain with little vegetation but much relief. Figs. 8.4 and 8.5 are the counterparts to Figs. 8.2 and 8.3 for these sections. Indeed, in parts of Section Y, the relief is so rugged that parts of the profile are in image shadow, and the photogrammetric elevation there can only be guessed. Such points should have been classified under Terrain Type 9 (bad photogrammetry), but by an oversight they were classified in Type 1 (open ground), to which they also belonged. Because of this need

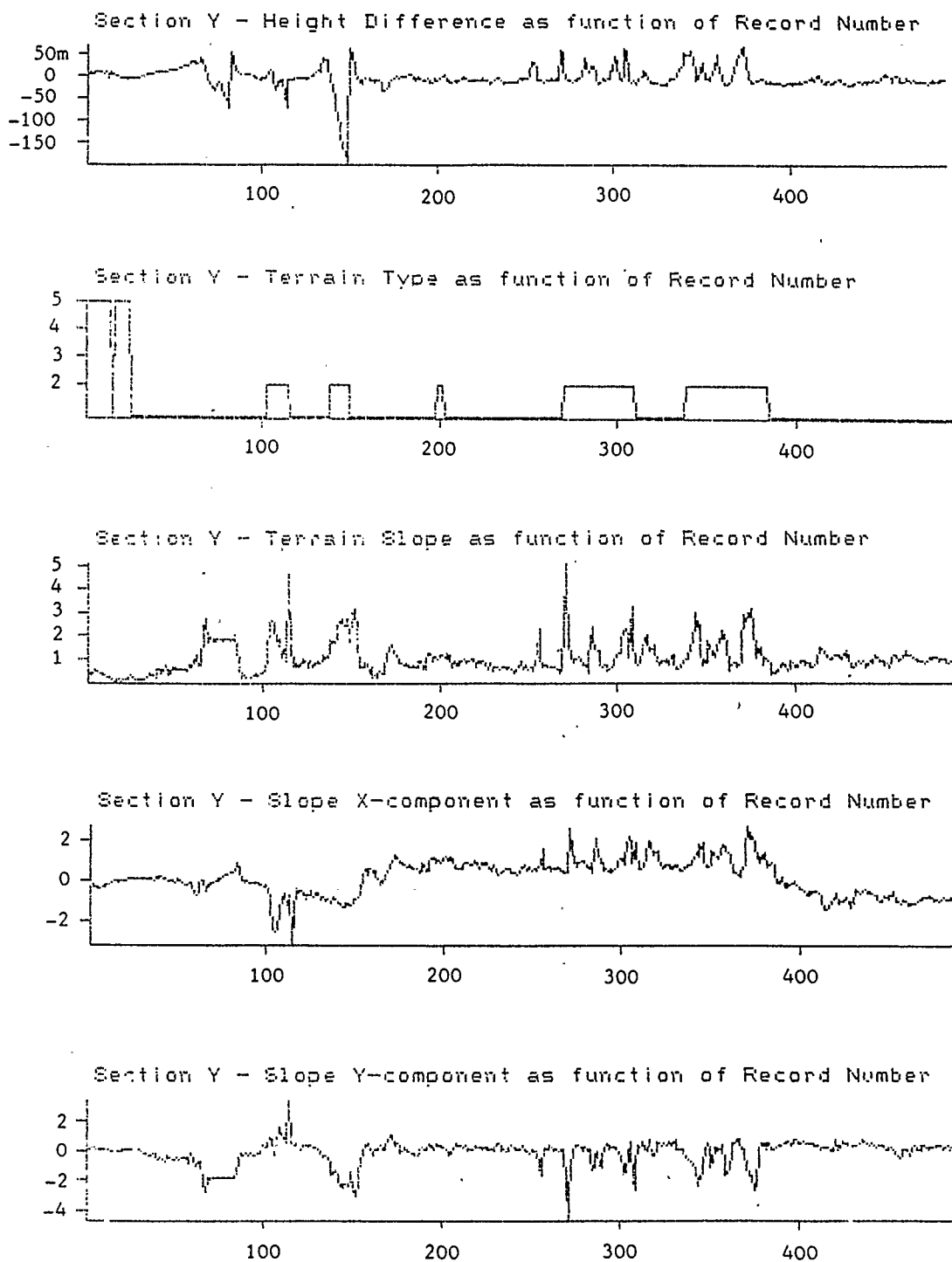


Fig. 8.4: Characteristics of Terrain Profile Section Y

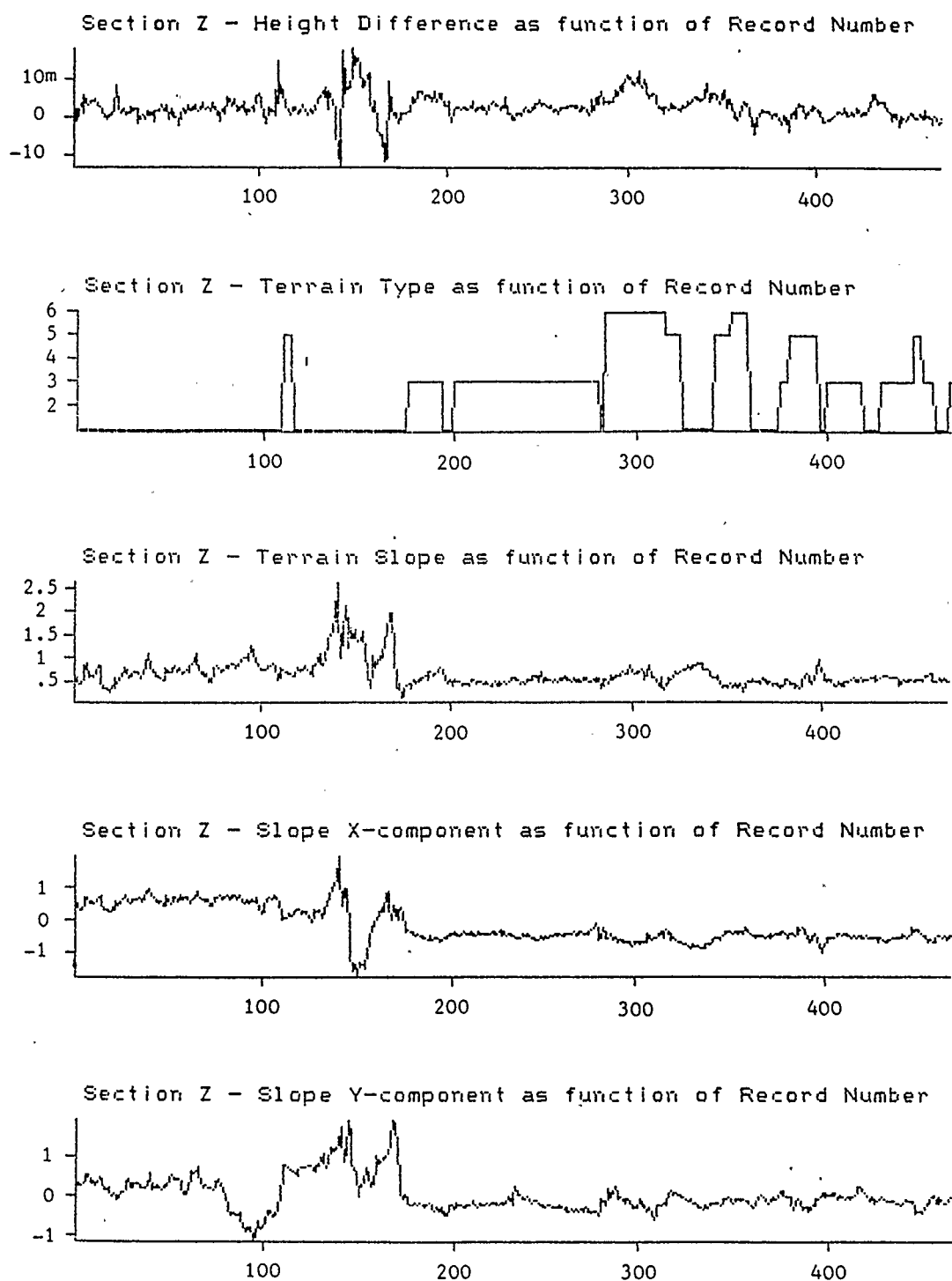


Fig. 8.5: Characteristics of Terrain Profile Section Z

for guessing, there occur some exceptionally large (in magnitude) values of the difference in Section Y, and rejection of points in the image shadow would now involve either repeating the photogrammetric measurements or using a purely arbitrary criterion for their rejection.

In spite of this problem, some conclusions can be drawn. The RMS values of difference generally increase as slope increases, and approximately in direct proportion to the slope value. In the case of Section Z, they are nearly 5m times the slope value, which is what one would expect with an uncertainty of 5m in the laser spot position.

Chapter 9

CONCLUSIONS AND RECOMMENDATIONS

Analyses have now been completed. The values of certain parameters, as measured by auxiliary systems, have been compared with the corresponding values as evaluated by various photogrammetric adjustments. The consistency of values derived from different photogrammetric adjustments has also been considered.

The parameters in question include the position coordinates and orientation angles of the camera (measured by an inertial system), increments in these quantities between consecutive camera stations, and also measures of camera displacement and rotation between stations which are independent of a coordinate system. Another parameter is the range from the camera to a point on the ground near the nadir, measured by a laser ranger/profiler. The values of this range have been analyzed not only at the camera stations but also along some profiles between camera stations.

It must be remembered that this experiment entailed the extreme conditions of high-altitude photography and very rugged terrain. Further, the auxiliary systems were not working under ideal conditions. The inertial systems were not present state-of-the-art equipment, they were not functioning at full capacity, due to a flaw in the data acquisition system, no updates were used, and a rather arbitrary assumption was made to replace the normal gravity model. More sophisticated error modelling, as outlined by Schwarz (1983) would probably have improved the

quality of the inertial system output. Also the laser alignment was initially unknown, and the crab-angle of the camera was not recorded.

With more modern technology, and the hindsight resulting from this analysis, the effects of most of these shortcomings could be reduced significantly.

The results are now summarized using two different approaches: first, according to the type of measurement and second, according to the application.

9.1 Results Classified According to Type of Measurement

(a) Camera Position

Different photogrammetric adjustments give different coordinates for a camera perspective centre, depending on the size of the block or sub-block used in the adjustment, the control points used, the use of constraints such as lake levels, and the type of adjustment, whether it is bundle or independent-model block. In the latter case, there are two estimates of the positions of many of the PC's. As mentioned in Chapter 3, the uncertainty in a photogrammetric estimate of a PC position is of the order of 10-20m in the horizontal, and 4m in the vertical. In one case, it is as great as 60m, but this applies to one of the points that were rejected from the SPACE-M adjustment because of their large residuals.

When auxiliary and photogrammetric estimates are compared, it is found that there is a bias of the order of hundreds of metres in all coordinates. While this bias is fairly constant in

the vertical, it changes significantly in the horizontal between the different flight lines. For this reason, auxiliary estimates of position cannot be used directly, unless the bias can be determined, and this determination would require updates of the inertial system.

If updates are not possible, the effect of the bias can be removed by considering the displacements between consecutive camera stations. For all three components (x , y and z) of these displacements, the agreement between auxiliary and photogrammetric values is as close as the discrepancy between the photogrammetric estimates. Further, in the case of estimates from SPACE-M, this agreement is better for the set of points that excluded those rejected in the adjustment than for the set that includes the rejected points, as can be seen by comparing values in Tables 4.1 and 4.2. Since the rejected points were those that gave large residuals in the adjustment, it follows that the accuracy of their position estimates could be improved by incorporating auxiliary estimates of the inter-station displacements into the adjustment. This improvement would occur mainly in the horizontal (planimetry); little improvement would be expected in the vertical because in that dimension the discrepancy between auxiliary and photogrammetric estimates is not significantly smaller than the uncertainty of the photogrammetric estimates.

Besides the bias that is present in each flight line, there is also a drift with time. Its effect on displacements between consecutive stations is negligible, and, like the bias, its value could be determined by updates.

Good agreement of individual components of displacement can only be expected when the coordinate systems used for the auxiliary and photogrammetric estimates are correctly aligned. Misalignments can easily occur in the absence of updates. However, there is no misalignment effect if one considers a rotation-invariant measure of the displacement. The absolute magnitude of the displacement vector is such a quantity. As Tables 4.1 and 4.2 indicate, this magnitude gives slightly better agreement between photogrammetry and auxiliary measurements than the horizontal components. The fact that improvement in agreement is small indicates that the misalignment was insignificant in this experiment.

To summarize, absolute positions of the camera, as given by an inertial system, are not of acceptable accuracy for input to a photogrammetric adjustment unless they receive adequate updates, in which case the inertial measurements, in effect, provide an interpolation between the update values. However, inertial estimates of relative camera positions, where the latter differ by 2.5km in space and 10 seconds in time, are of acceptable accuracy, especially when in a rotation-invariant form.

(b) Camera Orientation Angles

The outcome of the analysis of orientation angles (roll, pitch and heading) has some similarities to that of the position coordinates.

There is some discrepancy between the values of the orientation angles as deduced from different photogrammetric adjustments. This discrepancy is generally of magnitude about 0.05° , sometimes greater.

In the comparison of auxiliary and photogrammetric values, there are biases of up to 2° in all of the angles; this bias changes from one flight line to another. Therefore absolute values of orientation angles are unsuitable for input to an adjustment, unless the bias can be determined, e.g. from updates to the inertial system.

As with the position estimates, the effect of the bias can be removed by considering the changes in orientation angles between consecutive camera stations. The discrepancy between auxiliary and photogrammetric estimates (from SPACE-M) of these changes is generally less than 0.04° for roll and pitch, and 0.08° for heading (RMS values), as indicated by Tables 5.3, H.2 and H.4. These values apply to all camera stations. However, when points that were rejected in the SPACE-M adjustment are excluded from the analysis, these discrepancies are reduced to less than 0.03° for roll and pitch and 0.04° for heading, as shown by Tables 5.3, H.6 and H.8. This reduction shows that the use of auxiliary values of orientation angle changes could result in an improvement of accuracy, at least at some points of the network.

As was the case with the position estimates, good agreement of changes in specific orientation angles can only be expected when the auxiliary and photogrammetric axes are correctly aligned. The biases in the orientation angles indicate that misalignments of up to 2° may be present; however, the agreement is acceptably good in spite of this. Nevertheless, larger misalignments could lead to worse agreement. The biases could be removed by updating the inertial system, provided that there is no

significant misalignment within the system itself. It should be mentioned here that a misalignment correction for orientation angles may not necessarily be the same as the correction that should be applied for displacement between camera stations, as the heading angle is relative to true north, whereas the displacement is measured in the UTM grid.

Misalignment problems can also be avoided by considering measures of orientation change which are invariant with respect to rotations of the coordinate system. Two such measures were discussed in Chapter 6, and found, in this case, to give about the same agreement between auxiliary and photogrammetric values as the specific orientation angles.

(c) Laser Ranges

In this project, the main sources of errors in laser range proved to be outside the instrument itself.

Correct alignment is the primary problem in the use of a laser ranger to measure the distance from the instrument to a point on the ground that is close to the nadir. For a nominally vertical laser beam over a level land or water surface, the error due to misalignment is $R(1 - \cos m)$, where R is the measured range and m is the angle of misalignment. This error is proportional to R , and roughly proportional to the square of m for small angles. Further, over sloping ground, there is an additional error of $R s \sin m$, where s is the slope of the ground (i.e. the tangent of the slope angle).

For application with photogrammetry, the laser is normally installed so that its beam is parallel to the camera's principal

axis, as closely as can be achieved. However, its alignment needs to be checked and calibrated. If the laser is mounted separately from the camera, the crab angle must be measured, both in calibration and in use.

Essentially, calibration involves finding the position of the laser spot on the photographic image, and this can be determined by either of the methods described in Section 7.1, viz. photogrammetry involving several images such that the terrain near the laser spot gives a good random sample of slope steepness and orientation relative to the camera, or night photography over a dark area, so that the laser spot is the only feature on the image, or is otherwise clearly distinguishable.

Even if the orientation is known exactly, there can be some uncertainty in the range as measured, due to the nature of the terrain cover, such as when the laser beam may be reflected from both tree tops and ground, and to the terrain slope, where different parts of the laser spot are at different ranges. Estimates of any bias in the laser range associated with a given type of terrain have proved to be inconclusive; different samples of open ground give biases of varying sign, though generally there is a tendency for the laser ranger to give a higher terrain elevation than photogrammetry over forest, which is consistent with the assumption that the laser beam is reflected off the treetops.

Elevation profiles made by the laser over lakes show that the deviations of the laser-measured elevation from a plane surface are about 0.15m. Consequently this is the magnitude of the "noise" in the measurements.

9.2 Results Classified According to Application

(a) Independent Models

Apart from the case where the whole adjustment comprises only one stereomodel, absolute values of distance are irrelevant in an independent model because each model has its own scale, and this scale is adjusted when the model is incorporated into a block.

Consequently the errors that may occur at the independent model stage are likely to be deformations. In practice, relative values of distances could be used to show the presence of deformations; for instance, the ratios of distances between the perspective centres and their respective laser spots, and between the two perspective centres. In a case where the two laser beams were parallel, of equal length and perpendicular to a baseline of 2.5km, a change of 25cm in one of the laser ranges would correspond to a change of 0.006° in the angle between the base and the line joining the laser spots. In practice, however, such a small deformation could not be detected because of uncertainties in the other laser range, the base length, the relative orientations of the lines joining PC's and laser spots and of the baseline, as well as effects of terrain cover and slope.

The inertial system could only detect angular deformations of the order of 0.03° or greater. However, Schwarz et al. (1984) indicate that auxiliary orientation information is useful in independent models only if it is accurate to 10 arcseconds or better, i.e. 0.003° . Consequently it appears unlikely that use of auxiliary data can improve on the standard optical-analogue

method of relative orientation.

(b) Block Adjustments of Independent Models

A block adjustment involves, either directly or indirectly, determination of positions of perspective centres. Direct use of position coordinates for perspective centres, as given by an inertial system under the conditions of this experiment, is definitely unsatisfactory, because of the large biases present. However, the biases could be removed by updates of adequate quality at appropriate intervals, and the work of Goldfarb (1985) indicates that this approach, using GPS updates, is promising.

Otherwise, relative positions of perspective centres appear to be potential sources of improvement. Blais and Chapman (1985) have already incorporated first and second differences of PC coordinates into a SPACE-M adjustment, resulting in marginal improvements in residuals of ground point coordinates.

Tables 4.1 and 4.2 indicate that auxiliary measurements agree better with within-model estimates of baseline length than with between-model estimates, and also with rotation-invariant quantities such as absolute baseline length rather than individual components. Therefore one approach that may be worth investigating would be to relate the baseline length, as measured by the auxiliary system, to the baseline length within the individual model and the scale factor used to adjust the independent model to the ground coordinate system.

In principle, other distances, as determined by auxiliary systems, could be used as input to an adjustment to control the scale of the final block. The range from PC to laser spot is

suitable provided that the laser spot is accurately located on the image and the terrain cover and slope at that point are such that their effects on the measured range are known; at present, such effects are not sufficiently well known. Another example is the distance between the laser spots corresponding to two consecutive PC's. However, use of this could be too complicated to be practicable. It would involve locating both laser spots on both images and interpolating the laser readings to give their values corresponding to the instants of photographic exposure. The computation of distance between the spots would also be complex, as it would involve the distance between the PC's (measured by the inertial system), the change in camera orientation, and the change in local level due to earth curvature between the two camera stations.

Another point to be borne in mind is that a strengthening of the adjustment at flying height may not necessarily result in an improvement in the residuals of ground points. A similar situation was mentioned in Section 3.1, where it was noted that the lake-level constraint led to a greater uncertainty in the PC position. Such situations could arise from deformations within models, or errors in their integration into the block.

A block adjustment involves orientation of individual models to form an integrated whole. The orientation information from an auxiliary system refers to the orientation of the camera, while the orientation of an independent model is defined in terms of the coordinate system used in that model. In an independent model, it is customary to use a coordinate system in which one

axis corresponds to the baseline of the model (Blais, 1979). The relative orientation of two adjacent models could then be partly defined in terms of the directions of their two baselines, which are in turn defined by the PC coordinates. However, these two directions would not give any information on rotation of either model about its own baseline.

If the coordinate system of each independent model corresponded to the camera axes at the first PC of that model, then the relative orientation of the two models could be described in terms of the change of camera orientation from the first PC of one model to the first PC of the next. This change of camera orientation could be described either in terms of the three orientation angles (roll, pitch and heading, or ω , ϕ and κ) or by rotation-invariant quantities such as were defined in Chapter 6.

(c) Bundle Adjustments

A bundle adjustment differs from an independent model block adjustment in that whereas the latter comprises two stages (integration of two images into a model, and of several models into a block), a bundle adjustment combines the whole process into one stage.

Perspective centre positions still feature in the adjustment, and some of the comments made in Section 9.2(b) apply here too, namely on the direct use of PC coordinates only if properly updated, and on the use of relative PC positions in component form if there is no serious misalignment of axes, and in rotation-invariant form under any circumstances.

Camera orientation angles enter into a bundle adjustment more directly than they do in an independent model block adjustment. Normally they are expressed in terms of ω , ϕ and κ , but if an inertial system gives an output in terms of roll, pitch and heading, these angles can be converted to and from ω , ϕ and κ by the transformations given in Appendix D. Again, absolute values of these angles should be used only if biases are removed by updating of the inertial system. Otherwise, changes in these angles between adjacent PC's could be used as input on camera orientation. As before, rotation-invariant measures of the change in camera orientation, as described in Chapter 6, are preferable unless one can be sure that there is no serious misalignment.

Since the use of relative distances and orientation angles is intended to eliminate biases in these quantities, and since the biases may change significantly between flight lines, such relative data should only be used between consecutive stations on the same flight line.

Laser ranges from PC to laser spot can also be used to control scale; their use requires accurate identification of the laser spot on the image, and terrain cover and slope at that point such that their effects on the measured range are known to within a few decimetres.

Some further notes on the use of laser ranges in photogrammetric adjustment are given in Appendix F.

(d) Laser Profiling

The use of an airborne laser ranger for obtaining topographic profiles appears to be quite promising, especially in situations, such as over featureless terrain, where photogrammetry is less suitable. It is, however, essential to know the position and orientation of the instrument at all times. This information can be given by an inertial system, but the system requires updating at both ends of each profile.

For a high-flying aircraft, updating can be achieved by photogrammetry using ground control at the ends of the flight lines, but then the locations of the profiles are restricted by the locations of ground control. As Gibson (1984a) points out, straight flight lines between update points are very desirable because of degradation of the inertial system during turns. Therefore, if an area is to be mapped by a network of profiles, a considerable amount of ground control is needed around the periphery of the area.

GPS satellite positioning will probably be adequate for updating the aircraft position at sometime in the future, when the full constellation of satellites is in use. However, it does not give a complete update of the orientation.

If the updating problem could be solved, and the effects of terrain cover, vegetation and slope were more thoroughly investigated, then laser profiling from high-flying aircraft would have the potential of giving terrain elevations to accuracy of a few decimetres over smooth surface and topography.

In the meantime, profiling from a low-flying aircraft appears to be most practical at present, as errors in orientation then have less effect on the elevation measurements, and the size of the laser spot on the ground is less. Also there are better opportunities for obtaining zero velocity updates at the ends of straight flight lines if a helicopter is used.

Some suggested procedures for the use of photogrammetry in testing and using a laser profiler are given in Appendix F.

9.3 Recommendations

Although the quality of the auxiliary data has now been analyzed, there still remains the matter of including it in photogrammetric adjustments. Such inclusion has already been tried in the case of position information [Blais and Chapman (1984a),(1984b),(1985), Goldfarb (1985), Schwarz et al. (1985), Lucas (1987)], while both position and orientation information were used in the CCRS Bundle Adjustment whose output is discussed in this thesis. For the inclusion of inertial values of length of base in an independent model block adjustment, one should consider the feasibility of comparing them with the length of base in the stereomodel, multiplied by the scale factor used to integrate the model into the block, rather than with the length of base between mean perspective centres.

Further investigations could consider means of including camera orientation data into bundle adjustments, as well as its use in independent model block adjustments, as suggested in Section 9.2(b), by relating the orientation of a stereomodel to the orientation of the camera at the first PC in the model.

Improved knowledge of the behaviour of the laser profiler at high altitude is also desirable. This could be obtained by making further flights, together with photogrammetry, over specific types of terrain. Bias in the range reading, and its dependence on vegetation cover, could best be obtained from flights over flat terrain having large areas of uniform vegetation type such as grass, brush, open and thick forest, while effects of slope could best be studied from flights over terrain of simple, uniform vegetation cover, but varying topography, such as grassy hills.

REFERENCES

- Blais, J.A.R. (1976): SPACE-M: Spatial Photogrammetric Adjustment for Control Extensions using Independent Models. XIII Congress of the International Society for Photogrammetry, Helsinki, July 11-23, 1976.
- Blais, J.A.R. (1979): Least-Squares Block Adjustment of Stereoscopic Models and Error Analysis. Doctoral Thesis in the Department of Surveying Engineering, U.N.B. Technical Report No. 30001, Division of Surveying Engineering, The University of Calgary.
- Blais, J.A.R. and M.A. Chapman (1984a): The Use of Auxiliary Airborne Sensor Data in SPACE-M Photogrammetric Block Adjustments. The Canadian Surveyor, Vol. 38, No. 1, pp 3-14.
- Blais, J.A.R. and M.A. Chapman (1984b): The Use of Relative Terrestrial Control Data in SPACE-M Photogrammetric Block Adjustments. The Canadian Surveyor, Vol. 38, No. 4, pp 299-310.
- Blais, J.A.R. and M.A. Chapman (1985): Optimal Use of Auxiliary Airborne Inertial Data in Topographic Mapping Applications. Proceedings, Third International Symposium, Inertial Technology for Surveying and Geodesy, Banff, Canada, 16-20 Sept., 1985: Vol. 1, pp 359-373.
- Corten, F. (1984): Navigation Systems and Sensor Orientation Systems in Aerial Survey. Congress of the International Society for Photogrammetry and Remote Sensing, Rio de Janeiro.
- Frankich, K. (undated): Lecture notes. British Columbia Institute of Technology (unpublished).
- Gibson, J.R. (1984a): Auxiliary Airborne Data in Coastal Mapping and Other Applications. Lecture notes (unpublished).
- Gibson, J.R. (1984b): A Block Adjustment System Using External Navigation Data. Ph.D. Thesis, University of New Brunswick, Fredericton, N.B.
- Gibson, J.R. (1986): The Use of Auxiliary Data in Photogrammetric Adjustments, Proceedings of the International Symposium, ISPRS, Stuttgart, Sept. 1986.
- Goldfarb, J.M. (1985): Exposure Station Control for Aerotriangulation with an INS-Differential GPS. Proceedings of the Third International Symposium on Inertial Technology for Surveying and Geodesy, Banff, September, 1985, pp 777-789

- Goldfarb, J.M. and K.P. Schwarz (1985): Kinematic Positioning with an Integrated INS-Differential GPS. Proceedings of the First International Symposium on Precise Positioning with the Global Positioning System, Rockville, Md., Vol. 2, pp 757-772.
- Hursh, J.W. (undated): Aerial Profiling of Terrain System (APTS).
- Jepsky, J. (1986): Airborne Laser Profiling and Mapping Systems Come of Age. Technical Papers, 1986 ACBM-ASPRS Annual Convention, Volume 4: Photogrammetry, pp 229-238.
- Lucas, J.R. (1987): Aerotriangulation without Ground Control. Photogrammetric Engineering and Remote Sensing, Vol. 53, No. 3, pp 311-314.
- Masry, S.E. (1977): Coastal Mapping from a Stereomodel Established using Inertial Platform Data: Error Analysis. Technical Report No. 49, Department of Surveying Engineering, University of New Brunswick.
- Moffitt, F.H. & E.M. Mikhail (1980): Photogrammetry, 3rd edition, Harper & Row, New York, 648pp.
- Moreau, R. & L.M.A. Jeudy (1986): Profilometre Laser-Inertiel: Un Essai Qualitatif en Terrain Boisé.
- Schreier, H., J. Lougheed, J.R. Gibson & J. Russell (1984): Calibrating an Airborne Laser Profiling System. Photogrammetric Engineering and Remote Sensing, Vol. 50, No. 11, pp 1591-1598
- Schwarz, K.P. (1983): Inertial Surveying and Geodesy. Reviews of Geophysics and Space Physics, Vol. 21, No. 4, pp 878-890.
- Schwarz, K.P., C.S. Fraser & P.C. Gustafson (1984): Aerotriangulation without Ground Control, International Archives of Photogrammetry and Remote Sensing, Vol. 25, Part A1, XVth Congress, International Society for Photogrammetry and Remote Sensing, Rio de Janeiro, June 16-29.
- Wong, R.V.C., K.P. Schwarz, G. Lachapelle and J. Hagglund (1985): Integration of Inertial and GPS Satellite Techniques for Precise Marine Positioning. Marine Geodesy, Vol. 9, No. 2, pp 213-226.
- Zarzycki, J.M. (1972): The Use of Auxiliary Data in Aerial Triangulation. Twelfth Congress of the International Society for Photogrammetry. Ottawa.

APPENDIX A

Data on Individual Flight Lines

Numbering Systems, Coordinates and Times

Photo. (Spatial) Line 1 - Chron. Line 1 -	Page 127
Photo. (Spatial) Line 2 - Chron. Line 3 -	Page 128
Photo. (Spatial) Line 3 - Chron. Line 5 -	Page 129
Photo. (Spatial) Line 4 - Chron. Line 2 -	Page 130
Photo. (Spatial) Line 5 - Chron. Line 4 -	Page 131

Comparison of Point Numbering Systems for Photographic Images,
in Auxiliary Data Files (CCRS and working versions)
and in Photogrammetric Adjustment

Photo. Line 1				Chronological Line 1		
Photo Image	UTM Coordinates*		Time (h:m:s)	CCRS Point No.	Aux. Pt.No.	Photo. Pt.No.
	X	Y				
1	19000	68500	20:08:05	(1)		
2	18900	66200	20:08:16	2	1	1
3	18900	63800	20:08:27	3	2	2
4	18900	61600	20:08:39	4	3	3
5	19000	59200	20:08:50	5	4	4
6	19000	57300	20:09:00	6	5	5
7	19000	55400	20:09:09	7	6	6
8	19100	53400	20:09:19	8	7	7
9	19200	51100	20:09:29	9	8	8
10	19200	49000	20:09:40	10	9	9
11	19300	46800	20:09:51	11	10	10
12	19300	44600	20:10:01	12	11	11
13	19400	42400	20:10:12	13	12	12
14	19400	40200	20:10:23	14	13	13
15	19500	38000	20:10:33	15	14	14
16	19600	35800	20:10:44	16	15	15
17	19700	33700	20:10:55	17	16	16
18	19700	31400	20:11:06	18	17	17
19	19800	29300	20:11:16	19	18	18
20	19900	27000	20:11:27	20	19	19
21	19900	24800	20:11:38	21	20	20
22	20000	22600	20:11:48	22	21	21
23	20000	20500	20:11:59	23	22	22
24	20100	18300	20:12:09	24	23	23
25	20100	16200	20:12:20	25	24	24
26	20200	14000	20:12:30	26	25	25
27	20200	11900	20:12:41	27	26	26
28	20200	09700	20:12:51	28	27	27
29	20100	07700	20:13:02	29		
30	20000	05500	20:13:12	30		
31	20100	03400	20:13:23	31		
32	20200	01300	20:13:33	32		
33	20300	99100	20:13:44	33		

*For conciseness, the first digits of the x-coordinate, and the first 2 digits of the y-coordinate, have been omitted. These digits are 6 for the x-coordinate and 56 for all y-coordinates except Photo point 33 of Photo Line 1, for which they are 55.

Comparison of Point Numbering Systems for Photographic Images,
in Auxiliary Data Files (CCRS and working versions)
and in Photogrammetric Adjustment

Photo. Line 2				Chronological Line 3		
Photo Image	UTM Coordinates*		Time (h:m:s)	CCRS Point No.	Aux. Pt.No.	Photo. Pt.No.
	X	Y				
63	23100	70100				
64	23200	68400	20:30:39	1		
65	23300	66500	20:30:49	2		
66	23600	64400	20:30:59	3	1	1
67	23700	62500	20:31:08	4	2	2
68	23700	60500	20:31:18	5	3	3
69	23800	58600	20:31:27	6	4	4
70	23800	56400	20:31:38	7	5	5
71	23900	54300	20:31:48	8	6	6
72	23900	52000	20:31:59	9	7	7
73	23900	49700	20:32:10	10	8	8
74	24000	47400	20:32:22	11	9	9
75	24000	45000	20:32:33	12	10	10
76	24100	42600	20:32:45	13	11	11
77	24100	40200	20:32:57	14	12	12
78	24200	37800	20:33:08	15	13	13
79	24200	35400	20:33:20	16	14	14
80	24300	33000	20:33:32	17	15	15
81	24400	30600	20:33:43	18	16	16
82	24400	28200	20:33:55	19	17	17
83	24400	25800	20:34:07	20	18	18
84	24500	23500	20:34:18	21	19	19
85	24500	21200	20:34:29	22	20	20
86	24600	18800	20:34:40	23	21	21
87	24600	16500	20:34:52	24	22	22
88	24600	14200	20:35:03	25	23	23
89	24700	12000	20:35:14	26		
90	24700	09700	20:35:25	27		
91	24700	07300	20:35:36	28		
92	24800	04800	20:35:47	29		
93	24800	02900	20:35:59	30		
94	24800	00500	20:36:09	31		

*For conciseness, the first digit of the x-coordinate, and the first 2 digits of the y-coordinate, have been omitted. These digits are 6 for the x-coordinate and 56 for all y-coordinates except Photo point 33 of Photo Line 1, for which they are 55.

Comparison of Point Numbering Systems for Photographic Images,
in Auxiliary Data Files (CCRS and working versions)
and in Photogrammetric Adjustment

Photo. Line 3				Chronological Line 5		
Photo Image	UTM Coordinates*		Time (h:m:s)	CCRS Point No.	Aux. Pt.No.	Photo. Pt.No.
	X	Y				
128	27800	69900				
129	27800	67600	20:53:58	1		
130	28200	65400	20:54:08	2	1	1
131	28200	63300	20:54:19	3	2	2
132	28300	61100	20:54:29	4	3	3
133	28300	58900	20:54:40	5	4	4
134	28300	56700	20:54:50	6	5	5
135	28400	54400	20:55:01	7	6	6
136	28400	52300	20:55:12	8	7	7
137	28400	50000	20:55:23	9	8	8
138	28400	47700	20:55:34	10	9	9
139	28400	45300	20:55:46	11	10	10
140	28500	43000	20:55:57	12	11	11
141	28500	40600	20:56:09	13	12	12
142	28600	38200	20:56:20	14	13	13
143	28600	35800	20:56:32	15	14	14
144	28700	33500	20:56:43	16	15	15
145	28700	31100	20:56:54	17	16	16
146	28700	28700	20:57:06	18	17	17
147	28800	26300	20:57:17	19	18	18
148	28800	24000	20:57:29	20	19	19
149	28800	21600	20:57:40	21	20	20
150	28900	19200	20:57:52	22	21	21
151	28900	16800	20:58:03	23	22	22
152	29000	14500	20:58:14	24	23	23
153	29000	12100	20:58:26	25	24	24
154	29000	09700	20:58:38	26	25	25
155	29000	07300	20:58:49	27	26	26
156	29100	04900	20:59:00	28	27	27
157	29100	02500	20:59:12	29	28	28
158	29100	00200	20:59:23	30		

*For conciseness, the first digit of the x-coordinate, and the first 2 digits of the y-coordinate, have been omitted. These digits are 6 for the x-coordinate and 56 for all y-coordinates except Photo point 33 of Photo Line 1, for which they are 55.

Comparison of Point Numbering Systems for Photographic Images,
in Auxiliary Data Files (CCRS and working versions)
and in Photogrammetric Adjustment

Photo. Line 4				Chronological Line 2		
Photo Image	UTM Coordinates*		Time (h:m:s)	CCRS Point No.	Aux. Pt.No.	Photo. Pt.No.
	X	Y				
62	31600	67700	20:24:11	29	29	1
61	31600	65300	20:24:01	28	28	2
60	31600	62800	20:23:50	27	27	3
59	31600	60400	20:23:39	26	26	4
58	31600	58100	20:23:29	25	25	5
57	31700	55700	20:23:18	24	24	6
56	31700	53300	20:23:07	23	23	7
55	31700	50900	20:22:56	22	22	8
54	31800	48500	20:22:46	21	21	9
53	31800	46000	20:22:35	20	20	10
52	31900	43700	20:22:24	19	19	11
51	31900	41300	20:22:13	18	18	12
50	31900	38900	20:22:03	17	17	13
49	32000	36500	20:21:52	16	16	14
48	32000	34100	20:21:41	15	15	15
47	32000	31700	20:21:31	14	14	16
46	32100	29300	20:21:20	13	13	17
45	32100	26900	20:21:09	12	12	18
44	32100	24400	20:20:58	11	11	19
43	32200	21900	20:20:47	10	10	20
42	32200	19400	20:20:36	9	9	21
41	32200	16900	20:20:24	8	8	22
40	32200	14400	20:20:13	7	7	23
39	32300	12000	20:20:02	6	6	24
38	32300	09600	20:19:51	5	5	25
37	32300	07300	20:19:41	4	4	26
36	32300	05000	20:19:31	3	3	27
35	32400	02700	20:19:20	2	2	28
34	32400	00400	20:19:10	1	1	29

*For conciseness, the first digit of the x-coordinate, and the first 2 digits of the y-coordinate, have been omitted. These digits are 6 for the x-coordinate and 56 for all y-coordinates except Photo point 33 of Photo Line 1, for which they are 55.

Comparison of Point Numbering Systems for Photographic Images,
in Auxiliary Data Files (CCRS and working versions)
and in Photogrammetric Adjustment

Photo. Line 5				Chronological Line 4		
Photo Image	UTM Coordinates*		Time (h:m:s)	CCRS Point No.	Aux. Pt.No.	Photo. Pt.No.
	X	Y				
127	36400	66300	20:47:12	32	31	1
126	36400	63900	20:47:02	31	30	2
125	36500	61500	20:46:52	30	29	3
124	36600	59300	20:46:42	29	28	4
123	36600	57000	20:46:32	28	27	5
122	36700	54900	20:46:22	27	26	6
121	36800	52700	20:46:12	26	25	7
120	36800	50600	20:46:03	25	24	8
119	36800	48400	20:45:53	24	23	9
118	36900	46200	20:45:43	23	22	10
117	36900	44000	20:45:34	22	21	11
116	36900	41800	20:45:24	21	20	12
115	37000	39700	20:45:15	20	19	13
114	37000	37500	20:45:05	19	18	14
113	37100	35300	20:44:55	18	17	15
112	37200	33100	20:44:45	17	16	16
111	37200	31000	20:44:36	16	15	17
110	37300	28800	20:44:26	15	14	18
109	37300	26700	20:44:17	14	13	19
108	37300	24500	20:44:07	13	12	20
107	37300	22300	20:43:57	12	11	21
106	37300	20200	20:43:48	11	10	22
105	37300	18000	20:43:38	10	9	23
104	37300	15800	20:43:28	9	8	24
103	37300	13700	20:43:19	8	7	25
102	37300	11500	20:43:09	7	6	26
101	37300	09300	20:43:00	6	5	27
100	37300	07200	20:42:50	5	4	28
99	37300	05100	20:42:41	4	3	29
98	37400	03000	20:42:31	3	2	30
97	37400	01000	20:42:22	2	1	31
96			20:42:13	1		

*For conciseness, the first digit of the x-coordinate, and the first 2 digits of the y-coordinate, have been omitted. These digits are 6 for the x-coordinate and 56 for all y-coordinates except Photo point 33 of Photo Line 1, for which they are 55.

APPENDIX B

Calculation of convergence of meridians

For the convergence of meridians in the UTM projection, a linear approximation to the usual formula [Frankich] was developed, in order to simplify programming and reduce computing time.

The study area lies within a rectangle in the UTM projection whose boundaries are:

$$x = 610000, x = 650000, y = 5600000 \text{ and } y = 5670000.$$

The value of the convergence was found for each corner of this rectangle. The mean of all four values was 1.4324° . Corresponding to a change of 40000m in x between the west and east boundaries of the rectangle, there was a change of 0.440325° in the convergence (this was the mean of the changes along the south and north boundaries), equivalent to 1.10081×10^{-5} deg per metre change in x. Similarly there was a change of

4.581746×10^{-7} deg per metre change in y. The midpoint of the rectangle has coordinates $x = 630000, y = 5635000$. These values are therefore used in the following linear formula:

Convergence of meridians (degrees) =

$$1.4324 + 1.10081 \times 10^{-5}(x - 630000) + 4.58174 \times 10^{-7}(y - 5635000)$$

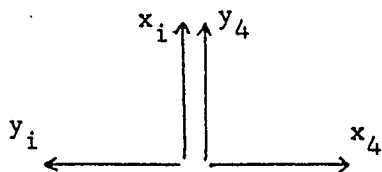
When the values derived from this formula are compared to the originally calculated ones for the corners of the rectangle, the discrepancies are less than 0.0025° in each case, being positive at the northwest and southeast corners and negative at the southwest and northeast corners.

APPENDIX C

Transformation between Ground-based and Camera-based
Coordinate Systems in terms of Roll, Pitch and Heading Angles

(1) Rotation in image plane

In the original image coordinates (x_i, y_i) , x_i is positive in the direction of flight. One rotates about the z-axis to the system (x_4, y_4, z_4) where y_4 is in the direction of flight.

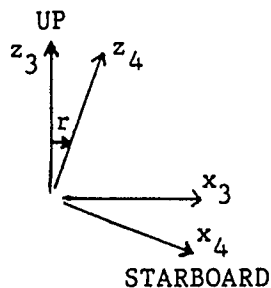


$$\begin{bmatrix} x_4 \\ y_4 \\ z_4 \end{bmatrix} = \begin{bmatrix} 0 & -1 & 0 \\ 1 & 0 & 0 \\ 0 & 0 & 1 \end{bmatrix} \begin{bmatrix} x_i \\ y_i \\ z_i \end{bmatrix}$$

$$\begin{aligned} x_4 &= -y_i \\ \text{or } y_4 &= x_i \\ z_4 &= z_i \end{aligned}$$

(2) Roll Angle

A roll angle of r is defined as a positive rotation through angle r about the fore-aft axis, i.e. about the y_4 axis. One now rotates about the y-axis through angle r to relate to the system (x_3, y_3, z_3) , where the z_3 axis is in a vertical plane.

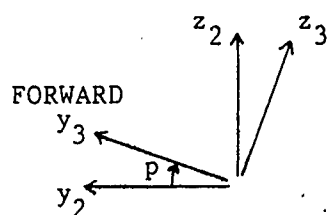


$$\begin{bmatrix} x_3 \\ y_3 \\ z_3 \end{bmatrix} = \begin{bmatrix} \cos r & 0 & \sin r \\ 0 & 1 & 0 \\ -\sin r & 0 & \cos r \end{bmatrix} \begin{bmatrix} x_4 \\ y_4 \\ z_4 \end{bmatrix}$$

$$\begin{aligned} x_3 &= x_4 \cos r + z_4 \sin r \\ \text{or } y_3 &= y_4 \\ z_3 &= -x_4 \sin r + z_4 \cos r \end{aligned}$$

(3) Pitch

Pitch angle p is measured in a vertical plane from the horizontal to the camera fore-aft axis, being positive when the aircraft is climbing. One rotates about the x -axis through angle p to relate to the system (x_2, y_2, z_2) , where z_2 is vertical.

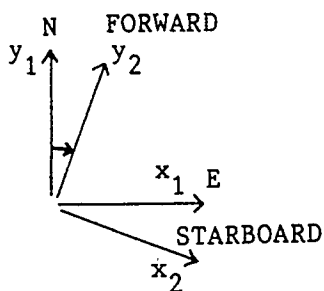


$$\begin{bmatrix} x_2 \\ y_2 \\ z_2 \end{bmatrix} = \begin{bmatrix} 1 & 0 & 0 \\ 0 & \cos p & -\sin p \\ 0 & \sin p & \cos p \end{bmatrix} \begin{bmatrix} x_3 \\ y_3 \\ z_3 \end{bmatrix}$$

$$\begin{aligned} x_2 &= x_3 \\ \text{or } y_2 &= y_3 \cos p - z_3 \sin p \\ z_2 &= y_3 \sin p + z_3 \cos p \end{aligned}$$

(4) Heading

Heading angle h is the bearing or azimuth towards which the aircraft (the x_1 axis) is headed. One now rotates about the z -axis through angle h to relate to the ground-based coordinate system (x_1, y_1, z_1) , in which y_1 is north and x_1 is east.



$$\begin{bmatrix} x_1 \\ y_1 \\ z_1 \end{bmatrix} = \begin{bmatrix} \cos h & \sin h & 0 \\ -\sin h & \cos h & 0 \\ 0 & 0 & 1 \end{bmatrix} \begin{bmatrix} x_2 \\ y_2 \\ z_2 \end{bmatrix}$$

$$\begin{aligned} x_1 &= x_2 \cos h + y_2 \sin h \\ \text{or } y_1 &= -x_2 \sin h + y_2 \cos h \\ z_1 &= z_2 \end{aligned}$$

Combining the four rotations,

$$\begin{bmatrix} x_1 \\ y_1 \\ z_1 \end{bmatrix} = \begin{bmatrix} \cos h & \sin h & 0 \\ -\sin h & \cos h & 0 \\ 0 & 0 & 1 \end{bmatrix} \begin{bmatrix} 1 & 0 & 0 \\ 0 & \cos p & -\sin p \\ 0 & \sin p & \cos p \end{bmatrix} \begin{bmatrix} \cos r & 0 & \sin r \\ 0 & 1 & 0 \\ -\sin r & 0 & \cos r \end{bmatrix} \begin{bmatrix} 0 & -1 & 0 \\ 1 & 0 & 0 \\ 0 & 0 & 1 \end{bmatrix} \begin{bmatrix} x_i \\ y_i \\ z_i \end{bmatrix}$$

$$\therefore \begin{bmatrix} x_1 \\ y_1 \\ z_1 \end{bmatrix} = \begin{bmatrix} \cos h & \cos p \sin h & -\sin p \sin h \\ -\sin h & \cos p \cos h & -\sin p \cos h \\ 0 & \sin p & \cos p \end{bmatrix} \begin{bmatrix} 0 & -\cos r & \sin r \\ 1 & 0 & 0 \\ 0 & \sin r & \cos r \end{bmatrix} \begin{bmatrix} x_i \\ y_i \\ z_i \end{bmatrix}$$

$$\therefore \begin{bmatrix} x_1 \\ y_1 \\ z_1 \end{bmatrix} = \begin{bmatrix} \cos p \sin h & -\cos r \cos h - \sin r \sin p \sin h & \sin r \cos h - \cos r \sin p \sin h \\ \cos p \cos h & \cos r \sin h - \sin r \sin p \cos h & -\sin r \sin h - \cos r \sin p \cos h \\ \sin p & \sin r \cos p & \cos r \cos p \end{bmatrix} \begin{bmatrix} x_i \\ y_i \\ z_i \end{bmatrix} \quad (C1)$$

When p and r are small angles, an approximation to this can be made, putting $\cos p = \cos r = 1$ and neglecting any product $\sin p \sin r$.

$$\text{Then } \begin{bmatrix} x_1 \\ y_1 \\ z_1 \end{bmatrix} = \begin{bmatrix} \sin h & -\cos h & \sin r \cos h - \sin p \sin h \\ \cos h & \sin h & -\sin r \sin h - \sin p \cos h \\ \sin p & \sin r & 1 \end{bmatrix} \begin{bmatrix} x_i \\ y_i \\ z_i \end{bmatrix} \quad (C2)$$

In a similar way, the reverse transformation can be determined:

$$\begin{bmatrix} x_i \\ y_i \\ z_i \end{bmatrix} = \begin{bmatrix} \cos p \sin h & \cos p \cos h & \sin p \\ -\cos r \cos h - \sin p \sin h \sin r & \sin h \cos r - \sin p \cos h \sin r & \cos p \sin r \\ \sin r \cos h - \cos r \sin p \sin h & -\sin r \sin h - \cos r \sin p \cos h & \cos p \cos r \end{bmatrix} \begin{bmatrix} x_1 \\ y_1 \\ z_1 \end{bmatrix} \quad (C3)$$

which is approximated by

$$\begin{bmatrix} x_i \\ y_i \\ z_i \end{bmatrix} = \begin{bmatrix} \sin h & \cos h & \sin p \\ \cos h & \sin h & \sin r \\ \sin r \cos h - \sin p \sin h & -\sin r \sin h - \sin p \cos h & 1 \end{bmatrix} \begin{bmatrix} x_1 \\ y_1 \\ z_1 \end{bmatrix} \quad (C4)$$

APPENDIX D

Determination of Range, Roll, Pitch and Heading from
Photogrammetry via Orientation Angles ϕ , ω and κ .

If components of a vector are (x_i, y_i, z_i) in the camera system, and (X, Y, Z) in the ground system, then from [Moffit and Mikhail, 1980, p598]

$$\begin{bmatrix} x_i \\ y_i \\ z_i \end{bmatrix} = \begin{bmatrix} \cos \phi \cos \kappa & \cos \omega \sin \kappa + \sin \omega \sin \phi \cos \kappa & \sin \omega \sin \kappa - \cos \omega \sin \phi \cos \kappa \\ -\cos \phi \sin \kappa & \cos \omega \cos \kappa - \sin \omega \sin \phi \sin \kappa & \sin \omega \cos \kappa + \cos \omega \sin \phi \sin \kappa \\ \sin \phi & -\sin \omega \cos \phi & \cos \omega \cos \phi \end{bmatrix} \begin{bmatrix} X \\ Y \\ Z \end{bmatrix} \quad (D1)$$

For the inverse transformation, one takes the transpose of the matrix, giving

$$\begin{bmatrix} X \\ Y \\ Z \end{bmatrix} = \begin{bmatrix} \cos \phi \cos \kappa & -\cos \phi \sin \kappa & \sin \phi \\ \cos \omega \sin \kappa + \sin \omega \sin \phi \cos \kappa & \cos \omega \cos \kappa - \sin \omega \sin \phi \sin \kappa & -\sin \omega \cos \phi \\ \sin \omega \sin \kappa - \cos \omega \sin \phi \cos \kappa & \sin \omega \cos \kappa + \cos \omega \sin \phi \sin \kappa & \cos \omega \cos \phi \end{bmatrix} \begin{bmatrix} x_i \\ y_i \\ z_i \end{bmatrix} \quad (D2)$$

To determine ϕ and ω :

(D2) is applied to the case where $[x_i, y_i, z_i]^T = [0 \ 0 \ R]^T$, which is perpendicular to the image plane, with z_i positive upwards. This is the vector from the QNP to the PC, if R is the distance between these two points.

$$\text{Then} \quad \begin{bmatrix} X \\ Y \\ Z \end{bmatrix} = \begin{bmatrix} R \sin \phi \\ -R \sin \omega \cos \phi \\ R \cos \omega \cos \phi \end{bmatrix} \quad (D3)$$

The SPACE-M output gives X , Y and Z , each of which is equal to the (PC coordinate) minus (QNP coordinate).

From (D3), it follows that $R^2 = X^2 + Y^2 + Z^2$

As $X = R \sin \phi$, then $\sin \phi = X/R$

As $Y = -R \sin \omega \cos \phi$, then $\sin \omega = -Y/R \cos \phi = -Y/(Y^2 + Z^2)^{1/2}$

Hence $\cos \omega = Z/(Y^2 + Z^2)^{1/2}$ and $\tan \omega = -Y/Z$

To determine κ :

Consider a vector whose components are X, Y, Z in the ground system and (x_i, y_i, z_i) in the camera system. For this application, a convenient vector is one from the QNP of the current image to the QNP of a neighbouring image. From (D1),

$$x_i = X \cos \phi \cos \kappa + Y \cos \omega \sin \kappa + Y \sin \omega \sin \phi \cos \kappa + Z \sin \omega \sin \kappa - Z \cos \omega \sin \phi \cos \kappa \quad (D4)$$

$$y_i = -X \cos \phi \sin \kappa + Y \cos \omega \cos \kappa - Y \sin \omega \sin \phi \sin \kappa + Z \sin \omega \cos \kappa + Z \cos \omega \sin \phi \sin \kappa \quad (D5)$$

which can be written

$$x_i = \cos \kappa (X \cos \phi + Y \sin \omega \sin \phi - Z \cos \omega \sin \phi) + \sin \kappa (Y \cos \omega + Z \sin \omega)$$

$$y_i = \cos \kappa (Y \cos \omega + Z \sin \omega) + \sin \kappa (-X \cos \phi - Y \sin \omega \sin \phi + Z \cos \omega \sin \phi)$$

$$\text{Putting } C_1 = X \cos \phi + Y \sin \omega \sin \phi - Z \cos \omega \sin \phi \quad (D6)$$

$$\text{and } C_2 = Y \cos \omega + Z \sin \omega \quad (D7)$$

$$\text{then } x_i = \cos \kappa C_1 + \sin \kappa C_2, \quad y_i = \cos \kappa C_2 - \sin \kappa C_1$$

To solve this pair of equations for κ ,

$$\text{let } C_1 = m \cos \psi, C_2 = m \sin \psi, \text{ so } \tan \psi = C_2/C_1.$$

$$\text{Then } x_i = m(\cos \kappa \cos \psi + \sin \kappa \sin \psi) = m \cos(\psi - \kappa)$$

$$y_i = m(\cos \kappa \sin \psi - \sin \kappa \cos \psi) = m \sin(\psi - \kappa)$$

$$\text{So } \tan(\psi - \kappa) = y_i/x_i \text{ and } \psi - \kappa = \tan^{-1}(y_i/x_i)$$

Hence,

$$\kappa = \psi - \tan^{-1}(y_i/x_i) = \tan^{-1}(C_2/C_1) - \tan^{-1}(y_i/x_i) \quad (D8)$$

In evaluating κ from this formula, one should first take the principal values of the inverse tangents, and then check the result in (D4) or (D5) to see whether 180° (π radians) should be

added or subtracted. x_1 and y_1 refer to the components of a vector between QNP's on the ground. However, since they are in the camera coordinate system, the ratio y_1/x_1 will still be the same if x_1 and y_1 refer to the components of the corresponding vector in the image plane. Therefore, in applying formula (D8), image coordinates can be used for x_1 and y_1 , and ground coordinates in the terms C_1 and C_2 , which are determined from (D6) and (D7).

In applying (D8) to the present situation, one should note that since the inter-QNP vectors are nearly parallel to the flight line, and the x_1 direction is also close to the flight line direction, then generally $|y_1| \ll |x_1|$. Also from (D6) and (D7), $C_1 \approx X$ and $C_2 \approx Y$. Since the flight lines are approximately in a N-S or S-N direction, then $|Y| \gg |X|$, so $|C_2| \gg |C_1|$. In the analysis of the accuracy of κ which follows, it is shown that it is desirable for the arguments of the inverse tangents to be small in magnitude. (D8) can be rewritten to satisfy this requirement.

$$\begin{aligned} \text{Putting } \psi &= \tan^{-1}(C_2/C_1), \text{ or } \tan \psi = C_2/C_1, \\ \text{then } C_1/C_2 &= \cot \psi = \tan(90^\circ - \psi), \\ \text{so } 90^\circ - \psi &= \tan^{-1}(C_1/C_2) \text{ and } \psi = 90^\circ - \tan^{-1}(C_1/C_2) \\ \text{Hence } \kappa &= 90^\circ - \tan^{-1}(C_1/C_2) - \tan^{-1}(y_1/x_1) \end{aligned} \quad (D9)$$

To ascertain the accuracy of κ , first consider Eq. (D8).

Putting $\psi = \tan^{-1}(C_2/C_1)$ and $\theta = \tan^{-1}(y_1/x_1)$, $\kappa = \psi - \theta$

Then the variance of κ is $\sigma^2(\kappa) = \left(\frac{\partial \kappa}{\partial \psi}\right)^2 \sigma^2(\psi) + \left(\frac{\partial \kappa}{\partial \theta}\right)^2 \sigma^2(\theta) = \sigma^2(\psi) + \sigma^2(\theta)$

$$\psi = \tan^{-1}(C_2/C_1) = \tan^{-1}t, \text{ where } t = C_2/C_1$$

$$\therefore \frac{\partial \psi}{\partial t} = \frac{1}{1+t^2} \quad \therefore \sigma^2(\psi) = \frac{1}{(1+t^2)^2} \cdot \sigma^2(t)$$

As $t = C_2/C_1$, $\sigma^2(t) = \sigma^2(C_2) \cdot \frac{1}{C_1^2} + \sigma^2(C_1) \left(\frac{-C_2}{C_1^2}\right)^2$

As $C_1 \approx X$ and $C_2 \approx Y$, $\sigma^2(t) \approx \frac{\sigma^2(Y)}{X^2} + \frac{\sigma^2(X) \cdot Y^2}{X^4} = \frac{1}{X^2} [\sigma^2(Y) + \frac{Y^2}{X^2} \sigma^2(X)]$

If $|X| \ll |Y|$, then $\sigma^2(t)$ will be very sensitive to errors in X .

Now consider Eq. (D9).

By the same method, and putting $\psi = \tan^{-1}(C_1/C_2) \approx \tan^{-1}(X/Y)$,

it is found that $\sigma^2(\kappa) = \sigma^2(\psi) + \sigma^2(\theta)$ as before

$$\sigma^2(\psi) = (1+t^2)^{-2} \cdot \sigma^2(t), \text{ where } t = C_1/C_2 \approx X/Y$$

$$\sigma^2(t) = \frac{1}{Y^2} [\sigma^2(X) + \frac{X^2}{Y^2} \sigma^2(Y)]$$

Now if $|X| \ll |Y|$, which is generally so, $\sigma^2(t) \approx \sigma^2(X)/Y^2$

$$\text{Also } (1+t^2)^2 \approx 1, \text{ so } \sigma^2(\psi) \approx \sigma^2(X)/Y^2$$

Similarly, if $|y_1| \ll |x_1|$, $\sigma^2(\theta) \approx \sigma^2(y_1)/x_1^2$

$$\text{So } \sigma^2(\kappa) = \sigma^2(X)/Y^2 + \sigma^2(y_1)/x_1^2$$

$\sigma^2(X)$ and $\sigma^2(y_1)$ are generally independent of position.

If the length of the QNP vector is doubled, then both Y and x_1 are doubled. Therefore $\sigma(\kappa)$ is halved. This fact can be used in choosing weighting factors to make the best estimate of κ .

At position i in a flight line, with QNP Q_i , the positions of Q_{i-2} , Q_{i-1} , Q_i , Q_{i+1} and Q_{i+2} are usually given. The vectors between Q_i and $Q_{i\pm 2}$ are twice as long as those between Q_i and $Q_{i\pm 1}$, therefore from the foregoing error analysis, the estimates of κ from the longer vectors should be twice as accurate as those from the shorter ones. The best estimate of κ is, consequently, made by taking a weighted mean of the individual estimates, with vectors between points Q_i and $Q_{i\pm 2}$ being given twice as much weight as those between points Q_i and $Q_{i\pm 1}$.

Once ϕ , ω and κ are determined, there is the final step of finding the roll angle r , pitch angle p and heading angle h .

From Eq. (C3),

$$\begin{bmatrix} x_i \\ y_i \\ z_i \end{bmatrix} = \begin{bmatrix} \cos p \sin h & \cos p \cos h & \sin p \\ -\cos r \cos h - \sin p \sin h \sin r & \sin h \cos r - \sin p \cos h \sin r & \cos p \sin r \\ \sin r \cos h - \cos r \sin p \sin h & -\sin r \sin h - \cos r \sin p \cos h & \cos p \cos r \end{bmatrix} \begin{bmatrix} X \\ Y \\ Z \end{bmatrix}$$

and from Eq. (D1),

$$\begin{bmatrix} x_i \\ y_i \\ z_i \end{bmatrix} = \begin{bmatrix} \cos \phi \cos \kappa & \cos \omega \sin \kappa + \sin \omega \sin \phi \cos \kappa & \sin \omega \sin \kappa - \cos \omega \sin \phi \cos \kappa \\ -\cos \phi \sin \kappa & \cos \omega \cos \kappa - \sin \omega \sin \phi \sin \kappa & \sin \omega \cos \kappa + \cos \omega \sin \phi \sin \kappa \\ \sin \phi & -\sin \omega \cos \phi & \cos \omega \cos \kappa \end{bmatrix} \begin{bmatrix} X \\ Y \\ Z \end{bmatrix}$$

and so elements in the two rotation matrices can be compared.

Comparing elements in position (1,3),

$$\sin p = \sin \omega \sin \kappa - \cos \omega \sin \phi \cos \kappa.$$

Assuming that the aircraft is not flying upside down, p will then be the principal value of $\sin^{-1}(\sin \omega \sin \kappa - \cos \omega \sin \phi \cos \kappa)$; as p is close to zero, the inverse sine function will give a good estimate.

Next comparing elements in position (2,3),

$\cos p \sin r = \sin \omega \cos \kappa + \cos \omega \sin \phi \sin \kappa$, and p is known.

Therefore $r = \sin^{-1}(\sin \omega \cos \kappa + \cos \omega \sin \phi \sin \kappa)/\cos p$

As r is close to zero, the principal value of the inverse sine is the value required. (If elements in position (3,3) were compared, r would be expressed as an inverse cosine, which would not only give a less accurate result for an angle near zero, but also involve an ambiguity, since r may or may not be a principal value.)

Finally, elements in positions (1,1) and (1,2) are compared:

$\cos p \sin h = \cos \phi \cos \kappa$, giving $h = \sin^{-1}(\cos \phi \cos \kappa/\cos p)$

$\cos p \cos h = \cos \omega \sin \kappa + \sin \omega \sin \phi \cos \kappa$, giving

$$h = \cos^{-1}(\cos \omega \sin \kappa + \sin \omega \sin \phi \cos \kappa)/\cos p$$

p is already known in these expressions.

h can be in any quadrant, so both of these expressions are needed for an unambiguous determination. In the present situation, h is close to $0^\circ/360^\circ$ or 180° , therefore, for best accuracy, h is determined first from $h = \sin^{-1}(\cos \phi \cos \kappa / \cos p)$, which gives a principal value between -90° and $+90^\circ$. For this range of angles, the argument of the inverse cosine in the second expression is positive. If that argument is negative, then the principal value of the inverse sine must be subtracted from 180° .

Summary

R is determined from $R = (X_p^2 + Y_p^2 + Z_p^2)^{1/2}$

ϕ and ω are determined from $\sin \phi = X_p/R$, $\sin \omega = -Y_p/R \cos \phi$, where X_p , Y_p , Z_p and R refer to components and length of the vector from QNP to PC.

$$\kappa = 90^\circ - \tan^{-1}(C_1/C_2) - \tan^{-1}(y_1/x_1)$$

where $C_1 = X_q \cos \phi + (Y_q \sin \omega - Z_q \cos \omega) \sin \phi$

$$C_2 = Y_q \cos \omega + Z_q \sin \omega$$

X_q , Y_q , Z_q are components of the vector between QNP's

x_1 , y_1 are components of the image of this vector.

To ensure that the value of κ is correct using principal values of \tan^{-1} , one checks whether the correct value of x_1 is given by $C_1 \cos \kappa + C_2 \sin \kappa$. If the sign is opposite, κ should be changed by 180° .

For a best estimate of κ , use a weighted mean of all values.

For a single interval (Q_i to Q_{i+1}), weight = 1

For a double interval (Q_i to Q_{i+2}), weight = 2

For a triple interval (Q_1 to Q_{1+3}), weight = 3.

(At this point, if there are 3 or more estimates of κ , one has the option of rejecting outliers. An arbitrary but practical criterion is to reject any estimate which differs from the mean of the estimates by more than 1.5 times the standard deviation of the estimates.)

Having found ϕ , ω and κ , then

$$p = \sin^{-1}(\sin \omega \sin \kappa - \cos \omega \sin \phi \cos \kappa) \quad (\text{Principal value})$$

$$r = \sin^{-1}(\sin \omega \cos \kappa + \cos \omega \sin \phi \sin \kappa) / \cos p \quad (\text{Princ. val.})$$

$$h = \sin^{-1}(\cos \phi \cos \kappa / \cos p)$$

-use principal value if $\cos \omega \sin \kappa + \sin \omega \sin \phi \cos \kappa > 0$

-subtract from 180° if $\cos \omega \sin \kappa + \sin \omega \sin \phi \cos \kappa < 0$

Comments

The effect of tilt in determining h from κ was found in practice to be negligible. It was found that $h = -(\kappa - 90^\circ)$ to within 0.001° in every case, even though tilt angles were almost as great as 3° .

It is assumed in these derivations that image coordinates (x_i, y_i) are measured in a right-handed system, i.e. such that the transformation from the image coordinates to the ground coordinates of any point does not involve a reflection. It is also assumed that the positive x-axis for the image coordinates is in the direction of flight. If this is not so (as was the case for (spatial) flight lines 4 and 5 in this project), then a rotation of 180° (i.e. a change of sign) must be applied to the image coordinates.

APPENDIX E

Derivation of Principal Point Offset Compensation

The formulas derived in Appendix D assume that the QNP ground coordinates correspond exactly to the principal point of the image. In practice, image measurements may have been made at a point having image coordinates (x_i, y_i) , which is near, but not exactly at, the principal point. Therefore correction to the image coordinates should be considered.

In Fig. E.1, let P be the perspective centre, let q be the image point, near the principal point, for which measurements were made, and let Q be the corresponding point on the ground.

In applying equation (D2) of Appendix D, one considered the situation where the vector $QP = [0 \ 0 \ R]^T$ in the camera coordinate system, corresponding to the case where $x_i = 0$ and $y_i = 0$.

Camera System

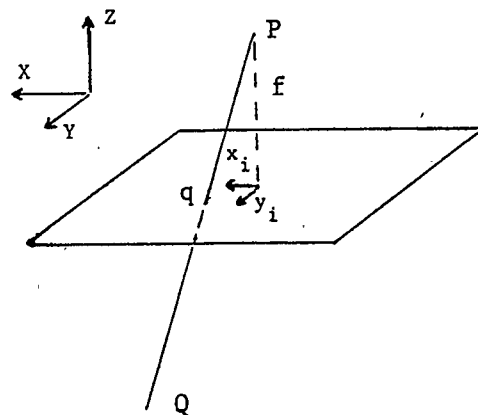


Fig. E.1: Geometry for Principal Point Offset Compensation.

When x_i and y_i are not zero, then $QP = k.Pq$, where k is some scale factor (k is negative, because QP and Pq are in opposite directions), and $Pq = [x_i \ y_i \ -f]^T$. Hence $QP = k[x_i \ y_i \ -f]^T$. Equation (D2) is now applied to the case where $[x_i \ y_i \ z_i]^T = QP$, giving

$$\begin{bmatrix} X \\ Y \\ Z \end{bmatrix} = k \begin{bmatrix} \cos \phi \cos \kappa & -\cos \phi \sin \kappa & \sin \phi \\ \cos \omega \sin \kappa + \sin \omega \sin \phi \cos \kappa & \cos \omega \cos \kappa - \sin \omega \sin \phi \sin \kappa & -\sin \omega \cos \phi \\ \sin \omega \sin \kappa - \cos \omega \sin \phi \cos \kappa & \sin \omega \cos \kappa + \cos \omega \sin \phi \sin \kappa & \cos \omega \cos \phi \end{bmatrix} \begin{bmatrix} x_i \\ y_i \\ -f \end{bmatrix} \quad (E1)$$

in which $[X \ Y \ Z]^T$ represents QP in ground coordinates.

Since the square matrix in (E1) is orthogonal, it follows that the vectors $[X \ Y \ Z]^T$ and $k[x_i \ y_i \ -f]^T$ have the same norm.

$$\text{Hence } k = -[(X^2 + Y^2 + Z^2)/(x_i^2 + y_i^2 + f^2)]^{1/2}$$

Given the values of X, Y, Z, x_i, y_i and f , equation (E1) must now be solved for ω and ϕ .

(E1) corresponds to three scalar equations, of which two are

$$X = k[x_i \cos \phi \cos \kappa - y_i \cos \phi \sin \kappa - f \sin \phi] \quad (E2)$$

$$\text{and } Y = k[x_i(\cos \omega \sin \kappa + \sin \omega \sin \phi \cos \kappa) + y_i(\cos \omega \cos \kappa - \sin \omega \sin \phi \sin \kappa) + f \sin \omega \cos \phi] \quad (E3)$$

One can note here that since $|x_i| \ll f$ and $|y_i| \ll f$, ω and ϕ will be close to the values ω_0 and ϕ_0 that would be obtained from the algorithm described in Appendix D. Therefore one can put

$$\phi = \phi_0 + \Delta\phi, \quad \omega = \omega_0 + \Delta\omega,$$

$$\text{where } \sin \phi_0 = X/(X^2 + Y^2 + Z^2)^{1/2}, \quad \sin \omega_0 = -Y/(Y^2 + Z^2)^{1/2}$$

$$\text{and so } \cos \phi_0 = [(Y^2 + Z^2)/(X^2 + Y^2 + Z^2)]^{1/2}, \quad \cos \omega_0 = Z/(Y^2 + Z^2)^{1/2}$$

$\cos \phi_0$ and $\cos \omega_0$ are both positive because ϕ_0 and ω_0 are small angles. Also $Z > 0$. Substituting thus for ϕ and ω in (E2),

$$\frac{X}{k} = x_i(\cos \phi_0 \cos \Delta\phi - \sin \phi_0 \Delta\phi) \cos \kappa - y_i(\cos \phi_0 \cos \Delta\phi - \sin \phi_0 \sin \Delta\phi) \sin \kappa - f(\sin \phi_0 \cos \Delta\phi + \cos \phi_0 \sin \Delta\phi)$$

Making the approximations $\cos \Delta\phi = \cos \Delta\omega = 1$, and neglecting the product $\sin \phi_0 \sin \Delta\phi$, then

$$\frac{X}{k} = x_i \cos \phi_0 \cos \kappa - y_i \cos \phi_0 \sin \kappa - f(\sin \phi_0 + \cos \phi_0 \sin \Delta\phi)$$

$$\text{Hence } f(\sin \phi_0 + \cos \phi_0 \sin \Delta\phi) = x_i \cos \kappa \cos \phi_0 - y_i \sin \kappa \cos \phi_0 - \frac{X}{k},$$

$$\text{giving } f \cos \phi_0 \sin \Delta\phi = x_i \cos \kappa \cos \phi_0 - y_i \sin \kappa \cos \phi_0 - \frac{X}{k} - f \sin \phi_0,$$

$$\text{and } \sin \Delta\phi = \frac{x_i}{f} \cos \kappa - \frac{y_i}{f} \sin \kappa - \frac{X}{f k \cos \phi_0} - \tan \phi_0.$$

$$\text{As } k \cos \phi_0 = -[(Y^2 + Z^2)/(x_i^2 + y_i^2 + z_i^2)]^{1/2} \quad \text{and} \quad \tan \phi_0 = X/(Y^2 + Z^2)^{1/2},$$

$$\begin{aligned} \text{then } \sin \Delta\phi &= \frac{x_i}{f} \cos \kappa - \frac{y_i}{f} \sin \kappa + \frac{X}{f} [(x_i^2 + y_i^2 + z_i^2)/(Y^2 + Z^2)]^{1/2} - X/(Y^2 + Z^2)^{1/2} \\ &= \frac{x_i}{f} \cos \kappa - \frac{y_i}{f} \sin \kappa + \frac{X}{(Y^2 + Z^2)^{1/2}} \left[\frac{(x_i^2 + y_i^2 + f^2)^{1/2}}{f} - 1 \right] \end{aligned}$$

Applying the binomial expansion of $[f^2 + (x_i^2 + y_i^2)]^{1/2}$, in which $x_i^2 + y_i^2 \ll f^2$, and neglecting the third and subsequent terms of that expansion,

$$\begin{aligned} \sin \Delta\phi &= \frac{x_i}{f} \cos \kappa - \frac{y_i}{f} \sin \kappa + \frac{X}{(Y^2 + Z^2)^{1/2}} \left(\frac{x_i^2 + y_i^2}{2f^2} \right) \\ &= \frac{x_i}{f} \cos \kappa - \frac{y_i}{f} \sin \kappa + \frac{X}{2(Y^2 + Z^2)^{1/2}} \left(\frac{x_i}{f} \right)^2 + \frac{X}{2(Y^2 + Z^2)^{1/2}} \left(\frac{y_i}{f} \right)^2 \end{aligned}$$

As, generally, $|X| \ll |Z|$, $|x_i| \ll f$ and $|y_i| \ll f$, while either $|\cos \kappa| > 0.7$ or $|\sin \kappa| > 0.7$, it follows that at least one of the first two terms in this expression for $\sin \Delta\phi$ must dominate.

Therefore, as an acceptable approximation,

$$\sin \Delta\phi = (x_i \cos \kappa - y_i \sin \kappa)/f$$

Substituting similarly for ϕ and ω in (E3),

$$\begin{aligned} \frac{Y}{k} &= x_i ([\cos \omega_0 \cos \Delta\omega - \sin \omega_0 \sin \Delta\omega] \sin \kappa + [\sin \omega_0 \cos \Delta\omega + \cos \omega_0 \sin \Delta\omega] \sin \phi \cos \kappa) \\ &+ y_i ([\cos \omega_0 \cos \Delta\omega - \sin \omega_0 \sin \Delta\omega] \cos \kappa - [\sin \omega_0 \cos \Delta\omega + \cos \omega_0 \sin \Delta\omega] \sin \phi \sin \kappa) \\ &+ f (\sin \omega_0 \cos \Delta\omega + \cos \omega_0 \sin \Delta\omega) \cos \phi \end{aligned}$$

and making the same approximations as before,

$$\begin{aligned}\frac{Y}{k} &= x_i (\cos \omega_0 \sin \kappa + [\sin \omega_0 + \cos \omega_0 \sin \Delta\omega] \sin \phi \cos \kappa) \\ &\quad + y_i (\cos \omega_0 \cos \kappa - [\sin \omega_0 + \cos \omega_0 \sin \Delta\omega] \sin \phi \sin \kappa) \\ &\quad + f (\sin \omega_0 + \cos \omega_0 \sin \Delta\omega) \cos \phi \\ &= x_i \cos \omega_0 \sin \kappa + y_i \cos \omega_0 \cos \kappa \\ &\quad + [\sin \omega_0 + \cos \omega_0 \sin \Delta\omega] (x_i \sin \phi \cos \kappa - y_i \sin \phi \sin \kappa + f \cos \phi)\end{aligned}$$

$$\text{Hence } \sin \omega_0 + \cos \omega_0 \sin \Delta\omega = \frac{\frac{Y}{k} - x_i \cos \omega_0 \sin \kappa - y_i \cos \omega_0 \cos \kappa}{x_i \sin \phi \cos \kappa - y_i \sin \phi \sin \kappa + f \cos \phi}$$

and so

$$\begin{aligned}\sin \Delta\omega &= \frac{\frac{Y}{k} - x_i \cos \omega_0 \sin \kappa - y_i \cos \omega_0 \cos \kappa}{(x_i \sin \phi \cos \kappa - y_i \sin \phi \sin \kappa + f \cos \phi) \cos \omega_0} - \tan \omega_0 \\ &= \frac{\frac{Y}{k} - \cos \omega_0 (x_i \sin \kappa + y_i \cos \kappa)}{\cos \omega_0 (\sin \phi [x_i \cos \kappa - y_i \sin \kappa] + f \cos \phi)} - \tan \omega_0 \\ &= \frac{\frac{Y}{k} - \cos \omega_0 (x_i \sin \kappa + y_i \cos \kappa)}{\cos \omega_0 (f \cos \phi - \sin \phi \cdot f \sin \Delta\phi)} - \tan \omega_0 \\ &= \frac{\frac{Y}{k} - \cos \omega_0 (x_i \sin \kappa + y_i \cos \kappa)}{f \cos \omega_0 (\cos \phi + \sin \phi \sin \Delta\phi)} - \tan \omega_0\end{aligned}$$

In the denominator, $\sin \phi \sin \Delta\phi \ll \cos \phi$, justifying the following approximation:

$$\begin{aligned}\sin \Delta\omega &= \frac{\frac{Y}{k} - \cos \omega_0 (x_i \sin \kappa + y_i \cos \kappa)}{f \cos \omega_0 \cos \phi} - \tan \omega_0 \\ &= - \frac{x_i \sin \kappa + y_i \cos \kappa}{f \cos \phi} + \frac{Y}{k f \cos \omega_0 \cos \phi} - \tan \omega_0 \\ &= - \frac{x_i \sin \kappa + y_i \cos \kappa}{f \cos \phi} + Y \left[\frac{1}{Z} + \frac{1}{k f \cos \omega_0 \cos \phi} \right] \quad \text{as } \tan \omega_0 = - \frac{Y}{Z}\end{aligned}$$

Substituting for $k \cos \phi$ and $\cos \omega_0$, the coefficient of Y in this expression can be shown to be $[1 - (f^2 + x_i^2 + y_i^2)/f]/Z$

$$\approx -(x_i^2 + y_i^2)/2f^2Z,$$

using the same binomial approximation as before.

$$\text{Hence } \sin \Delta\omega = - \frac{1}{f \cos \phi} (x_i \sin \kappa + y_i \cos \kappa) - \frac{Y}{2Z} \left[\left(\frac{x_i}{f} \right)^2 + \left(\frac{y_i}{f} \right)^2 \right]$$

For the same reasons as before, it can be assumed that the first term dominates this expression, giving as an acceptable approximation,

$$\sin \Delta\omega = - \frac{1}{f \cos \phi} (x_i \sin \kappa + y_i \cos \kappa)$$

Appendix F

SUGGESTED PROCEDURES FOR USE OF LASER RANGER WITH PHOTOGRAMMETRY

1. Laser Profiling

(a) Application: Determination of terrain elevation.

The laser gives the distance from the instrument to a point on the ground. In addition to this distance, the laser's position and orientation at every reading need to be known. This information can be given by an inertial navigation/positioning system. It is essential to know the laser's alignment relative to the inertial system accurately.

As inertial systems suffer from drift, updates are needed at sufficiently frequent intervals, and these updates should apply to both position and orientation. For an aircraft, an update can be obtained by (a) landing

(b) GPS positioning system

(c) photogrammetry with ground control.

In case (a), there is a zero-velocity, and possibly a position, update. Also the direction of the gravity vector may give some direct input on orientation.

In case (b), the input is on position only, and its usefulness in updating the orientation is questionable.

In case (c), complete position and orientation data are available, provided that the crab angle is known.

Photogrammetry alone could also give the terrain profile without using the laser. However, a combination of photogrammetry

and laser might be desirable

- (i) if the profile itself is more easily obtained from laser readings than from photogrammetry,
- (ii) if the photogrammetry can be used as update at the two ends of a long profile, but cannot be used in the intervening space.

These situations could occur when conjugate images of points in the profile are difficult to identify, e.g. when there is uniform snow, grass or sand cover, or in forested areas (Moreau & Jeudy).

(b) Testing

To avoid errors such as can arise from misalignment, the laser reading needs to be tested against a standard whose accuracy is already known. Photogrammetry is one such standard.

Fig. F.1 shows a photogrammetric model. With adequate ground control and an adjustment, one can find the positions of the two perspective centres PC_1 and PC_2 .

If $p_1, p_2, p_3, p_4, \dots$ represent positions of the laser instrument, and $q_1, q_2, q_3, q_4, \dots$ represent the corresponding positions of the laser spot on the ground, then $p_1q_1, p_2q_2, p_3q_3,$

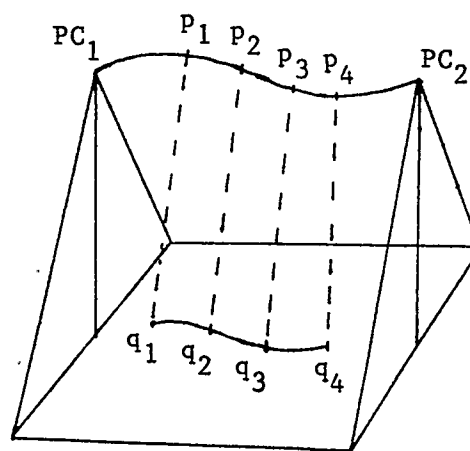


Fig. F.1: Positions of Laser and Laser Spot in Profiling.

p_4q_4 are the distances measured by the laser. Therefore these distances need to be determined by an independent method, to compare them with the actual laser readings.

The positions p_1, p_2, p_3, p_4 and the orientations of the camera can be determined from an inertial system. The inertial system can be updated at the two perspective centres, where the position and camera orientation can be determined from a photogrammetric adjustment (bundle or SPACE-M). The laser beam direction is then determinable if its alignment relative to the camera axis is known.

Knowing the position of p_1 and the direction of the laser beam, then in principle one can determine from the photogrammetric model the point q_1 at which the laser beam meets the ground, as this is a unique point (assuming that there are not any nearly-vertical cliffs). Knowing the position of q_1 , the distance p_1q_1 is easily calculated. This can then be compared with the laser reading taken from p_1 .

In summary, then, the distances p_1q_1, p_2q_2 etc. have been determined

- (i) from a combination of photogrammetric and inertial data
- (ii) from the laser ranger

and these two ranges can be compared.

In practice, there could be a problem in determining exactly where the points q_1, q_2 lie in the photogrammetric model, so another approach should be considered. Essentially, there is a redundancy of information in the combination of photogrammetric, inertial and laser systems. The redundancy permits at least two

different estimates of the value of some parameter, and the discrepancy between these estimates, to be made. In the foregoing paragraph, the discrepancy between two estimates of the range itself was sought. However, the same data could also be combined in a different way to give two estimates of some other quantity.

One way of doing this is to determine two estimates of the terrain elevation. One estimate is derived from the positions p_1 , p_2 , p_3 , p_4 and the laser directions at these points, exactly as before, and then by combining these positions and directions with the laser range to give the x, y and z coordinates of the laser spot.

If these same x and y values are inserted into the photogrammetric model, then the model can give a second estimate of the z-coordinate. So there exist two estimates of the z-coordinate. Since the laser beam is almost vertical, the difference between the two estimates of the z-coordinate should be almost equal to the difference between the two estimates of the laser range that were discussed earlier.

2. Laser Ranges in Photogrammetric Adjustment

(a) Application:

A photogrammetric adjustment can be strengthened by the use of extra data of acceptable accuracy. Positions of control points (absolute or relative) are the most commonly used forms of such data. However, in principle, any quantity that is uniquely defined by the geometry of the photogrammetric model, and can be measured independently, can be used as input to the adjustment.

The laser range could be such a quantity.

The beam from a laser ranger intercepts the ground at a certain point which can be called the laser spot. The ranger measures the distance from the instrument itself to the laser spot. This distance can also be determined from photogrammetry, provided that the ranger is close to the camera. Hence the laser range can be compared with the photogrammetric range as part of the adjustment process.

Perspective centre positions are defined by the photogrammetric model, and their coordinates are often the by-product of an adjustment. Coordinates of points on the ground are often used in adjustments; this is the case not only for points whose coordinates are already known (control points) but also for points whose coordinates are not previously known (e.g. tie points and pass points) but can be found from the model. Knowing the coordinates of the perspective centre (PC) and a ground point, the distance between them is determined too. If the ground point happens to be the laser spot, then the distance from PC to laser spot can be measured independently by the laser ranger.

To use the laser with photogrammetry, the position of the laser spot in the model must be known. Normally this spot is near the principal point of one image. Its actual displacement from the principal point depends on the misalignment of laser beam and camera axis. If the laser is mounted close to the camera, the variation of this displacement with height of instrument above ground (parallax effect) will be negligible. The direction of displacement of the laser spot from the principal point in the

image will be constant if the laser is attached to the camera. If the laser is mounted separately from the camera, this direction will depend on the crab-angle κ . (See Fig. F.2)

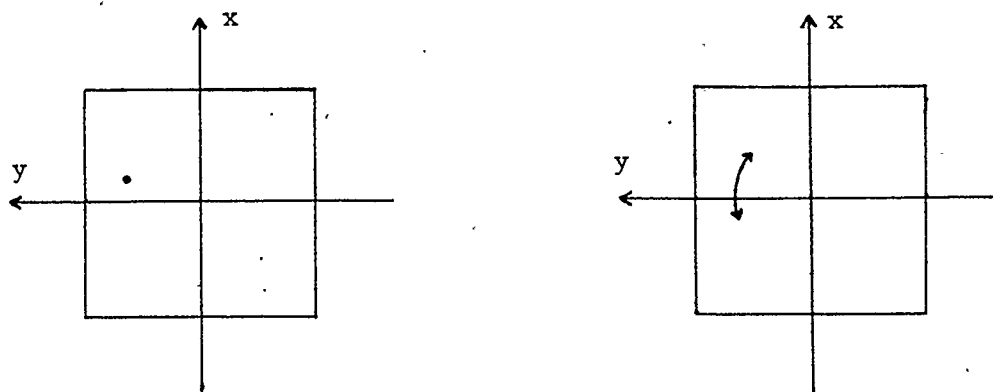


Fig. F.2

Position of Laser Spot with
Laser Attached to Camera.

Range of Positions of Laser
Spot with Laser Mounted
Separately from Camera.

Having identified the laser spot in one image, it should be identified in the conjugate image so that its coordinates in the model can be determined.

Combining the model or ground coordinates of the PC and the laser spot, there is enough information to determine the range from PC to laser spot from the photogrammetry. The photogrammetric adjustment process must be formulated in such a way that it involves the range from PC to laser spot, either directly or indirectly.

Being a single distance in the ground coordinate system, the laser range is irrelevant to interior and relative orientation processes, and is only applicable to absolute orientation, where it essentially determines the scale of the model.

(b) Testing

It is desirable to check the accuracy of the ranger, to avoid errors such as can arise from misalignment.

The laser ranger's measurement of a given distance is to be compared with an independent measurement of the same distance.

The distance in this case is the distance from the laser ranger to the laser spot. This is practically identical to the distance from the camera to the laser spot.

Measurement of this distance photogrammetrically requires knowing the coordinates of (i) the PC (ii) the laser spot in the ground coordinate system.

The coordinates of the PC are normal by-products of an adjustment (bundle or SPACE-M). For the laser spot coordinates, the position of the laser spot must be found in one image. (See "Application" above) It can then be located in the conjugate image, and so its ground coordinates can be determined when the adjustment is done. Knowing the PC and laser spot coordinates in the ground system, the distance between them is easily calculated, and can be compared with the actual laser measurement.

APPENDIX G

Tables of Profile Elevation Discrepancies

G.1 - G.5 as Functions of Terrain Type and Slope Separately

G.1	Section A	Page 155
G.2	Section W	Page 156
G.3	Section X	Page 157
G.4	Section Y	Page 158
G.5	Section Z	Page 159

G.6 - G.10 as Functions of Terrain Type and Slope Jointly

G.6	Section A	Page 160
G.7	Section W	Page 161
G.8	Section X	Page 162
G.9	Section Y	Page 163
G.10	Section Z	Page 164

Table G.1

Section A

Elevation Discrepancies as Function of Terrain Type

Terrain Type	Sample No.	Size	Mean Discr.	Mean Abs. Value	RMS Value	Min. Value	Max. Value	S.D.
1	70		-0.76	3.11	4.02	-8.30	11.75	3.95
2	35		1.83	5.26	6.73	-8.77	15.04	6.47
3	9		-1.39	1.39	1.60	-2.84	-0.37	0.79
4	62		0.47	3.47	4.32	-6.73	14.59	4.29
5	134		3.87	4.39	5.14	-6.52	12.23	3.38
6	38		-0.77	7.10	8.94	-20.39	14.00	8.91
7	47		3.77	6.52	7.82	-19.95	15.05	6.85
8	79		4.77	4.90	6.44	-2.10	19.55	4.33
9	34		1.79	3.94	5.67	-7.54	20.36	5.38
All	508		2.23	4.56	5.91	-20.39	20.36	5.47

Elevation Discrepancies as Function of Total Slope

Terrain Slope	Sample Size	Mean Discr.	Mean Abs. Value	RMS Value	Min. Value	Max. Value	S.D.
0 -0.24	8	-0.38	3.32	3.77	-4.42	6.76	3.75
0.25-0.49	25	1.46	4.62	5.45	-7.51	13.63	5.26
0.50-0.74	172	1.89	4.02	5.04	-19.95	15.05	4.67
0.75-0.99	142	2.80	4.52	5.81	-8.77	19.55	5.10
1.00-1.24	44	0.74	7.00	9.05	-20.39	20.36	9.02
1.25-1.49	27	0.84	4.98	5.88	-12.10	10.70	5.82
1.50-1.74	11	7.32	7.35	9.55	-0.15	15.60	6.13
1.75-1.99	7	3.19	5.71	7.31	-5.64	15.92	6.57
>1.99	15	4.18	4.61	6.30	-1.65	14.17	4.71
All	451	2.17	4.68	6.06	-20.39	20.36	5.65

Table G.2

Section W

Elevation Discrepancies as Function of Terrain Type

Terrain Type No.	Sample Size	Mean Discr.	Mean Abs. Value	RMS Value	Min. Value	Max. Value	S.D.
1	179	-1.82	3.93	4.68	-7.06	26.29	4.31
2	2	-1.96	1.96	2.23	-3.03	-0.88	1.07
3	58	-0.70	2.47	3.04	-4.26	7.37	2.96
4	48	0.96	3.58	4.35	-4.49	9.60	4.24
5	89	4.96	5.91	7.28	-4.67	17.65	5.33
6	20	4.98	6.47	6.97	-4.46	13.43	4.89
7	0	0.00	0.00	0.00	0.00	0.00	0.00
8	18	6.63	7.67	9.61	-3.96	17.06	6.96
9	0	0.00	0.00	0.00	0.00	0.00	0.00
All	414	0.81	4.39	5.55	-7.06	26.29	5.49

Elevation Discrepancies as Function of Total Slope

Terrain Slope	Sample Size	Mean Discr.	Mean Abs. Value	RMS Value	Min. Value	Max. Value	S.D.
0 -0.24	396	0.59	4.28	5.31	-7.06	17.06	5.28
0.25-0.49	15	4.53	5.64	7.32	-3.49	17.65	5.76
0.50-0.74	1	8.12	8.12	8.12	8.12	8.12	0.00
0.75-0.99	2	13.59	13.59	18.60	0.89	26.29	12.70
1.00-1.24	0	0.00	0.00	0.00	-0.00	0.00	0.00
1.25-1.49	0	0.00	0.00	0.00	-0.00	0.00	0.00
1.50-1.74	0	0.00	0.00	0.00	-0.00	0.00	0.00
1.75-1.99	0	0.00	0.00	0.00	-0.00	0.00	0.00
>1.99	0	0.00	0.00	0.00	-0.00	0.00	0.00
All	414	0.81	4.39	5.55	-7.06	26.29	5.49

Table G.3

Section X

Elevation Discrepancies as Function of Terrain Type

Terrain Type No.	Sample Size	Mean Discr.	Mean Abs. Value	RMS Value	Min. Value	Max. Value	S.D.
1	34	1.60	7.20	8.92	-8.50	23.47	8.78
2	0	0.00	0.00	0.00	-0.00	0.00	0.00
3	31	-1.80	2.70	3.41	-6.19	7.07	2.90
4	0	0.00	0.00	0.00	0.00	0.00	0.00
5	130	6.20	7.17	8.62	-7.32	19.53	5.98
6	96	12.70	13.17	14.40	-7.55	25.21	6.79
7	3	8.43	8.43	8.55	6.85	10.33	1.44
8	175	1.48	3.76	5.00	-6.31	15.61	4.78
9	0	0.00	0.00	0.00	0.00	0.00	0.00
All	469	4.92	6.84	8.91	-8.50	25.21	7.43

Elevation Discrepancies as Function of Total Slope

Terrain Slope	Sample Size	Mean Discr.	Mean Abs. Value	RMS Value	Min. Value	Max. Value	S.D.
0 -0.24	430	4.66	6.74	8.84	-8.50	25.21	7.51
0.25-0.49	27	5.12	5.35	6.53	-2.64	15.61	4.06
0.50-0.74	5	11.50	11.50	11.70	7.72	13.45	2.15
0.75-0.99	5	16.10	16.10	16.58	11.78	23.47	3.96
1.00-1.24	2	14.00	14.00	14.35	10.86	17.14	3.14
1.25-1.49	0	0.00	0.00	0.00	0.00	0.00	0.00
1.50-1.74	0	0.00	0.00	0.00	0.00	0.00	0.00
1.75-1.99	0	0.00	0.00	0.00	0.00	0.00	0.00
>1.99	0	0.00	0.00	0.00	0.00	0.00	0.00
All	469	4.92	6.84	8.91	-8.50	25.21	7.43

Table G.4

Section Y

Elevation Discrepancies as Function of Terrain Type

Terrain Type No.	Sample Size	Mean Discr.	Mean Abs.	RMS Value	Min. Value	Max. Value	S.D.
1	350	-5.72	12.35	17.58	-152.08	64.54	16.62
2	115	-1.94	28.11	44.32	-195.58	69.69	44.27
3	0	0.00	0.00	0.00	0.00	0.00	0.00
4	0	0.00	0.00	0.00	0.00	0.00	0.00
5	24	1.65	5.61	6.17	-8.40	10.13	5.95
6	0	0.00	0.00	0.00	0.00	0.00	0.00
7	0	0.00	0.00	0.00	0.00	0.00	0.00
8	0	0.00	0.00	0.00	0.00	0.00	0.00
9	0	0.00	0.00	0.00	0.00	0.00	0.00
All	489	-4.47	15.73	26.17	-195.58	69.69	25.78

Elevation Discrepancies as Function of Total Slope

Terrain Slope	Sample Size	Mean Discr.	Mean Abs.	RMS Value	Min. Value	Max. Value	S.D.
0 -0.24	35	-1.50	5.10	5.96	-12.91	9.11	5.77
0.25-0.49	54	-2.84	9.47	11.13	-20.22	27.52	10.77
0.50-0.74	114	-4.88	11.38	13.31	-32.67	38.01	12.38
0.75-0.99	120	-5.40	11.87	14.89	-47.08	60.68	13.88
1.00-1.24	60	-2.17	13.49	17.21	-32.84	52.19	17.08
1.25-1.49	23	-0.06	11.53	15.69	-27.33	48.83	15.69
1.50-1.74	13	-18.86	24.88	45.54	-152.08	39.18	41.45
1.75-1.99	29	-5.94	28.47	33.63	-75.07	52.03	33.11
>1.99	41	-5.52	50.13	69.31	-195.58	69.69	69.09
All	489	-4.47	15.73	26.17	-195.58	69.69	25.78

Table G.5

Section Z

Elevation Discrepancies as Function of Terrain Type

Terrain Type No.	Sample Size	Mean Discr.	Mean Abs. Value	RMS Value	Min. Value	Max. Value	S.D.
1	229	2.36	3.20	4.47	-12.50	18.13	3.80
2	0	0.00	0.00	0.00	-0.00	0.00	0.00
3	151	2.16	2.34	2.83	-2.41	6.95	1.83
4	0	0.00	0.00	0.00	-0.00	0.00	0.00
5	45	2.77	3.21	4.28	-3.68	14.84	3.26
6	43	6.21	6.25	6.87	-0.82	12.22	2.94
7	0	0.00	0.00	0.00	-0.00	0.00	0.00
8	0	0.00	0.00	0.00	-0.00	0.00	0.00
9	0	0.00	0.00	0.00	-0.00	0.00	0.00
All	468	2.69	3.20	4.30	-12.50	18.13	3.35

Elevation Discrepancies as Function of Total Slope

Terrain Slope	Sample Size	Mean Discr.	Mean Abs. Value	RMS Value	Min. Value	Max. Value	S.D.
0 -0.24	2	-0.89	0.89	1.08	-1.50	-0.27	0.62
0.25-0.49	123	1.91	2.30	2.96	-4.19	10.93	2.26
0.50-0.74	221	2.84	3.00	3.91	-1.85	14.84	2.69
0.75-0.99	82	3.12	3.34	4.09	-3.86	11.51	2.64
1.00-1.24	16	1.67	3.87	4.53	-10.20	7.62	4.21
1.25-1.49	7	7.73	9.14	10.23	-4.93	15.47	6.70
1.50-1.74	11	3.91	9.59	10.49	-12.50	18.13	9.73
1.75-1.99	3	0.59	8.17	8.82	-11.36	9.58	8.80
>1.99	3	5.43	7.41	10.15	-2.97	17.21	8.58
All	468	2.69	3.20	4.30	-12.50	18.13	3.35

Table G.6

Section A

Sample size, mean, s.d. and rms values for various
slope categories and terrain types (left column)

	Slope Category								
	1	2	3	4	5	6	7	8	9
1	6	8	11	20	2	3	1	2	1
	-2.26	-2.98	-0.36	1.52	1.78	-3.77	-0.15	-4.42	-1.65
	1.97	2.99	4.15	5.15	1.43	1.25	0.00	1.22	0.00
2	2.99	4.22	4.16	5.37	2.28	3.97	0.15	4.58	1.65
	0	1	10	10	1	3	2	0	8
	0.00	13.63	-1.60	0.39	8.22	-0.62	6.42	0.00	5.42
3	0.00	0.00	4.31	6.50	0.00	5.89	5.68	0.00	5.11
	0.00	13.63	4.60	6.51	8.22	5.92	8.57	0.00	7.45
	0	2	4	3	0	0	0	0	0
4	0.00	-0.44	-1.96	-1.26	0.00	0.00	0.00	0.00	0.00
	0.00	0.07	0.63	0.52	0.00	0.00	0.00	0.00	0.00
	0.00	0.44	2.06	1.36	0.00	0.00	0.00	0.00	0.00
5	0	2	17	13	0	0	0	0	0
	0.00	-5.44	-2.26	-1.66	0.00	0.00	0.00	0.00	0.00
	0.00	0.82	2.70	4.97	0.00	0.00	0.00	0.00	0.00
6	0.00	5.50	3.52	5.23	0.00	0.00	0.00	0.00	0.00
	2	6	55	35	9	11	2	2	1
	5.26	5.88	4.14	3.10	1.50	2.42	4.36	4.58	0.19
7	1.50	1.39	2.78	3.81	4.39	3.31	0.25	1.08	0.00
	5.47	6.04	4.99	4.91	4.64	4.10	4.36	4.71	0.19
	0	0	16	6	9	5	2	0	0
8	0.00	0.00	2.68	5.70	-13.68	-1.85	13.16	0.00	0.00
	0.00	0.00	2.71	3.70	4.43	7.80	0.84	0.00	0.00
	0.00	0.00	3.81	6.79	14.38	8.01	13.19	0.00	0.00
9	0	0	24	17	5	1	0	0	0
	0.00	0.00	1.84	5.11	7.94	6.19	0.00	0.00	0.00
	0.00	0.00	8.14	4.28	4.33	0.00	0.00	0.00	0.00
10	0.00	0.00	8.34	6.67	9.05	6.19	0.00	0.00	0.00
	0	5	29	28	13	1	2	1	0
	0.00	3.55	2.85	5.52	5.70	1.17	15.26	15.92	0.00
11	0.00	2.94	2.27	4.52	4.08	0.00	0.34	0.00	0.00
	0.00	4.61	3.64	7.14	7.01	1.17	15.26	15.92	0.00
	0	1	6	10	5	3	2	2	5
12	0.00	5.41	-1.02	0.47	3.28	3.69	1.16	3.05	4.15
	0.00	0.00	3.49	3.66	8.62	8.02	1.00	2.80	3.53
	0.00	5.41	3.63	3.69	9.22	8.83	1.53	4.13	5.45

Slope Categories

1	< 0.25	6	1.25 to 1.49
2	0.25 to 0.49	7	1.50 to 1.74
3	0.50 to 0.74	8	1.75 to 1.99
4	0.75 to 0.99	9	> 1.99
5	1.00 to 1.24		

Table G.7

Section W

Sample size, mean, s.d. and rms values for various
slope categories and terrain types (left column)

	Slope Category								
	1	2	3	4	5	6	7	8	9
1	173	3	1	2	0	0	0	0	0
	-2.17	4.80	8.12	13.59	0.00	0.00	0.00	0.00	0.00
	3.56	5.24	0.00	12.70	0.00	0.00	0.00	0.00	0.00
	4.17	7.11	8.12	18.60	0.00	0.00	0.00	0.00	0.00
2	2	0	0	0	0	0	0	0	0
	-1.96	0.00	0.00	0.00	0.00	0.00	0.00	0.00	0.00
	1.07	0.00	0.00	0.00	0.00	0.00	0.00	0.00	0.00
	2.23	0.00	0.00	0.00	0.00	0.00	0.00	0.00	0.00
3	58	0	0	0	0	0	0	0	0
	-0.70	0.00	0.00	0.00	0.00	0.00	0.00	0.00	0.00
	2.96	0.00	0.00	0.00	0.00	0.00	0.00	0.00	0.00
	3.04	0.00	0.00	0.00	0.00	0.00	0.00	0.00	0.00
4	42	6	0	0	0	0	0	0	0
	1.04	0.39	0.00	0.00	0.00	0.00	0.00	0.00	0.00
	4.36	3.22	0.00	0.00	0.00	0.00	0.00	0.00	0.00
	4.48	3.24	0.00	0.00	0.00	0.00	0.00	0.00	0.00
5	83	6	0	0	0	0	0	0	0
	4.70	8.52	0.00	0.00	0.00	0.00	0.00	0.00	0.00
	5.26	5.06	0.00	0.00	0.00	0.00	0.00	0.00	0.00
	7.05	9.91	0.00	0.00	0.00	0.00	0.00	0.00	0.00
6	20	0	0	0	0	0	0	0	0
	4.98	0.00	0.00	0.00	0.00	0.00	0.00	0.00	0.00
	4.89	0.00	0.00	0.00	0.00	0.00	0.00	0.00	0.00
	6.97	0.00	0.00	0.00	0.00	0.00	0.00	0.00	0.00
7	0	0	0	0	0	0	0	0	0
	0.00	0.00	0.00	0.00	0.00	0.00	0.00	0.00	0.00
	0.00	0.00	0.00	0.00	0.00	0.00	0.00	0.00	0.00
	0.00	0.00	0.00	0.00	0.00	0.00	0.00	0.00	0.00
8	18	0	0	0	0	0	0	0	0
	6.63	0.00	0.00	0.00	0.00	0.00	0.00	0.00	0.00
	6.96	0.00	0.00	0.00	0.00	0.00	0.00	0.00	0.00
	9.61	0.00	0.00	0.00	0.00	0.00	0.00	0.00	0.00
9	0	0	0	0	0	0	0	0	0
	0.00	0.00	0.00	0.00	0.00	0.00	0.00	0.00	0.00
	0.00	0.00	0.00	0.00	0.00	0.00	0.00	0.00	0.00
	0.00	0.00	0.00	0.00	0.00	0.00	0.00	0.00	0.00

Slope Categories

1	< 0.25	6	1.25 to 1.49
2	0.25 to 0.49	7	1.50 to 1.74
3	0.50 to 0.74	8	1.75 to 1.99
4	0.75 to 0.99	9	> 1.99
5	1.00 to 1.24		

Table G.8

Section X

Sample size, mean, s.d. and rms values for various
slope categories and terrain types (left column)

	Slope Category								
	1	2	3	4	5	6	7	8	9
1	31	2	0	1	0	0	0	0	0
	0.38	9.46	0.00	23.47	0.00	0.00	0.00	0.00	0.00
	7.92	3.75	0.00	0.00	0.00	0.00	0.00	0.00	0.00
	7.93	10.18	0.00	23.47	0.00	0.00	0.00	0.00	0.00
2	0	0	0	0	0	0	0	0	0
	0.00	0.00	0.00	0.00	0.00	0.00	0.00	0.00	0.00
	0.00	0.00	0.00	0.00	0.00	0.00	0.00	0.00	0.00
	0.00	0.00	0.00	0.00	0.00	0.00	0.00	0.00	0.00
3	31	0	0	0	0	0	0	0	0
	-1.80	0.00	0.00	0.00	0.00	0.00	0.00	0.00	0.00
	2.90	0.00	0.00	0.00	0.00	0.00	0.00	0.00	0.00
	3.41	0.00	0.00	0.00	0.00	0.00	0.00	0.00	0.00
4	0	0	0	0	0	0	0	0	0
	0.00	0.00	0.00	0.00	0.00	0.00	0.00	0.00	0.00
	0.00	0.00	0.00	0.00	0.00	0.00	0.00	0.00	0.00
	0.00	0.00	0.00	0.00	0.00	0.00	0.00	0.00	0.00
5	116	9	0	4	1	0	0	0	0
	5.96	4.53	0.00	14.26	17.14	0.00	0.00	0.00	0.00
	6.02	1.36	0.00	1.62	0.00	0.00	0.00	0.00	0.00
	8.48	4.73	0.00	14.35	17.14	0.00	0.00	0.00	0.00
6	95	1	0	0	0	0	0	0	0
	12.84	-0.54	0.00	0.00	0.00	0.00	0.00	0.00	0.00
	6.69	0.00	0.00	0.00	0.00	0.00	0.00	0.00	0.00
	14.47	0.54	0.00	0.00	0.00	0.00	0.00	0.00	0.00
7	3	0	0	0	0	0	0	0	0
	8.43	0.00	0.00	0.00	0.00	0.00	0.00	0.00	0.00
	1.44	0.00	0.00	0.00	0.00	0.00	0.00	0.00	0.00
	8.55	0.00	0.00	0.00	0.00	0.00	0.00	0.00	0.00
8	154	15	5	0	1	0	0	0	0
	0.73	5.27	11.50	0.00	10.86	0.00	0.00	0.00	0.00
	4.23	4.67	2.15	0.00	0.00	0.00	0.00	0.00	0.00
	4.29	7.04	11.70	0.00	10.86	0.00	0.00	0.00	0.00
9	0	0	0	0	0	0	0	0	0
	0.00	0.00	0.00	0.00	0.00	0.00	0.00	0.00	0.00
	0.00	0.00	0.00	0.00	0.00	0.00	0.00	0.00	0.00
	0.00	0.00	0.00	0.00	0.00	0.00	0.00	0.00	0.00

Slope Categories

1	< 0.25	6	1.25 to 1.49
2	0.25 to 0.49	7	1.50 to 1.74
3	0.50 to 0.74	8	1.75 to 1.99
4	0.75 to 0.99	9	> 1.99
5	1.00 to 1.24		

Table G.9

Section Y

Sample size, mean, s.d. and rms values for various
slope categories and terrain types (left column)

	Slope Category								
	1	2	3	4	5	6	7	8	9
1	21 -1.21 6.14 6.26	42 -5.12 9.69 10.96	99 -4.59 12.76 13.56	99 -6.97 9.96 12.16	44 -4.85 14.36 15.16	14 -3.93 9.50 10.28	7 -31.51 49.48 58.66	16 -21.96 32.01 38.81	8 27.84 20.75 34.72
2	0 0.00 0.00 0.00	3 0.46 20.00 20.01	14 -7.74 8.92 11.81	21 1.99 23.80 23.89	16 5.19 21.26 21.89	9 5.97 20.72 21.56	6 -4.10 21.49 21.87	13 13.77 21.90 25.87	33 -13.61 74.10 75.34
3	0 0.00 0.00 0.00	0 0.00 0.00 0.00	0 0.00 0.00 0.00	0 0.00 0.00 0.00	0 0.00 0.00 0.00	0 0.00 0.00 0.00	0 0.00 0.00 0.00	0 0.00 0.00 0.00	0 0.00 0.00 0.00
4	0 0.00 0.00 0.00	0 0.00 0.00 0.00	0 0.00 0.00 0.00	0 0.00 0.00 0.00	0 0.00 0.00 0.00	0 0.00 0.00 0.00	0 0.00 0.00 0.00	0 0.00 0.00 0.00	0 0.00 0.00 0.00
5	14 -1.94 5.13 5.49	9 6.70 2.27 7.08	1 6.54 0.00 6.54	0 0.00 0.00 0.00	0 0.00 0.00 0.00	0 0.00 0.00 0.00	0 0.00 0.00 0.00	0 0.00 0.00 0.00	0 0.00 0.00 0.00
6	0 0.00 0.00 0.00	0 0.00 0.00 0.00	0 0.00 0.00 0.00	0 0.00 0.00 0.00	0 0.00 0.00 0.00	0 0.00 0.00 0.00	0 0.00 0.00 0.00	0 0.00 0.00 0.00	0 0.00 0.00 0.00
7	0 0.00 0.00 0.00	0 0.00 0.00 0.00	0 0.00 0.00 0.00	0 0.00 0.00 0.00	0 0.00 0.00 0.00	0 0.00 0.00 0.00	0 0.00 0.00 0.00	0 0.00 0.00 0.00	0 0.00 0.00 0.00
8	0 0.00 0.00 0.00	0 0.00 0.00 0.00	0 0.00 0.00 0.00	0 0.00 0.00 0.00	0 0.00 0.00 0.00	0 0.00 0.00 0.00	0 0.00 0.00 0.00	0 0.00 0.00 0.00	0 0.00 0.00 0.00
9	0 0.00 0.00 0.00	0 0.00 0.00 0.00	0 0.00 0.00 0.00	0 0.00 0.00 0.00	0 0.00 0.00 0.00	0 0.00 0.00 0.00	0 0.00 0.00 0.00	0 0.00 0.00 0.00	0 0.00 0.00 0.00

Slope Categories

1	< 0.25	6	1.25 to 1.49
2	0.25 to 0.49	7	1.50 to 1.74
3	0.50 to 0.74	8	1.75 to 1.99
4	0.75 to 0.99	9	> 1.99
5	1.00 to 1.24		

Table G.10

Section 2

Sample size, mean, s.d. and rms values for various
slope categories and terrain types (left column)

		Slope Category							
	1	2	3	4	5	6	7	8	9
1	1	31	82	75	16	7	11	3	3
	-1.50	1.47	1.86	2.70	1.67	7.73	3.91	0.59	5.43
	0.00	2.75	1.84	2.18	4.21	6.70	9.73	8.80	8.58
	1.50	3.12	2.62	3.48	4.53	10.23	10.49	8.82	10.15
2	0	0	0	0	0	0	0	0	0
	0.00	0.00	0.00	0.00	0.00	0.00	0.00	0.00	0.00
	0.00	0.00	0.00	0.00	0.00	0.00	0.00	0.00	0.00
	0.00	0.00	0.00	0.00	0.00	0.00	0.00	0.00	0.00
3	1	60	89	1	0	0	0	0	0
	-0.27	1.79	2.44	2.41	0.00	0.00	0.00	0.00	0.00
	0.00	1.51	1.97	0.00	0.00	0.00	0.00	0.00	0.00
	0.27	2.34	3.14	2.41	0.00	0.00	0.00	0.00	0.00
4	0	0	0	0	0	0	0	0	0
	0.00	0.00	0.00	0.00	0.00	0.00	0.00	0.00	0.00
	0.00	0.00	0.00	0.00	0.00	0.00	0.00	0.00	0.00
	0.00	0.00	0.00	0.00	0.00	0.00	0.00	0.00	0.00
5	0	17	26	2	0	0	0	0	0
	0.00	1.45	3.37	6.18	0.00	0.00	0.00	0.00	0.00
	0.00	2.44	3.42	2.34	0.00	0.00	0.00	0.00	0.00
	0.00	2.84	4.80	6.61	0.00	0.00	0.00	0.00	0.00
6	0	15	24	4	0	0	0	0	0
	0.00	3.86	7.11	9.64	0.00	0.00	0.00	0.00	0.00
	0.00	2.42	2.35	0.76	0.00	0.00	0.00	0.00	0.00
	0.00	4.56	7.49	9.67	0.00	0.00	0.00	0.00	0.00
7	0	0	0	0	0	0	0	0	0
	0.00	0.00	0.00	0.00	0.00	0.00	0.00	0.00	0.00
	0.00	0.00	0.00	0.00	0.00	0.00	0.00	0.00	0.00
	0.00	0.00	0.00	0.00	0.00	0.00	0.00	0.00	0.00
8	0	0	0	0	0	0	0	0	0
	0.00	0.00	0.00	0.00	0.00	0.00	0.00	0.00	0.00
	0.00	0.00	0.00	0.00	0.00	0.00	0.00	0.00	0.00
	0.00	0.00	0.00	0.00	0.00	0.00	0.00	0.00	0.00
9	0	0	0	0	0	0	0	0	0
	0.00	0.00	0.00	0.00	0.00	0.00	0.00	0.00	0.00
	0.00	0.00	0.00	0.00	0.00	0.00	0.00	0.00	0.00
	0.00	0.00	0.00	0.00	0.00	0.00	0.00	0.00	0.00

Slope Categories

1	< 0.25	6	1.25 to 1.49
2	0.25 to 0.49	7	1.50 to 1.74
3	0.50 to 0.74	8	1.75 to 1.99
4	0.75 to 0.99	9	> 1.99
5	1.00 to 1.24		

APPENDIX H

Detailed Comparisons of Orientation Angles

H.1 - H.10: Angles from Auxiliary Systems and Photogrammetry

H.1)	SPACE-M	(Single Differences	Page 166
H.2)	Case (a)	(Double Differences	167
H.3)	SPACE-M	(Single Differences	Page 168
H.4)	Case (b)	(Double Differences	169
H.5)	SPACE-M	(Single Differences	Page 170
H.6)	Case (c)	(Double Differences	171
H.7)	SPACE-M	(Single Differences	Page 172
H.8)	Case (d)	(Double Differences	173
H.9)	CCRS Bundle	(Single Differences	Page 174
H.10)	Adjustment	(Double Differences	175

H.11 - H.18: Angles from CCRS Bundle and SPACE-M Adjustment

H.11)	SPACE-M	(Single Differences	Page 176
H.12)	Case (a)	(Double Differences	177
H.13)	SPACE-M	(Single Differences	Page 178
H.14)	Case (b)	(Double Differences	179
H.15)	SPACE-M	(Single Differences	Page 180
H.16)	Case (c)	(Double Differences	181
H.17)	SPACE-M	(Single Differences	Page 182
H.18)	Case (d)	(Double Differences	183

Table H.1

Single Differences of Orientation Angles (Degrees)

Mean, RMS and Max./Min. Values from
Auxiliary Systems and SPACE-M case (a)

		Roll			
Chron. Line No.	Pts.	Mean	RMS	Max.	Min.
1	25	-2.008	2.008	-1.901	-2.098
2	28	-1.798	1.799	-1.718	-1.990
3	23	-1.814	1.814	-1.748	-1.881
4	31	-1.631	1.631	-1.583	-1.687
5	28	-1.451	1.451	-1.414	-1.550
ALL	135	-1.729	1.740	-1.414	-2.098

		Pitch			
Chron. Line No.	Pts.	Mean	RMS	Max.	Min.
1	25	1.169	1.171	1.340	1.036
2	28	2.105	2.106	2.268	1.977
3	23	0.943	0.944	1.061	0.849
4	31	2.030	2.030	2.120	1.957
5	28	1.237	1.238	1.317	1.077
ALL	135	1.537	1.609	2.268	0.849

		Heading			
Chron. Line No.	Pts.	Mean	RMS	Max.	Min.
1	25	-1.484	1.489	-1.219	-1.999
2	28	2.167	2.169	2.620	2.019
3	23	-0.831	0.833	-0.629	-0.883
4	31	0.398	0.402	0.690	0.310
5	28	-0.133	0.198	0.589	-0.340
ALL	135	0.097	1.245	2.620	-1.999

Table H.2

Double Differences of Orientation Angles (Degrees)

Mean, RMS and Max./Min. Values from
Auxiliary Systems and SPACE-M case (a)

Roll						
Chron. Line No.	Pts.	Mean	RMS	Max.	Min.	
1	22	-0.003	0.035	0.087	-0.071	
2	26	0.000	0.057	0.183	-0.181	
3	22	-0.004	0.028	0.059	-0.057	
4	30	-0.000	0.023	0.056	-0.054	
5	27	-0.005	0.027	0.047	-0.077	
ALL	127	-0.002	0.036	0.183	-0.181	

Pitch						
Chron. Line No.	Pts.	Mean	RMS	Max.	Min.	
1	22	-0.005	0.041	0.095	-0.082	
2	26	-0.007	0.040	0.113	-0.102	
3	22	-0.010	0.032	0.041	-0.073	
4	30	-0.005	0.041	0.074	-0.075	
5	27	-0.008	0.041	0.059	-0.082	
ALL	127	-0.007	0.040	0.113	-0.102	

Heading						
Chron. Line No.	Pts.	Mean	RMS	Max.	Min.	
1	22	-0.020	0.129	0.266	-0.496	
2	26	-0.016	0.109	0.169	-0.495	
3	22	0.001	0.082	0.234	-0.166	
4	30	0.001	0.077	0.251	-0.301	
5	27	0.004	0.206	0.743	-0.699	
ALL	127	-0.006	0.130	0.743	-0.699	

Table H.3

Single Differences of Orientation Angles (Degrees)

Mean, RMS and Max./Min. Values from
Auxiliary Systems and SPACE-M case (b)

		Roll			
Chron. Line No.	Pts.	Mean	RMS	Max.	Min.
1	25	-2.008	2.008	-1.901	-2.098
2	28	-1.798	1.799	-1.718	-1.990
3	23	-1.814	1.814	-1.748	-1.881
4	31	-1.631	1.631	-1.583	-1.687
5	28	-1.451	1.451	-1.414	-1.550
ALL	135	-1.729	1.740	-1.414	-2.098

		Pitch			
Chron. Line No.	Pts.	Mean	RMS	Max.	Min.
1	25	1.169	1.171	1.340	1.036
2	28	2.105	2.106	2.268	1.977
3	23	0.942	0.943	1.061	0.849
4	31	2.030	2.030	2.120	1.957
5	28	1.238	1.239	1.317	1.077
ALL	135	1.536	1.609	2.268	0.849

		Heading			
Chron. Line No.	Pts.	Mean	RMS	Max.	Min.
1	25	-1.493	1.497	-1.219	-1.999
2	28	2.167	2.169	2.620	2.019
3	23	-0.855	0.855	-0.795	-0.894
4	31	0.392	0.393	0.453	0.335
5	28	-0.149	0.151	-0.099	-0.196
ALL	135	0.087	1.247	2.620	-1.999

Table H.4

Double Differences of Orientation Angles (Degrees)

Mean, RMS and Max./Min. Values from
Auxiliary Systems and SPACE-M case (b)

Roll						
Chron. Line No.	Pts.	Mean	RMS	Max.	Min.	
1	22	-0.003	0.035	0.087	-0.071	
2	26	0.000	0.057	0.183	-0.181	
3	22	-0.004	0.028	0.059	-0.057	
4	30	-0.000	0.023	0.056	-0.054	
5	27	-0.005	0.028	0.047	-0.077	
ALL	127	-0.002	0.036	0.183	-0.181	
Pitch						
Chron. Line No.	Pts.	Mean	RMS	Max.	Min.	
1	22	-0.005	0.041	0.094	-0.082	
2	26	-0.007	0.040	0.113	-0.102	
3	22	-0.010	0.032	0.041	-0.070	
4	30	-0.005	0.040	0.074	-0.075	
5	27	-0.008	0.041	0.060	-0.083	
ALL	127	-0.007	0.039	0.113	-0.102	
Heading						
Chron. Line No.	Pts.	Mean	RMS	Max.	Min.	
1	22	-0.020	0.134	0.270	-0.496	
2	26	-0.015	0.110	0.169	-0.495	
3	22	0.001	0.038	0.084	-0.067	
4	30	0.001	0.029	0.055	-0.059	
5	27	0.004	0.030	0.058	-0.048	
ALL	127	-0.005	0.079	0.270	-0.496	

Table H.5

Single Differences of Orientation Angles (Degrees)

Mean, RMS and Max./Min. Values from
Auxiliary Systems and SPACE-M case (c)

		Roll			
Chron. Line No.	Pts.	Mean	RMS	Max.	Min.
1	15	-2.000	2.001	-1.909	-2.091
2	19	-1.787	1.788	-1.716	-1.848
3	17	-1.811	1.811	-1.748	-1.881
4	23	-1.632	1.633	-1.583	-1.685
5	19	-1.450	1.450	-1.415	-1.550
ALL	93	-1.719	1.728	-1.415	-2.091

		Pitch			
Chron. Line No.	Pts.	Mean	RMS	Max.	Min.
1	15	1.162	1.164	1.338	1.036
2	19	2.113	2.114	2.260	2.024
3	17	0.942	0.944	1.061	0.850
4	23	2.038	2.039	2.120	1.957
5	19	1.241	1.242	1.317	1.077
ALL	93	1.549	1.624	2.260	0.850

		Heading			
Chron. Line No.	Pts.	Mean	RMS	Max.	Min.
1	15	-1.481	1.481	-1.451	-1.560
2	19	2.155	2.156	2.217	2.108
3	17	-0.854	0.854	-0.798	-0.895
4	23	0.393	0.395	0.437	0.332
5	19	-0.155	0.157	-0.099	-0.205
ALL	93	0.111	1.217	2.217	-1.560

Table H.6

Double Differences of Orientation Angles (Degrees)

Mean, RMS and Max./Min. Values from
Auxiliary Systems and SPACE-M case (c)

		Roll			
Chron. Line No.	Pts.	Mean	RMS	Max.	Min.
1	10	0.003	0.028	0.074	-0.026
2	11	-0.005	0.024	0.036	-0.039
3	10	-0.018	0.030	0.025	-0.059
4	17	-0.000	0.019	0.053	-0.022
5	11	-0.003	0.021	0.037	-0.034
ALL	59	-0.004	0.024	0.074	-0.059

		Pitch			
Chron. Line No.	Pts.	Mean	RMS	Max.	Min.
1	10	-0.000	0.034	0.094	-0.030
2	11	0.000	0.017	0.025	-0.028
3	10	-0.019	0.030	0.009	-0.054
4	17	-0.010	0.027	0.047	-0.054
5	11	-0.009	0.031	0.035	-0.048
ALL	59	-0.008	0.028	0.094	-0.054

		Heading			
Chron. Line No.	Pts.	Mean	RMS	Max.	Min.
1	10	0.005	0.017	0.029	-0.022
2	11	-0.006	0.037	0.048	-0.061
3	10	0.011	0.044	0.089	-0.035
4	17	-0.007	0.026	0.044	-0.047
5	11	0.007	0.034	0.058	-0.047
ALL	59	0.001	0.032	0.089	-0.061

Table H.7

Single Differences of Orientation Angles (Degrees)

Mean, RMS and Max./Min. Values from
Auxiliary Systems and SPACE-M case (d)

		Roll			
Chron. Line No.	Pts.	Mean	RMS	Max.	Min.
1	15	-2.003	2.003	-1.911	-2.096
2	19	-1.792	1.792	-1.737	-1.846
3	17	-1.813	1.814	-1.752	-1.848
4	23	-1.635	1.635	-1.597	-1.679
5	19	-1.450	1.450	-1.423	-1.551
ALL	93	-1.721	1.731	-1.423	-2.096

		Pitch			
Chron. Line No.	Pts.	Mean	RMS	Max.	Min.
1	15	1.160	1.162	1.333	1.028
2	19	2.109	2.110	2.268	2.016
3	17	0.948	0.949	1.061	0.867
4	23	2.035	2.036	2.121	1.949
5	19	1.244	1.245	1.323	1.076
ALL	93	1.549	1.623	2.268	0.867

		Heading			
Chron. Line No.	Pts.	Mean	RMS	Max.	Min.
1	15	-1.481	1.481	-1.451	-1.559
2	19	2.155	2.156	2.217	2.108
3	17	-0.854	0.854	-0.797	-0.896
4	23	0.393	0.395	0.437	0.332
5	19	-0.155	0.158	-0.097	-0.205
ALL	93	0.111	1.217	2.217	-1.559

Table H.8

Double Differences of Orientation Angles (Degrees)

Mean, RMS and Max./Min. Values from
Auxiliary Systems and SPACE-M case (d)

		Roll			
Chron. Line No.	Pts.	Mean	RMS	Max.	Min.
1	10	0.001	0.030	0.078	-0.031
2	11	-0.002	0.026	0.039	-0.043
3	10	-0.015	0.023	0.005	-0.046
4	17	0.000	0.016	0.028	-0.021
5	11	0.004	0.012	0.029	-0.020
ALL	59	-0.002	0.022	0.078	-0.046

		Pitch			
Chron. Line No.	Pts.	Mean	RMS	Max.	Min.
1	10	-0.001	0.037	0.102	-0.037
2	11	0.001	0.022	0.032	-0.059
3	10	-0.013	0.022	0.015	-0.045
4	17	-0.006	0.023	0.046	-0.034
5	11	-0.007	0.017	0.023	-0.026
ALL	59	-0.005	0.025	0.102	-0.059

		Heading			
Chron. Line No.	Pts.	Mean	RMS	Max.	Min.
1	10	0.004	0.017	0.030	-0.022
2	11	-0.006	0.037	0.048	-0.061
3	10	0.011	0.044	0.090	-0.035
4	17	-0.007	0.026	0.044	-0.047
5	11	0.007	0.034	0.058	-0.048
ALL	59	0.001	0.032	0.090	-0.061

Table H.9

Single Differences of Orientation Angles

Mean, RMS and Max./Min. Values (deg)

Auxiliary Systems and CCRS Bundle Adjustment

		Roll			
Chron.					
Line No.	Pts.	Mean	RMS	Max.	Min.
1	27	-2.007	2.007	-1.980	-2.022
2	29	-1.748	1.748	-1.727	-1.764
3	23	-1.802	1.802	-1.796	-1.813
4	31	-1.582	1.582	-1.522	-1.630
5	28	-1.459	1.459	-1.446	-1.474
ALL	138	-1.712	1.722	-1.446	-2.022

		Pitch			
Chron.					
Line No.	Pts.	Mean	RMS	Max.	Min.
1	27	1.163	1.164	1.190	1.141
2	29	2.114	2.114	2.134	2.094
3	23	0.932	0.932	0.946	0.911
4	31	2.039	2.039	2.087	1.998
5	28	1.247	1.247	1.263	1.229
ALL	138	1.538	1.612	2.134	0.911

		Heading			
Chron.					
Line No.	Pts.	Mean	RMS	Max.	Min.
1	27	-1.483	1.483	-1.468	-1.505
2	29	2.145	2.145	2.154	2.134
3	23	-0.862	0.862	-0.844	-0.884
4	31	0.389	0.389	0.398	0.375
5	28	-0.150	0.150	-0.135	-0.179
ALL	138	0.074	1.249	2.154	-1.505

Table H.10

Double Differences of Orientation Angles

Mean, RMS and Max./Min. Values (deg)

Auxiliary Systems and CCRS Bundle Adjustment

		Roll			
Chron. Line No.	Pts.	Mean	RMS	Max.	Min.
1	26	-0.001	0.004	0.007	-0.010
2	28	0.001	0.007	0.017	-0.014
3	22	-0.000	0.004	0.008	-0.007
4	30	-0.002	0.012	0.018	-0.024
5	27	-0.001	0.005	0.009	-0.011
ALL	133	-0.001	0.008	0.018	-0.024

		Pitch			
Chron. Line No.	Pts.	Mean	RMS	Max.	Min.
1	26	-0.001	0.007	0.012	-0.015
2	28	-0.000	0.006	0.014	-0.013
3	22	0.000	0.007	0.016	-0.015
4	30	-0.002	0.010	0.013	-0.019
5	27	-0.001	0.006	0.011	-0.015
ALL	133	-0.001	0.007	0.016	-0.019

		Heading			
Chron. Line No.	Pts.	Mean	RMS	Max.	Min.
1	26	0.001	0.008	0.021	-0.010
2	28	-0.000	0.005	0.008	-0.011
3	22	0.001	0.010	0.020	-0.019
4	30	0.001	0.003	0.010	-0.005
5	27	0.001	0.008	0.021	-0.020
ALL	133	0.000	0.007	0.021	-0.020

Table H.11

Single Differences of Orientation Angles

Mean, RMS and Max./Min. Values (deg) from
CCRS Bundle Adjustment and SPACE-M case (a)

		Roll			
Chron.					
Line No.	Pts.	Mean	RMS	Max.	Min.
1	25	-0.000	0.047	0.081	-0.098
2	28	-0.051	0.076	0.027	-0.234
3	23	-0.012	0.028	0.054	-0.075
4	31	-0.049	0.061	-0.002	-0.136
5	28	0.008	0.025	0.049	-0.081
ALL	135	-0.022	0.052	0.081	-0.234

		Pitch			
Line No.	Pts.	Mean	RMS	Max.	Min.
1	25	0.006	0.055	0.149	-0.126
2	28	-0.009	0.059	0.147	-0.119
3	23	0.011	0.047	0.135	-0.079
4	31	-0.009	0.043	0.070	-0.090
5	28	-0.010	0.046	0.059	-0.157
ALL	135	-0.003	0.050	0.149	-0.157

		Heading			
Line No.	Pts.	Mean	RMS	Max.	Min.
1	25	-0.001	0.123	0.268	-0.520
2	28	0.023	0.096	0.470	-0.124
3	23	0.031	0.066	0.225	-0.027
4	31	0.008	0.064	0.306	-0.084
5	28	0.017	0.147	0.737	-0.192
ALL	135	0.015	0.104	0.737	-0.520

Table H.12

Double Differences of Orientation Angles (Degrees)

Mean, RMS and Max./Min. Values from
CCRS Bundle Adjustment and SPACE-M case (a)

		Roll			
Chron. Line No.	Pts.	Mean	RMS	Max.	Min.
1	22	-0.003	0.035	0.089	-0.068
2	26	-0.001	0.057	0.182	-0.170
3	22	-0.004	0.028	0.058	-0.055
4	30	0.002	0.027	0.056	-0.060
5	27	-0.005	0.027	0.058	-0.078
ALL	127	-0.002	0.037	0.182	-0.170

		Pitch			
Chron. Line No.	Pts.	Mean	RMS	Max.	Min.
1	22	-0.005	0.043	0.099	-0.074
2	26	-0.008	0.040	0.115	-0.092
3	22	-0.010	0.032	0.039	-0.064
4	30	-0.003	0.042	0.091	-0.085
5	27	-0.007	0.039	0.070	-0.068
ALL	127	-0.006	0.039	0.115	-0.092

		Heading			
Chron. Line No.	Pts.	Mean	RMS	Max.	Min.
1	22	-0.021	0.133	0.260	-0.516
2	26	-0.016	0.109	0.169	-0.492
3	22	0.001	0.083	0.229	-0.165
4	30	0.000	0.077	0.255	-0.297
5	27	0.004	0.208	0.754	-0.698
ALL	127	-0.006	0.131	0.754	-0.698

Table H.13

Single Differences of Orientation Angles

Mean, RMS and Max./Min. Values (deg) from
CCRS Bundle Adjustment and SPACE-M case (b)

		Roll			
Chron. Line No.	Pts.	Mean	RMS	Max.	Min.
1	25	-0.000	0.047	0.081	-0.098
2	28	-0.051	0.076	0.027	-0.234
3	23	-0.012	0.028	0.054	-0.075
4	31	-0.049	0.061	-0.002	-0.136
5	28	0.008	0.025	0.049	-0.081
ALL	135	-0.022	0.052	0.081	-0.234

		Pitch			
Line No.	Pts.	Mean	RMS	Max.	Min.
1	25	0.006	0.055	0.149	-0.126
2	28	-0.009	0.059	0.147	-0.119
3	23	0.010	0.047	0.135	-0.079
4	31	-0.009	0.043	0.070	-0.089
5	28	-0.010	0.046	0.059	-0.157
ALL	135	-0.003	0.050	0.149	-0.157

		Heading			
Line No.	Pts.	Mean	RMS	Max.	Min.
1	25	-0.009	0.118	0.268	-0.520
2	28	0.023	0.096	0.470	-0.124
3	23	0.007	0.030	0.080	-0.042
4	31	0.003	0.031	0.065	-0.056
5	28	0.001	0.027	0.060	-0.044
ALL	135	0.005	0.071	0.470	-0.520

Table H.14

Double Differences of Orientation Angles (Degrees)

Mean, RMS and Max./Min. Values from
CCRS Bundle Adjustment and SPACE-M case (b)

		Roll			
Chron. Line No.	Pts.	Mean	RMS	Max.	Min.
1	22	-0.003	0.035	0.089	-0.068
2	26	-0.001	0.057	0.182	-0.170
3	22	-0.004	0.028	0.058	-0.055
4	30	0.002	0.027	0.056	-0.060
5	27	-0.005	0.027	0.058	-0.078
ALL	127	-0.002	0.037	0.182	-0.170

		Pitch			
Chron. Line No.	Pts.	Mean	RMS	Max.	Min.
1	22	-0.005	0.043	0.097	-0.074
2	26	-0.008	0.040	0.115	-0.091
3	22	-0.010	0.032	0.039	-0.064
4	30	-0.003	0.041	0.090	-0.085
5	27	-0.007	0.039	0.070	-0.068
ALL	127	-0.006	0.039	0.115	-0.091

		Heading			
Chron. Line No.	Pts.	Mean	RMS	Max.	Min.
1	22	-0.021	0.138	0.264	-0.516
2	26	-0.016	0.110	0.169	-0.492
3	22	0.001	0.041	0.102	-0.062
4	30	0.000	0.028	0.051	-0.058
5	27	0.004	0.033	0.058	-0.057
ALL	127	-0.006	0.081	0.264	-0.516

Table H.15

Single Differences of Orientation Angles

Mean, RMS and Max./Min. Values (deg) from
CCRS Bundle Adjustment and SPACE-M case (c)

		Roll			
Chron.					
Line No.	Pts.	Mean	RMS	Max.	Min.
1	15	0.011	0.035	0.071	-0.080
2	19	-0.042	0.052	0.029	-0.097
3	17	-0.008	0.029	0.054	-0.075
4	23	-0.053	0.063	-0.002	-0.121
5	19	0.008	0.027	0.045	-0.081
ALL	93	-0.020	0.045	0.071	-0.121

		Pitch			
Line No.	Pts.	Mean	RMS	Max.	Min.
1	15	0.001	0.059	0.148	-0.126
2	19	-0.002	0.058	0.137	-0.094
3	17	0.012	0.052	0.135	-0.078
4	23	-0.003	0.042	0.056	-0.072
5	19	-0.009	0.046	0.059	-0.157
ALL	93	-0.001	0.051	0.148	-0.157

		Heading			
Line No.	Pts.	Mean	RMS	Max.	Min.
1	15	0.003	0.022	0.029	-0.055
2	19	0.009	0.029	0.078	-0.043
3	17	0.008	0.031	0.056	-0.042
4	23	0.005	0.028	0.047	-0.049
5	19	-0.005	0.027	0.041	-0.046
ALL	93	0.004	0.028	0.078	-0.055

Table H.16

Double Differences of Orientation Angles (Degrees)

Mean, RMS and Max./Min. Values from
CCRS Bundle Adjustment and SPACE-M case (c)

		Roll			
Chron. Line No.	Pts.	Mean	RMS	Max.	Min.
1	10	0.003	0.031	0.081	-0.027
2	11	-0.007	0.029	0.042	-0.056
3	10	-0.017	0.029	0.023	-0.053
4	17	0.002	0.026	0.054	-0.031
5	11	-0.000	0.021	0.048	-0.030
ALL	59	-0.003	0.027	0.081	-0.056

		Pitch			
Chron. Line No.	Pts.	Mean	RMS	Max.	Min.
1	10	-0.002	0.036	0.097	-0.034
2	11	-0.001	0.016	0.030	-0.029
3	10	-0.018	0.030	0.016	-0.057
4	17	-0.008	0.031	0.066	-0.064
5	11	-0.006	0.026	0.031	-0.035
ALL	59	-0.007	0.029	0.097	-0.064

		Heading			
Chron. Line No.	Pts.	Mean	RMS	Max.	Min.
1	10	0.007	0.020	0.036	-0.030
2	11	-0.005	0.039	0.058	-0.068
3	10	0.015	0.048	0.090	-0.036
4	17	-0.008	0.025	0.033	-0.046
5	11	0.006	0.037	0.058	-0.053
ALL	59	0.002	0.034	0.090	-0.068

Table H.17

Single Differences of Orientation Angles

Mean, RMS and Max./Min. Values (deg) from
CCRS Bundle Adjustment and SPACE-M case (d)

		Roll			
Chron.					
Line No.	Pts.	Mean	RMS	Max.	Min.
1	15	-0.009	0.035	0.069	-0.085
2	19	-0.047	0.055	0.008	-0.116
3	17	-0.011	0.025	0.049	-0.042
4	23	-0.056	0.064	-0.011	-0.121
5	19	0.007	0.026	0.040	-0.082
ALL	93	-0.022	0.046	0.069	-0.121

		Pitch			
Line No.	Pts.	Mean	RMS	Max.	Min.
1	15	-0.001	0.060	0.143	-0.134
2	19	-0.006	0.061	0.145	-0.102
3	17	0.017	0.049	0.134	-0.061
4	23	-0.006	0.041	0.052	-0.082
5	19	-0.006	0.047	0.065	-0.158
ALL	93	-0.001	0.052	0.145	-0.158

		Heading			
Line No.	Pts.	Mean	RMS	Max.	Min.
1	15	0.003	0.022	0.029	-0.054
2	19	0.009	0.029	0.078	-0.043
3	17	0.008	0.031	0.057	-0.043
4	23	0.005	0.028	0.047	-0.049
5	19	-0.005	0.028	0.041	-0.046
ALL	93	0.004	0.028	0.078	-0.054

Table H.18

Double Differences of Orientation Angles (Degrees)

Mean, RMS and Max./Min. Values from
CCRS Bundle Adjustment and SPACE-M case (d)

		Roll			
Chron. Line No.	Pts.	Mean	RMS	Max.	Min.
1	10	0.001	0.032	0.085	-0.028
2	11	-0.004	0.032	0.038	-0.053
3	10	-0.015	0.023	0.009	-0.047
4	17	0.003	0.025	0.046	-0.035
5	11	0.006	0.015	0.040	-0.018
ALL	59	-0.001	0.026	0.085	-0.053

		Pitch			
Chron. Line No.	Pts.	Mean	RMS	Max.	Min.
1	10	-0.004	0.039	0.106	-0.041
2	11	0.000	0.023	0.022	-0.067
3	10	-0.012	0.025	0.017	-0.048
4	17	-0.004	0.028	0.065	-0.043
5	11	-0.004	0.014	0.027	-0.022
ALL	59	-0.004	0.027	0.106	-0.067

		Heading			
Chron. Line No.	Pts.	Mean	RMS	Max.	Min.
1	10	0.007	0.020	0.037	-0.030
2	11	-0.005	0.039	0.058	-0.068
3	10	0.015	0.048	0.091	-0.034
4	17	-0.008	0.025	0.033	-0.046
5	11	0.006	0.038	0.057	-0.054
ALL	59	0.002	0.034	0.091	-0.068

APPENDIX I

Detailed Comparisons of PC Positions

I.1 - I.7 - Positions from Auxiliary Systems
and Photogrammetric Adjustments

I.1 - I.3	SPACE-M including rejected points	Pages 185-187
I.4 - I.6	SPACE-M excluding rejected points	Pages 188-190
I.7	CCRS Bundle Adjustment	Page 191

I.8 - I.14 - Position Increments from Auxiliary Systems
and Photogrammetric Adjustments

I.8 - I.10	SPACE-M including rejected points	Pages 192-194
I.11 - I.13	SPACE-M excluding rejected points	Pages 195-197
I.14	CCRS Bundle Adjustment	Page 198

I.15 - I.23 Comparisons of CCRS Bundle and SPACE-M Adjustments

I.15 - I.17	Position Comparisons	Pages 199-201
-------------	----------------------	---------------

I.18 - I.23 Position Increments

I.18 - I.20	SPACE-M including rejected points	Pages 202-204
I.21 - I.23	SPACE-M excluding rejected points	Pages 205-207

Table I.1

Comparison of P.C. Positions by
Auxiliary Systems and SPACE-M Adjustments

Values are Auxiliary minus Photogrammetric (metres)

Old (Spring, 1985) data including rejected points

Column Headings are explained in Section 4.2

X-Coordinate

Chr. Flight Line	No. of Points	Mean t	Mean DepVar	Regr. Slope	Corr. Coeff	RMS Devn.
1	27	10.564	637.86	0.372	0.126	31.03
2	29	21.678	528.52	-0.199	-0.069	62.46
3	23	32.963	174.11	-0.020	-0.037	17.71
4	31	44.763	-180.41	-0.032	-0.031	46.05
5	28	56.633	-101.83	0.030	0.027	63.76

Y-Coordinate

Chr. Flight Line	No. of Points	Mean t	Mean DepVar	Regr. Slope	Corr. Coeff	RMS Devn.
1	27	10.564	980.00	-0.023	-0.028	8.84
2	29	21.678	102.59	0.160	0.066	52.26
3	23	32.963	1325.82	-0.009	-0.034	8.64
4	31	44.763	345.57	0.027	0.032	37.68
5	28	56.633	1439.56	-0.008	-0.021	22.05

Z-Coordinate

Chr. Flight Line	No. of Points	Mean t	Mean DepVar	Regr. Slope	Corr. Coeff	RMS Devn.
1	27	10.564	-274.98	-0.127	-0.110	12.13
2	29	21.678	-295.85	0.046	0.068	14.83
3	23	32.963	-290.49	0.003	0.024	4.67
4	31	44.763	-290.38	0.002	0.016	4.90
5	28	56.633	-284.91	0.001	0.018	3.08

Horizontal Distance

Chr. Flight Line	No. of Points	Mean t	Mean DepVar	Regr. Slope	Corr. Coeff	RMS Devn.
1	27	10.564	1169.66	0.185	0.123	15.76
2	29	21.678	542.19	-0.159	-0.068	50.54
3	23	32.963	1337.31	-0.011	-0.036	10.55
4	31	44.763	390.77	0.038	0.032	52.98
5	28	56.633	1444.52	-0.010	-0.023	25.08

Total Distance

Chr. Flight Line	No. of Points	Mean t	Mean DepVar	Regr. Slope	Corr. Coeff	RMS Devn.
1	27	10.564	1201.58	0.209	0.123	17.86
2	29	21.678	617.79	-0.162	-0.069	51.10
3	23	32.963	1368.50	-0.012	-0.035	11.05
4	31	44.763	488.03	0.029	0.032	40.98
5	28	56.633	1472.35	-0.010	-0.023	24.97

Table I.2.

Comparison of P.C. Positions by
Auxiliary Systems and SPACE-M Adjustments

Values are Auxiliary minus Photogrammetric (metres)

New (Autumn, 1985) data with lakes including rejected points

Column Headings are explained in Section 4.2

X-Coordinate						
Chr. Flight Line	No. of Points	Mean t	Mean DepVar	Regr. Slope	Corr. Coeff	RMS Devn.
1	27	10.564	637.87	0.378	0.126	31.53
2	29	21.678	527.96	-0.199	-0.069	62.46
3	23	32.963	174.01	-0.018	-0.037	16.36
4	31	44.763	-182.10	-0.032	-0.031	46.49
5	28	56.633	-101.44	0.030	0.027	64.19

Y-Coordinate						
Chr. Flight Line	No. of Points	Mean t	Mean DepVar	Regr. Slope	Corr. Coeff	RMS Devn.
1	27	10.564	980.51	-0.014	-0.018	8.67
2	29	21.678	102.18	0.160	0.066	52.21
3	23	32.963	1325.91	-0.009	-0.035	8.57
4	31	44.763	346.07	0.027	0.032	37.65
5	28	56.633	1440.02	-0.008	-0.021	21.97

Z-Coordinate						
Chr. Flight Line	No. of Points	Mean t	Mean DepVar	Regr. Slope	Corr. Coeff	RMS Devn.
1	27	10.564	-275.22	-0.117	-0.106	11.64
2	29	21.678	-296.71	0.046	0.068	14.53
3	23	32.963	-290.80	0.004	0.026	4.58
4	31	44.763	-289.94	0.002	0.021	4.87
5	28	56.633	-285.30	0.001	0.019	3.13

Horizontal Distance						
Chr. Flight Line	No. of Points	Mean t	Mean DepVar	Regr. Slope	Corr. Coeff	RMS Devn.
1	27	10.564	1170.08	0.196	0.124	16.60
2	29	21.678	541.58	-0.158	-0.068	50.44
3	23	32.963	1337.36	-0.011	-0.036	10.38
4	31	44.763	392.00	0.038	0.032	53.25
5	28	56.633	1444.97	-0.010	-0.023	25.07

Total Distance						
Chr. Flight Line	No. of Points	Mean t	Mean DepVar	Regr. Slope	Corr. Coeff	RMS Devn.
1	27	10.564	1202.04	0.217	0.123	19.52
2	29	21.678	617.66	-0.161	-0.068	50.95
3	23	32.963	1368.62	-0.012	-0.036	10.90
4	31	44.763	488.80	0.029	0.032	40.85
5	28	56.633	1472.87	-0.010	-0.024	24.96

Table I.3

Comparison of P.C. Positions by
Auxiliary Systems and SPACE-M Adjustments

Values are Auxiliary minus Photogrammetric (metres)

New (Autumn, 1985) data without lakes including rejected points

Column Headings are explained in Section 4.2

X-Coordinate						
Chr. Flight Line	No. of Points	Mean t	Mean DepVar	Regr. Slope	Corr. Coeff	RMS Devn.
1	27	10.564	639.69	0.388	0.127	32.10
2	29	21.678	525.99	-0.202	-0.069	63.35
3	23	32.963	174.90	-0.017	-0.037	15.56
4	31	44.763	-184.07	-0.033	-0.031	47.44
5	28	56.633	-100.90	0.031	0.027	64.88

Y-Coordinate						
Chr. Flight Line	No. of Points	Mean t	Mean DepVar	Regr. Slope	Corr. Coeff	RMS Devn.
1	27	10.564	980.48	-0.004	-0.005	9.18
2	29	21.678	101.58	0.157	0.067	51.01
3	23	32.963	1325.64	-0.008	-0.034	7.79
4	31	44.763	345.46	0.026	0.032	36.08
5	28	56.633	1440.13	-0.008	-0.020	21.07

Z-Coordinate						
Chr. Flight Line	No. of Points	Mean t	Mean DepVar	Regr. Slope	Corr. Coeff	RMS Devn.
1	27	10.564	-274.06	-0.108	-0.098	11.54
2	29	21.678	-296.38	0.048	0.068	15.32
3	23	32.963	-290.40	0.004	0.026	4.66
4	31	44.763	-288.49	0.003	0.021	6.30
5	28	56.633	-285.05	0.001	0.017	3.32

Horizontal Distance						
Chr. Flight Line	No. of Points	Mean t	Mean DepVar	Regr. Slope	Corr. Coeff	RMS Devn.
1	27	10.564	1171.06	0.210	0.123	17.95
2	29	21.678	539.42	-0.163	-0.068	51.57
3	23	32.963	1337.21	-0.010	-0.035	9.51
4	31	44.763	392.45	0.038	0.032	52.50
5	28	56.633	1445.08	-0.010	-0.023	23.99

Total Distance						
Chr. Flight Line	No. of Points	Mean t	Mean DepVar	Regr. Slope	Corr. Coeff	RMS Devn.
1	27	10.564	1202.72	0.229	0.122	19.74
2	29	21.678	615.61	-0.166	-0.069	52.26
3	23	32.963	1368.38	-0.011	-0.035	10.07
4	31	44.763	488.32	0.028	0.032	39.88
5	28	56.633	1472.93	-0.010	-0.023	23.95

Table I.4

Comparison of P.C. Positions by
Auxiliary Systems and SPACE-M Adjustments

Values are Auxiliary minus Photogrammetric (metres)

Old (Spring, 1985) data excluding rejected points

Column Headings are explained in Section 4.2

X-Coordinate						
Chr. Flight Line	No. of Points	Mean t	Mean DepVar	Regr. Slope	Corr. Coeff	RMS Devn.
1	16	10.899	646.51	0.339	0.121	30.33
2	17	21.784	522.63	-0.184	-0.066	60.56
3	18	32.907	174.19	-0.019	-0.036	17.71
4	23	44.635	-178.16	-0.026	-0.029	41.03
5	19	56.297	-115.56	0.026	0.024	59.68

Y-Coordinate						
Chr. Flight Line	No. of Points	Mean t	Mean DepVar	Regr. Slope	Corr. Coeff	RMS Devn.
1	16	10.899	978.28	-0.026	-0.034	8.37
2	17	21.784	106.20	0.154	0.064	52.53
3	18	32.907	1327.19	-0.009	-0.034	8.48
4	23	44.635	341.64	0.024	0.029	35.87
5	19	56.297	1445.37	-0.006	-0.018	19.80

Z-Coordinate						
Chr. Flight Line	No. of Points	Mean t	Mean DepVar	Regr. Slope	Corr. Coeff	RMS Devn.
1	16	10.899	-277.46	-0.116	-0.110	11.36
2	17	21.784	-295.07	0.041	0.065	13.80
3	18	32.907	-291.33	0.004	0.028	4.44
4	23	44.635	-291.31	0.001	0.011	4.54
5	19	56.297	-285.62	0.001	0.017	3.17

Horizontal Distance						
Chr. Flight Line	No. of Points	Mean t	Mean DepVar	Regr. Slope	Corr. Coeff	RMS Devn.
1	16	10.899	1172.94	0.165	0.118	15.11
2	17	21.784	537.18	-0.144	-0.065	48.11
3	18	32.907	1338.68	-0.011	-0.035	10.42
4	23	44.635	385.98	0.033	0.029	49.44
5	19	56.297	1451.17	-0.008	-0.021	22.70

Total Distance						
Chr. Flight Line	No. of Points	Mean t	Mean DepVar	Regr. Slope	Corr. Coeff	RMS Devn.
1	16	10.899	1205.34	0.187	0.118	17.16
2	17	21.784	613.01	-0.146	-0.066	48.57
3	18	32.907	1370.02	-0.012	-0.035	10.95
4	23	44.635	484.58	0.026	0.029	38.63
5	19	56.297	1479.02	-0.008	-0.021	22.58

Table I.5

Comparison of P.C. Positions by
Auxiliary Systems and SPACE-M Adjustments

Values are Auxiliary minus Photogrammetric (metres)

New (Autumn, 1985) data with lakes excluding rejected points

Column Headings are explained in Section 4.2

X-Coordinate						
Chr. Flight Line	No. of Points	Mean t	Mean DepVar	Regr. Slope	Corr. Coeff	RMS Devn.
1	17	10.942	647.85	0.329	0.118	30.33
2	18	21.738	523.35	-0.178	-0.065	59.48
3	19	32.930	174.10	-0.017	-0.035	15.88
4	24	44.640	-180.44	-0.025	-0.028	40.67
5	20	56.356	-113.09	0.025	0.024	59.12

Y-Coordinate						
Chr. Flight Line	No. of Points	Mean t	Mean DepVar	Regr. Slope	Corr. Coeff	RMS Devn.
1	17	10.942	979.26	-0.017	-0.024	7.93
2	18	21.738	104.02	0.151	0.063	52.07
3	19	32.930	1326.84	-0.008	-0.033	8.32
4	24	44.640	342.43	0.023	0.029	35.15
5	20	56.356	1445.64	-0.006	-0.018	19.09

Z-Coordinate						
Chr. Flight Line	No. of Points	Mean t	Mean DepVar	Regr. Slope	Corr. Coeff	RMS Devn.
1	17	10.942	-277.76	-0.101	-0.105	10.57
2	18	21.738	-296.21	0.039	0.064	13.24
3	19	32.930	-291.14	0.004	0.028	4.62
4	24	44.640	-290.73	0.002	0.016	4.30
5	20	56.356	-285.82	0.001	0.018	3.22

Horizontal Distance						
Chr. Flight Line	No. of Points	Mean t	Mean DepVar	Regr. Slope	Corr. Coeff	RMS Devn.
1	17	10.942	1174.48	0.167	0.116	15.70
2	18	21.738	537.38	-0.139	-0.064	47.11
3	19	32.930	1338.30	-0.011	-0.034	10.09
4	24	44.640	387.73	0.032	0.029	48.71
5	20	56.356	1451.22	-0.008	-0.021	22.03

Total Distance						
Chr. Flight Line	No. of Points	Mean t	Mean DepVar	Regr. Slope	Corr. Coeff	RMS Devn.
1	17	10.942	1206.90	0.185	0.115	17.53
2	18	21.738	613.72	-0.141	-0.064	47.49
3	19	32.930	1369.60	-0.011	-0.034	10.68
4	24	44.640	485.63	0.024	0.029	37.62
5	20	56.356	1479.11	-0.008	-0.021	21.93

Table I.6

Comparison of P.C. Positions by
Auxiliary Systems and SPACE-M Adjustments

Values are Auxiliary minus Photogrammetric (metres)

New (Autumn, 1985) data without lakes excluding rejected points

Column Headings are explained in Section 4.2

X-Coordinate						
Chr. Flight Line	No. of Points	Mean t	Mean DepVar	Regr. Slope	Corr. Coeff	RMS Devn.
1	17	10.942	649.60	0.340	0.119	31.11
2	18	21.738	521.95	-0.180	-0.065	60.18
3	19	32.930	174.98	-0.016	-0.035	15.13
4	24	44.640	-182.30	-0.026	-0.028	41.57
5	20	56.356	-112.80	0.025	0.024	59.40

Y-Coordinate						
Chr. Flight Line	No. of Points	Mean t	Mean DepVar	Regr. Slope	Corr. Coeff	RMS Devn.
1	17	10.942	979.46	-0.008	-0.011	8.52
2	18	21.738	102.85	0.146	0.063	50.34
3	19	32.930	1326.64	-0.008	-0.033	7.62
4	24	44.640	341.65	0.022	0.029	33.63
5	20	56.356	1445.53	-0.006	-0.017	18.34

Z-Coordinate						
Chr. Flight Line	No. of Points	Mean t	Mean DepVar	Regr. Slope	Corr. Coeff	RMS Devn.
1	17	10.942	-276.28	-0.093	-0.100	10.20
2	18	21.738	-295.87	0.042	0.064	14.14
3	19	32.930	-290.84	0.004	0.029	4.72
4	24	44.640	-289.46	0.002	0.019	5.46
5	20	56.356	-285.69	0.001	0.016	3.31

Horizontal Distance						
Chr. Flight Line	No. of Points	Mean t	Mean DepVar	Regr. Slope	Corr. Coeff	RMS Devn.
1	17	10.942	1175.62	0.180	0.114	17.12
2	18	21.738	535.61	-0.143	-0.064	48.17
3	19	32.930	1338.20	-0.010	-0.034	9.31
4	24	44.640	387.96	0.031	0.029	47.98
5	20	56.356	1451.11	-0.008	-0.020	21.10

Total Distance						
Chr. Flight Line	No. of Points	Mean t	Mean DepVar	Regr. Slope	Corr. Coeff	RMS Devn.
1	17	10.942	1207.67	0.196	0.114	18.80
2	18	21.738	612.01	-0.145	-0.065	48.78
3	19	32.930	1369.45	-0.010	-0.034	9.95
4	24	44.640	485.07	0.024	0.029	36.59
5	20	56.356	1478.97	-0.008	-0.020	21.06

Table I.7

Comparison of P.C. Positions by
Auxiliary Systems and CCRS Bundle Adjustment

Values are Auxiliary minus Photogrammetric (metres)

Column Headings are explained in Section 4.2

X-Coordinate						
Chr. Flight Line	No. of Points	Mean t	Mean DepVar	Regr. Slope	Corr. Coeff	RMS Devn.
1	27	10.564	636.77	0.385	0.129	31.27
2	29	21.678	521.10	-0.202	-0.069	63.17
3	23	32.963	175.55	-0.018	-0.038	15.87
4	31	44.763	-191.62	-0.030	-0.031	42.73
5	28	56.633	-104.33	0.030	0.027	63.70
Y-Coordinate						
Chr. Flight Line	No. of Points	Mean t	Mean DepVar	Regr. Slope	Corr. Coeff	RMS Devn.
1	27	10.564	980.11	-0.083	-0.101	8.65
2	29	21.678	102.01	0.178	0.067	57.10
3	23	32.963	1326.59	-0.015	-0.037	12.80
4	31	44.763	344.59	0.026	0.032	36.81
5	28	56.633	1437.20	-0.010	-0.023	24.19
Z-Coordinate						
Chr. Flight Line	No. of Points	Mean t	Mean DepVar	Regr. Slope	Corr. Coeff	RMS Devn.
1	27	10.564	-286.01	-0.094	-0.119	8.30
2	29	21.678	-305.91	0.045	0.069	13.93
3	23	32.963	-300.11	0.004	0.030	4.17
4	31	44.763	-292.32	0.002	0.015	4.83
5	28	56.633	-293.76	0.001	0.025	1.86
Horizontal Distance						
Chr. Flight Line	No. of Points	Mean t	Mean DepVar	Regr. Slope	Corr. Coeff	RMS Devn.
1	27	10.564	1169.20	0.141	0.121	12.20
2	29	21.678	535.48	-0.158	-0.068	50.08
3	23	32.963	1338.23	-0.017	-0.038	14.72
4	31	44.763	394.92	0.037	0.032	51.80
5	28	56.633	1442.33	-0.012	-0.025	27.64
Total Distance						
Chr. Flight Line	No. of Points	Mean t	Mean DepVar	Regr. Slope	Corr. Coeff	RMS Devn.
1	27	10.564	1203.69	0.159	0.121	13.81
2	29	21.678	616.84	-0.159	-0.069	50.27
3	23	32.963	1371.47	-0.017	-0.037	15.16
4	31	44.763	492.43	0.029	0.032	40.36
5	28	56.633	1471.95	-0.012	-0.025	27.32

Table I.8

Comparison of P.C. Position Increments by
Auxiliary Systems and SPACE-M Adjustments

Old (Spring, 1985) data including rejected points

Photogrammetric Increments Within Models

RMS Discrepancies (metres)

Chr.Flight Line	No. of Points	X-Compt.	Y-Compt.	Z-Compt.	Horiz. Dist	Total Dist.
1	26	4.60	2.57	3.30	2.52	2.52
2	28	7.83	6.58	3.74	6.65	6.65
3	22	3.03	2.12	1.98	2.13	2.13
4	30	6.17	4.00	2.60	4.04	4.04
5	27	8.20	3.82	2.54	3.88	3.88

Max. Absolute Discrepancies (metres)

Chr.Flight Line	No. of Points	X-Compt.	Y-Compt.	Z-Compt.	Horiz. Dist	Total Dist.
1	26	8.71	6.25	8.43	6.19	6.17
2	28	10.58	14.26	8.21	14.28	14.28
3	22	6.47	4.67	5.29	4.63	4.62
4	30	11.20	7.12	7.31	7.18	7.19
5	27	15.53	9.50	5.83	9.46	9.44

Photogrammetric Increments Between Mean P.C.'s

RMS Discrepancies (metres)

Chr.Flight Line	No. of Points	X-Compt.	Y-Compt.	Z-Compt.	Horiz. Dist	Total Dist.
1	26	5.35	4.63	3.77	4.64	4.64
2	28	9.04	8.29	3.54	8.37	8.37
3	22	4.14	3.39	1.99	3.38	3.39
4	30	6.55	5.70	2.70	5.71	5.70
5	27	8.73	5.61	2.38	5.66	5.66

Max. Absolute Discrepancies (metres)

Chr.Flight Line	No. of Points	X-Compt.	Y-Compt.	Z-Compt.	Horiz. Dist	Total Dist.
1	26	14.03	11.15	9.98	10.86	10.81
2	28	17.97	17.39	7.38	17.60	17.60
3	22	8.59	7.93	4.22	7.96	7.96
4	30	11.37	12.23	7.21	12.24	12.24
5	27	16.01	12.93	5.01	13.27	13.27

Table I.9

Comparison of P.C. Position Increments by
Auxiliary Systems and SPACE-M Adjustments

New (Autumn, 1985) data with lakes including rejected points

Photogrammetric Increments Within Models

RMS Discrepancies (metres)

Chr.Flight Line	No. of Points	X-Compt.	Y-Compt.	Z-Compt.	Horiz. Dist	Total Dist.
1	26	4.57	2.63	3.33	2.58	2.57
2	28	7.90	6.44	3.99	6.51	6.50
3	22	3.09	2.16	1.87	2.17	2.17
4	30	6.20	3.90	2.39	3.95	3.94
5	27	8.18	3.80	2.40	3.86	3.85

Max. Absolute Discrepancies (metres)

Chr.Flight Line	No. of Points	X-Compt.	Y-Compt.	Z-Compt.	Horiz. Dist	Total Dist.
1	26	8.61	6.08	8.83	6.02	5.99
2	28	10.84	13.92	12.78	13.94	13.94
3	22	7.04	4.68	4.87	4.64	4.63
4	30	11.23	7.26	6.21	7.28	7.28
5	27	15.49	9.62	5.72	9.58	9.56

Photogrammetric Increments Between Mean P.C.'s

RMS Discrepancies (metres)

Chr.Flight Line	No. of Points	X-Compt.	Y-Compt.	Z-Compt.	Horiz. Dist	Total Dist.
1	26	5.56	4.55	3.65	4.55	4.55
2	28	10.54	8.67	3.58	8.77	8.77
3	22	3.83	3.15	1.87	3.14	3.14
4	30	6.64	5.29	2.41	5.31	5.31
5	27	8.59	5.12	2.25	5.18	5.18

Max. Absolute Discrepancies (metres)

Chr.Flight Line	No. of Points	X-Compt.	Y-Compt.	Z-Compt.	Horiz. Dist	Total Dist.
1	26	14.85	11.64	9.81	11.33	11.29
2	28	29.04	22.04	8.39	22.45	22.44
3	22	7.11	6.88	4.09	6.92	6.92
4	30	11.41	10.68	5.76	10.64	10.64
5	27	15.11	12.39	4.71	12.39	12.39

Table I.10

Comparison of P.C. Position Increments by
Auxiliary Systems and SPACE-M Adjustments

New (Autumn, 1985) data without lakes including rejected points

Photogrammetric Increments Within Models

RMS Discrepancies (metres)

Chr.Flight Line	No. of Points	X-Compt.	Y-Compt.	Z-Compt.	Horiz. Dist	Total Dist.
1	26	4.57	2.62	3.51	2.56	2.56
2	28	7.90	6.45	3.83	6.52	6.52
3	22	3.09	2.16	1.93	2.17	2.17
4	30	6.21	3.89	2.52	3.94	3.94
5	27	8.20	3.79	2.43	3.85	3.84

Max. Absolute Discrepancies (metres)

Chr.Flight Line	No. of Points	X-Compt.	Y-Compt.	Z-Compt.	Horiz. Dist	Total Dist.
1	26	8.64	6.02	9.62	5.96	5.93
2	28	10.84	13.96	10.22	13.98	13.98
3	22	7.05	4.69	4.78	4.65	4.64
4	30	11.24	7.31	5.13	7.33	7.33
5	27	15.55	9.59	6.53	9.55	9.53

Photogrammetric Increments Between Mean P.C.'s

RMS Discrepancies (metres)

Chr.Flight Line	No. of Points	X-Compt.	Y-Compt.	Z-Compt.	Horiz. Dist	Total Dist.
1	26	4.97	4.55	3.72	4.55	4.55
2	28	9.36	7.79	3.44	7.89	7.88
3	22	3.70	3.20	1.98	3.19	3.19
4	30	6.64	4.65	2.57	4.68	4.68
5	27	8.63	5.09	2.27	5.14	5.13

Max. Absolute Discrepancies (metres)

Chr.Flight Line	No. of Points	X-Compt.	Y-Compt.	Z-Compt.	Horiz. Dist	Total Dist.
1	26	12.68	10.45	10.63	10.18	10.14
2	28	22.87	18.87	7.42	19.23	19.22
3	22	6.90	6.78	3.99	6.76	6.75
4	30	12.16	9.14	5.80	9.18	9.17
5	27	15.40	13.00	5.13	12.96	12.94

Table I.11

Comparison of P.C. Position Increments by
Auxiliary Systems and SPACE-M Adjustments

Old (Spring, 1985) data excluding rejected points

Photogrammetric Increments Within Models

RMS Discrepancies (metres)

Chr.Flight Line	No. of Points	X-Compt.	Y-Compt.	Z-Compt.	Horiz. Dist	Total Dist.
1	11	4.00	2.50	2.14	2.44	2.44
2	9	7.78	5.34	3.91	5.39	5.38
3	14	3.09	1.88	1.60	1.89	1.88
4	17	7.10	4.13	2.03	4.15	4.15
5	13	6.84	3.43	2.06	3.43	3.42

Max. Absolute Discrepancies (metres)

Chr.Flight Line	No. of Points	X-Compt.	Y-Compt.	Z-Compt.	Horiz. Dist	Total Dist.
1	11	5.90	4.81	4.12	4.71	4.71
2	9	10.53	8.96	6.71	8.97	8.93
3	14	6.47	4.67	2.60	4.63	4.62
4	17	11.20	7.12	4.02	7.14	7.14
5	13	12.31	9.50	4.00	9.46	9.44

Photogrammetric Increments Between Mean P.C.'s

RMS Discrepancies (metres)

Chr.Flight Line	No. of Points	X-Compt.	Y-Compt.	Z-Compt.	Horiz. Dist	Total Dist.
1	11	5.11	2.79	2.30	2.78	2.78
2	9	7.01	5.39	3.73	5.44	5.43
3	14	4.47	3.39	1.70	3.38	3.39
4	17	7.13	4.73	2.13	4.75	4.75
5	13	7.04	4.53	2.01	4.52	4.51

Max. Absolute Discrepancies (metres)

Chr.Flight Line	No. of Points	X-Compt.	Y-Compt.	Z-Compt.	Horiz. Dist	Total Dist.
1	11	10.09	5.60	4.41	5.70	5.70
2	9	9.80	11.22	7.38	11.29	11.29
3	14	8.59	6.70	2.76	6.67	6.66
4	17	11.24	9.06	4.33	9.23	9.22
5	13	13.13	12.73	4.01	12.71	12.69

Table I.12

Comparison of P.C. Position Increments by
Auxiliary Systems and SPACE-M Adjustments

New (Autumn, 1985) data with lakes excluding rejected points

Photogrammetric Increments Within Models

RMS Discrepancies (metres)

Chr.Flight Line	No. of Points	X-Compt.	Y-Compt.	Z-Compt.	Horiz. Dist	Total Dist.
1	13	4.18	2.52	2.13	2.45	2.44
2	10	7.97	5.01	3.63	5.07	5.06
3	16	3.04	1.87	1.66	1.87	1.87
4	19	6.84	3.92	1.93	3.95	3.95
5	15	6.82	3.69	1.83	3.70	3.70

Max. Absolute Discrepancies (metres)

Chr.Flight Line	No. of Points	X-Compt.	Y-Compt.	Z-Compt.	Horiz. Dist	Total Dist.
1	13	5.82	4.76	4.26	4.67	4.66
2	10	10.84	8.50	6.15	8.52	8.48
3	16	7.04	4.68	3.22	4.64	4.63
4	19	11.23	7.26	3.60	7.28	7.28
5	15	12.32	9.62	3.58	9.58	9.56

Photogrammetric Increments Between Mean P.C.'s

RMS Discrepancies (metres)

Chr.Flight Line	No. of Points	X-Compt.	Y-Compt.	Z-Compt.	Horiz. Dist	Total Dist.
1	13	5.46	2.52	1.99	2.52	2.52
2	10	7.76	5.75	3.31	5.82	5.81
3	16	3.97	3.15	1.72	3.14	3.14
4	19	7.06	4.86	1.98	4.90	4.90
5	15	7.08	5.04	1.83	5.06	5.06

Max. Absolute Discrepancies (metres)

Chr.Flight Line	No. of Points	X-Compt.	Y-Compt.	Z-Compt.	Horiz. Dist	Total Dist.
1	13	11.46	5.19	4.26	5.25	5.25
2	10	9.83	10.99	5.96	11.05	11.05
3	16	7.11	6.73	3.46	6.72	6.70
4	19	11.41	9.20	4.29	9.23	9.23
5	15	13.34	12.39	3.59	12.36	12.34

Table I.13

Comparison of P.C. Position Increments by
Auxiliary Systems and SPACE-M Adjustments

New (Autumn, 1985) data without lakes excluding rejected points

Photogrammetric Increments Within Models

RMS Discrepancies (metres)

Chr.Flight Line	No. of Points	X-Compt.	Y-Compt.	Z-Compt.	Horiz. Dist	Total Dist.
1	13	4.18	2.51	2.27	2.44	2.44
2	10	7.96	5.05	4.19	5.11	5.10
3	16	3.04	1.88	1.72	1.88	1.87
4	19	6.85	3.92	2.14	3.95	3.95
5	15	6.82	3.68	2.04	3.69	3.69

Max. Absolute Discrepancies (metres)

Chr.Flight Line	No. of Points	X-Compt.	Y-Compt.	Z-Compt.	Horiz. Dist	Total Dist.
1	13	5.81	4.74	4.52	4.65	4.64
2	10	10.81	8.56	7.64	8.57	8.53
3	16	7.05	4.69	3.60	4.65	4.64
4	19	11.24	7.31	5.13	7.33	7.33
5	15	12.32	9.59	4.67	9.55	9.53

Photogrammetric Increments Between Mean P.C.'s

RMS Discrepancies (metres)

Chr.Flight Line	No. of Points	X-Compt.	Y-Compt.	Z-Compt.	Horiz. Dist	Total Dist.
1	13	5.12	2.42	2.09	2.43	2.43
2	10	7.78	5.53	3.91	5.60	5.59
3	16	3.85	3.21	1.83	3.20	3.20
4	19	7.21	4.66	2.19	4.70	4.70
5	15	7.07	5.16	2.05	5.17	5.17

Max. Absolute Discrepancies (metres)

Chr.Flight Line	No. of Points	X-Compt.	Y-Compt.	Z-Compt.	Horiz. Dist	Total Dist.
1	13	9.11	5.08	4.62	5.13	5.14
2	10	9.91	9.01	7.42	9.03	8.98
3	16	6.90	6.78	3.82	6.76	6.75
4	19	12.16	9.14	5.80	9.18	9.17
5	15	13.52	13.00	4.71	12.96	12.94

Table I.14

Comparison of P.C. Position Increments by
Auxiliary Systems and CCRS Bundle Adjustment

RMS Discrepancies (metres)

Chr.Flight Line	No. of Points	X-Compt.	Y-Compt.	Z-Compt.	Horiz. Dist	Total Dist.
1	26	4.09	1.74	1.36	1.80	1.80
2	28	7.57	7.53	1.69	7.61	7.61
3	22	2.39	1.95	0.92	1.91	1.91
4	30	5.29	4.14	1.08	4.20	4.19
5	27	7.86	4.22	0.29	4.30	4.30

Max. Discrepancies

Chr.Flight Line	No. of Points	X-Compt.	Y-Compt.	Z-Compt.	Horiz. Dist	Total Dist.
1	26	4.48	3.38	2.71	3.46	3.46
2	28	8.52	12.43	2.13	12.45	12.45
3	22	2.87	2.57	1.60	2.52	2.52
4	30	8.47	4.87	2.19	4.87	4.87
5	27	8.48	8.19	0.53	8.32	8.32

Table I.15

Comparison of P.C. Positions by
CCRS Bundle and SPACE-M Adjustments

Old (Spring, 1985) data including rejected points

Chr. Flight Line	No. of Points	RMS Discrepancies (metres)			Horiz. Dist	Total Dist.
		X-Compt.	Y-Compt.	Z-Compt.		
1	27	7.19	6.93	11.94	9.99	15.56
2	29	9.45	7.79	10.46	12.25	16.11
3	23	4.51	6.50	10.11	7.91	12.84
4	31	12.50	5.35	4.27	13.60	14.25
5	28	7.33	6.82	9.17	10.01	13.58

Chr. Flight Line	No. of Points	Max. Absolute Discrepancies (metres)			Horiz. Dist	Total Dist.
		X-Compt.	Y-Compt.	Z-Compt.		
1	27	20.83	14.07	26.78	24.76	36.48
2	29	26.21	21.50	16.23	28.43	30.10
3	23	11.49	16.54	18.08	16.67	24.60
4	31	20.19	10.22	8.83	22.54	22.63
5	28	13.70	19.73	14.30	22.71	26.51

Old (Spring, 1985) data excluding rejected points

Chr. Flight Line	No. of Points	RMS Discrepancies (metres)			Horiz. Dist	Total Dist.
		X-Compt.	Y-Compt.	Z-Compt.		
1	16	5.96	6.40	11.01	8.75	14.07
2	17	7.05	7.24	10.14	10.11	14.32
3	18	4.93	6.04	9.12	7.80	12.00
4	23	12.60	5.31	4.28	13.67	14.33
5	19	7.22	4.97	8.67	8.77	12.34

Chr. Flight Line	No. of Points	Max. Absolute Discrepancies (metres)			Horiz. Dist	Total Dist.
		X-Compt.	Y-Compt.	Z-Compt.		
1	16	17.57	14.07	22.33	22.51	31.71
2	17	13.81	21.50	15.10	24.60	27.40
3	18	11.49	13.04	14.50	14.48	19.54
4	23	19.85	10.22	8.83	21.75	21.77
5	19	13.70	10.51	12.63	13.70	18.00

Table I.16

Comparison of P.C. Positions by
CCRS Bundle and SPACE-M Adjustments

New (Autumn, 1985) data with lakes including rejected points

Chr. Flight Line	No. of Points	RMS Discrepancies (metres)			Horiz. Dist	Total Dist.
		X-Compt.	Y-Compt.	Z-Compt.		
1	27	7.32	7.49	11.63	10.47	15.65
2	29	10.18	7.91	9.52	12.89	16.03
3	23	3.62	6.19	9.76	7.17	12.11
4	31	11.25	5.06	4.26	12.34	13.05
5	28	6.82	6.40	8.78	9.35	12.83

Chr. Flight Line	No. of Points	Max. Absolute Discrepancies (metres)			Horiz. Dist	Total Dist.
		X-Compt.	Y-Compt.	Z-Compt.		
1	27	20.85	15.56	26.19	25.49	36.54
2	29	33.19	19.49	15.27	37.71	39.01
3	23	8.28	15.46	17.05	15.46	23.01
4	31	18.69	9.61	8.60	21.02	21.17
5	28	13.14	19.25	13.02	21.75	25.16

New (Autumn, 1985) data with lakes excluding rejected points

Chr. Flight Line	No. of Points	RMS Discrepancies (metres)			Horiz. Dist	Total Dist.
		X-Compt.	Y-Compt.	Z-Compt.		
1	17	6.00	6.78	10.89	9.05	14.16
2	18	5.72	6.53	9.41	8.68	12.80
3	19	3.87	5.61	9.12	6.82	11.39
4	24	11.16	5.14	4.40	12.29	13.05
5	20	6.59	4.49	8.40	7.98	11.58

Chr. Flight Line	No. of Points	Max. Absolute Discrepancies (metres)			Horiz. Dist	Total Dist.
		X-Compt.	Y-Compt.	Z-Compt.		
1	17	17.13	15.56	21.64	23.14	31.68
2	18	10.76	19.49	12.31	21.92	24.07
3	19	8.28	12.27	14.09	12.62	18.92
4	24	18.15	9.14	8.60	19.78	19.79
5	20	13.14	8.82	11.88	13.16	16.30

Table I.17

Comparison of P.C. Positions by
CCRS Bundle and SPACE-M Adjustments

New (Autumn, 1985) data without lakes including rejected points

Chr. Flight Line	No. of Points	RMS Discrepancies (metres)			Horiz. Dist	Total Dist.
		X-Compt.	Y-Compt.	Z-Compt.		
1	27	6.85	8.41	12.90	10.84	16.85
2	29	7.31	7.87	10.00	10.74	14.67
3	23	3.34	7.17	10.33	7.91	13.01
4	31	10.13	4.99	5.39	11.29	12.51
5	28	6.86	7.46	9.17	10.13	13.67

Max. Absolute Discrepancies (metres)

Chr. Flight Line	No. of Points	Max. Absolute Discrepancies (metres)			Horiz. Dist	Total Dist.
		X-Compt.	Y-Compt.	Z-Compt.		
1	27	20.12	18.34	28.85	26.66	39.28
2	29	23.57	17.42	18.55	26.97	28.60
3	23	6.40	18.72	19.49	18.72	27.02
4	31	17.31	11.59	12.03	20.83	20.84
5	28	15.13	21.92	16.55	23.11	26.64

New (Autumn, 1985) data without lakes excluding rejected points

Chr. Flight Line	No. of Points	RMS Discrepancies (metres)			Horiz. Dist	Total Dist.
		X-Compt.	Y-Compt.	Z-Compt.		
1	17	6.19	7.80	12.36	9.95	15.87
2	18	4.32	7.26	9.90	8.44	13.01
3	19	3.42	6.42	9.52	7.27	11.98
4	24	9.93	4.70	5.27	10.99	12.19
5	20	6.59	5.09	8.62	8.33	11.98

Max. Absolute Discrepancies (metres)

Chr. Flight Line	No. of Points	Max. Absolute Discrepancies (metres)			Horiz. Dist	Total Dist.
		X-Compt.	Y-Compt.	Z-Compt.		
1	17	16.45	18.34	23.43	24.64	34.00
2	18	7.11	17.42	16.81	18.57	22.26
3	19	6.40	15.24	15.70	15.56	22.10
4	24	17.09	9.80	10.10	19.47	19.48
5	20	13.91	12.85	14.30	14.24	20.18

Table I.18

Comparison of P.C. Position Increments by
CCRS Bundle and SPACE-M Adjustments

Old (Spring, 1985) data including rejected points

Photogrammetric Increments Within Models

RMS Discrepancies (metres)

Chr. Flight Line	No. of Points	X-Compt.	Y-Compt.	Z-Compt.	Horiz. Dist	Total Dist.
1	26	1.89	3.09	2.56	3.09	3.09
2	28	1.84	2.74	2.98	2.74	2.74
3	22	2.18	2.66	2.03	2.66	2.66
4	30	1.87	2.21	2.40	2.20	2.20
5	27	3.13	2.87	2.60	2.89	2.89

Max. Absolute Discrepancies (metres)

Chr. Flight Line	No. of Points	X-Compt.	Y-Compt.	Z-Compt.	Horiz. Dist	Total Dist.
1	26	4.63	6.44	5.93	6.48	6.46
2	28	4.16	7.32	6.55	7.32	7.31
3	22	4.01	5.66	5.19	5.66	5.66
4	30	4.17	4.02	6.16	4.03	4.05
5	27	7.39	7.13	5.93	7.19	7.17

Photogrammetric Increments Between Mean P.C.'s

RMS Discrepancies (metres)

Chr. Flight Line	No. of Points	X-Compt.	Y-Compt.	Z-Compt.	Horiz. Dist	Total Dist.
1	26	4.17	4.45	3.02	4.44	4.44
2	28	4.62	4.63	3.02	4.64	4.64
3	22	3.29	3.45	2.08	3.46	3.46
4	30	3.07	4.19	2.52	4.17	4.17
5	27	5.03	4.57	2.41	4.62	4.61

Max. Absolute Discrepancies (metres)

Chr. Flight Line	No. of Points	X-Compt.	Y-Compt.	Z-Compt.	Horiz. Dist	Total Dist.
1	26	9.95	11.34	8.56	11.14	11.11
2	28	16.16	11.57	6.18	11.49	11.50
3	22	5.88	6.96	4.26	7.02	7.03
4	30	6.83	8.85	7.03	8.79	8.80
5	27	11.39	10.35	5.11	10.44	10.42

Table I.19

Comparison of P.C. Position Increments by
CCRS Bundle and SPACE-M Adjustments

New (Autumn, 1985) data with lakes including rejected points

Photogrammetric Increments Within Models

RMS Discrepancies (metres)

Chr. Flight Line	No. of Points	X-Compt.	Y-Compt.	Z-Compt.	Horiz. Dist	Total Dist.
1	26	1.83	3.22	2.61	3.22	3.22
2	28	1.91	2.77	3.24	2.76	2.77
3	22	2.24	2.67	1.91	2.68	2.68
4	30	1.97	2.20	2.20	2.19	2.19
5	27	3.13	2.88	2.44	2.90	2.90

Max. Absolute Discrepancies (metres)

Chr. Flight Line	No. of Points	X-Compt.	Y-Compt.	Z-Compt.	Horiz. Dist	Total Dist.
1	26	4.53	6.27	6.33	6.30	6.28
2	28	4.33	7.24	10.94	7.24	7.23
3	22	4.28	5.76	4.77	5.75	5.76
4	30	4.44	3.76	5.06	3.78	3.78
5	27	7.34	7.25	5.82	7.31	7.29

Photogrammetric Increments Between Mean P.C.'s

RMS Discrepancies (metres)

Chr. Flight Line	No. of Points	X-Compt.	Y-Compt.	Z-Compt.	Horiz. Dist	Total Dist.
1	26	4.51	4.36	2.86	4.35	4.35
2	28	7.18	5.13	3.10	5.20	5.20
3	22	3.02	3.18	1.95	3.19	3.19
4	30	3.23	3.60	2.20	3.58	3.58
5	27	4.68	3.93	2.28	3.97	3.97

Max. Absolute Discrepancies (metres)

Chr. Flight Line	No. of Points	X-Compt.	Y-Compt.	Z-Compt.	Horiz. Dist	Total Dist.
1	26	10.77	11.83	7.86	11.61	11.58
2	28	28.54	13.32	8.78	13.85	13.86
3	22	4.74	6.48	4.01	6.55	6.55
4	30	7.58	6.94	5.06	6.99	6.99
5	27	9.68	10.01	4.81	10.09	10.07

Table I.20

Comparison of P.C. Position Increments by
CCRS Bundle and SPACE-M Adjustments

New (Autumn, 1985) data without lakes including rejected points

Photogrammetric Increments Within Models

RMS Discrepancies (metres)

Chr. Flight Line	No. of Points	X-Compt.	Y-Compt.	Z-Compt.	Horiz. Dist	Total Dist.
1	26	1.84	3.21	2.74	3.21	3.21
2	28	1.90	2.76	2.93	2.76	2.76
3	22	2.24	2.66	2.07	2.67	2.67
4	30	1.98	2.20	2.14	2.20	2.20
5	27	3.13	2.88	2.50	2.90	2.90

Max. Absolute Discrepancies (metres)

Chr. Flight Line	No. of Points	X-Compt.	Y-Compt.	Z-Compt.	Horiz. Dist	Total Dist.
1	26	4.56	6.21	7.12	6.25	6.23
2	28	4.30	7.22	8.38	7.22	7.21
3	22	4.29	5.75	4.68	5.74	5.75
4	30	4.46	3.73	3.66	3.75	3.76
5	27	7.41	7.21	6.63	7.28	7.26

Photogrammetric Increments Between Mean P.C.'s

RMS Discrepancies (metres)

Chr. Flight Line	No. of Points	X-Compt.	Y-Compt.	Z-Compt.	Horiz. Dist	Total Dist.
1	26	3.64	4.35	2.88	4.34	4.34
2	28	5.28	3.96	2.79	4.00	4.00
3	22	2.97	3.35	2.14	3.36	3.36
4	30	3.18	2.90	2.16	2.90	2.90
5	27	4.52	3.96	2.33	4.00	3.99

Max. Absolute Discrepancies (metres)

Chr. Flight Line	No. of Points	X-Compt.	Y-Compt.	Z-Compt.	Horiz. Dist	Total Dist.
1	26	9.48	10.64	8.13	10.47	10.44
2	28	21.01	8.89	6.81	9.24	9.25
3	22	4.73	6.56	4.71	6.55	6.54
4	30	6.94	5.44	4.83	5.47	5.47
5	27	7.60	10.63	5.23	10.70	10.67

Table I.21

Comparison of P.C. Position Increments
by CCRS Bundle and SPACE-M Adjustments

Old (Spring, 1985) data excluding rejected points

Photogrammetric Increments Within Models

Chr. Flight Line	No. of Points	RMS Discrepancies (metres)			Horiz. Dist	Total Dist.
		X-Compt.	Y-Compt.	Z-Compt.		
1	11	1.14	3.03	1.62	3.03	3.03
2	9	1.67	3.98	2.61	3.98	3.98
3	14	2.17	2.34	1.66	2.35	2.35
4	17	2.25	2.06	2.02	2.04	2.04
5	13	3.26	3.00	2.17	3.03	3.02

Chr. Flight Line	No. of Points	Max. Absolute Discrepancies (metres)			Horiz. Dist	Total Dist.
		X-Compt.	Y-Compt.	Z-Compt.		
1	11	2.18	5.33	3.11	5.38	5.37
2	9	4.02	7.32	4.65	7.32	7.31
3	14	3.71	3.99	3.54	4.05	4.05
4	17	4.17	3.19	4.05	3.13	3.13
5	13	5.33	7.13	4.50	7.19	7.17

Photogrammetric Increments Between Mean P.C.'s

Chr. Flight Line	No. of Points	RMS Discrepancies (metres)			Horiz. Dist	Total Dist.
		X-Compt.	Y-Compt.	Z-Compt.		
1	11	2.03	3.23	1.64	3.22	3.22
2	9	2.13	3.69	2.52	3.69	3.70
3	14	3.33	3.81	1.82	3.81	3.81
4	17	3.07	3.53	2.06	3.51	3.51
5	13	4.78	3.89	2.09	3.93	3.92

Chr. Flight Line	No. of Points	Max. Absolute Discrepancies (metres)			Horiz. Dist	Total Dist.
		X-Compt.	Y-Compt.	Z-Compt.		
1	11	6.02	5.64	3.26	5.65	5.65
2	9	3.96	6.91	5.25	6.90	6.90
3	14	5.88	6.96	4.26	7.02	7.03
4	17	6.83	6.09	4.34	6.01	6.00
5	13	7.85	10.35	4.51	10.44	10.42

Table I.22

Comparison of P.C. Position Increments by
CCRS Bundle and SPACE-M Adjustments

New (Autumn, 1985) data with lakes excluding rejected points

Photogrammetric Increments Within Models

RMS Discrepancies (metres)

Chr. Flight Line	No. of Points	X-Compt.	Y-Compt.	Z-Compt.	Horiz. Dist	Total Dist.
1	13	1.10	3.41	1.73	3.40	3.40
2	10	1.74	3.86	2.38	3.86	3.86
3	16	2.33	2.28	1.67	2.28	2.28
4	19	2.26	2.21	1.95	2.20	2.20
5	15	3.10	2.80	1.91	2.83	2.83

Max. Absolute Discrepancies (metres)

Chr. Flight Line	No. of Points	X-Compt.	Y-Compt.	Z-Compt.	Horiz. Dist	Total Dist.
1	13	2.09	5.73	3.86	5.78	5.78
2	10	4.33	7.24	4.44	7.24	7.23
3	16	4.28	4.20	3.40	4.27	4.26
4	19	4.44	3.76	3.75	3.78	3.78
5	15	5.53	7.25	4.08	7.31	7.29

Photogrammetric Increments Between Mean P.C.'s

RMS Discrepancies (metres)

Chr. Flight Line	No. of Points	X-Compt.	Y-Compt.	Z-Compt.	Horiz. Dist	Total Dist.
1	13	2.60	2.88	1.46	2.86	2.86
2	10	2.00	3.33	2.24	3.33	3.33
3	16	3.07	3.35	1.79	3.35	3.35
4	19	3.34	3.11	1.93	3.10	3.10
5	15	4.39	3.70	1.88	3.73	3.72

Max. Absolute Discrepancies (metres)

Chr. Flight Line	No. of Points	X-Compt.	Y-Compt.	Z-Compt.	Horiz. Dist	Total Dist.
1	13	7.40	6.27	2.93	6.25	6.25
2	10	3.84	6.12	3.83	6.10	6.10
3	16	4.52	6.48	4.01	6.55	6.55
4	19	7.58	5.07	3.62	5.06	5.06
5	15	7.73	10.01	4.09	10.09	10.07

Table I.23

Comparison of P.C. Position Increments by
CCRS Bundle and SPACE-M Adjustments

New (Autumn, 1985) data without lakes excluding rejected points

Photogrammetric Increments Within Models

RMS Discrepancies (metres)

Chr. Flight Line	No. of Points	X-Compt.	Y-Compt.	Z-Compt.	Horiz. Dist	Total Dist.
1	13	1.10	3.40	1.90	3.40	3.40
2	10	1.73	3.84	2.84	3.84	3.84
3	16	2.33	2.27	1.83	2.27	2.26
4	19	2.27	2.22	2.00	2.21	2.21
5	15	3.09	2.80	2.15	2.82	2.82

Max. Absolute Discrepancies (metres)

Chr. Flight Line	No. of Points	X-Compt.	Y-Compt.	Z-Compt.	Horiz. Dist	Total Dist.
1	13	2.09	5.72	4.10	5.77	5.77
2	10	4.30	7.22	5.51	7.22	7.21
3	16	4.29	4.18	4.07	4.25	4.25
4	19	4.46	3.73	3.66	3.75	3.76
5	15	5.47	7.21	5.17	7.28	7.26

Photogrammetric Increments Between Mean P.C.'s

RMS Discrepancies (metres)

Chr. Flight Line	No. of Points	X-Compt.	Y-Compt.	Z-Compt.	Horiz. Dist	Total Dist.
1	13	2.09	2.77	1.63	2.76	2.76
2	10	1.96	2.92	2.68	2.92	2.93
3	16	3.03	3.53	1.99	3.53	3.53
4	19	3.40	2.62	1.99	2.61	2.61
5	15	4.35	3.65	2.14	3.68	3.67

Max. Absolute Discrepancies (metres)

Chr. Flight Line	No. of Points	X-Compt.	Y-Compt.	Z-Compt.	Horiz. Dist	Total Dist.
1	13	5.04	6.30	3.17	6.27	6.27
2	10	3.79	5.82	5.29	5.82	5.81
3	16	4.73	6.56	4.71	6.55	6.54
4	19	6.94	5.02	3.81	5.01	5.01
5	15	7.51	10.63	5.21	10.70	10.67

APPENDIX J

Graphs of Orientation Angles and Range as Functions of Time

J.1 - J.4 Actual Angles as Functions of Time

J.1 - J.2	Flight Line 1	Pages 209-210
-----------	---------------	---------------

J.3 - J.4	Flight Line 4	Pages 211-212
-----------	---------------	---------------

J.5 - J.8 Angle Discrepancies as Functions of Time

J.5 - J.6	Flight Line 1	Pages 213-214
-----------	---------------	---------------

J.7 - J.8	Flight Line 4	Pages 215-216
-----------	---------------	---------------

J.9	Effect of Kappa Outliers - All Flight Lines	Page 217
-----	---	----------

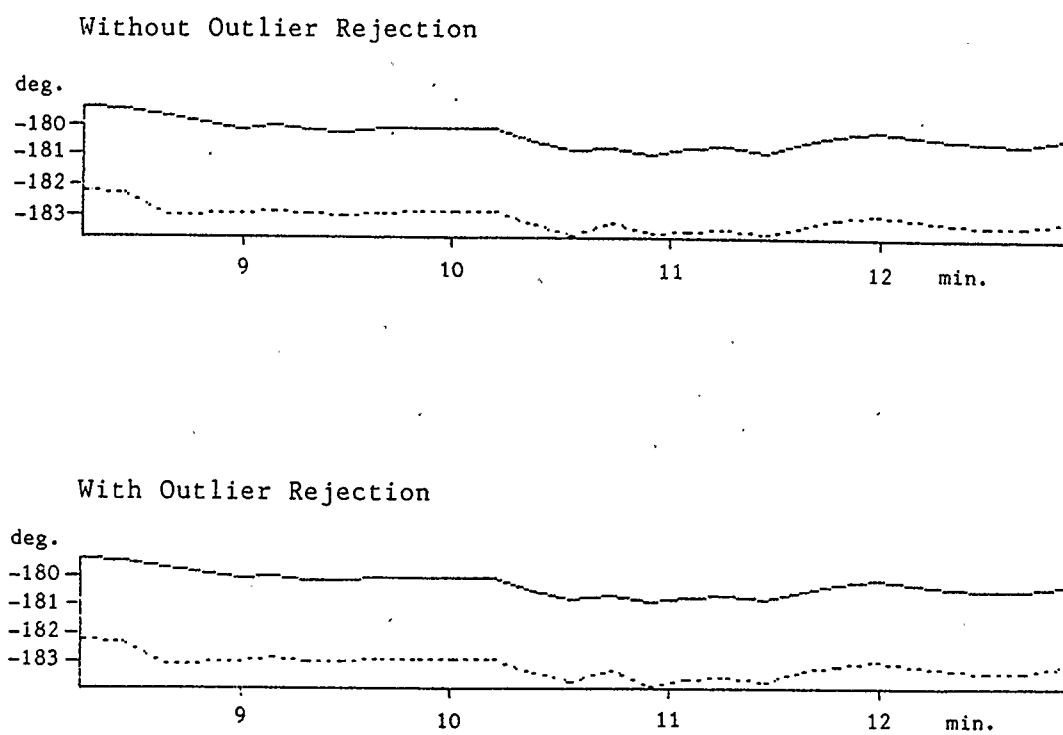
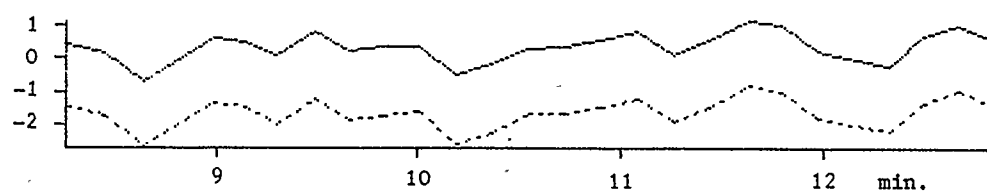


Fig. J.1: Heading Angle as a Function of Time - Chron. Flight Line 1
Continuous Graph for Aux. - Broken Graph for Photo.

Range (metres)



Roll Angle (deg)



Pitch Angle (deg)

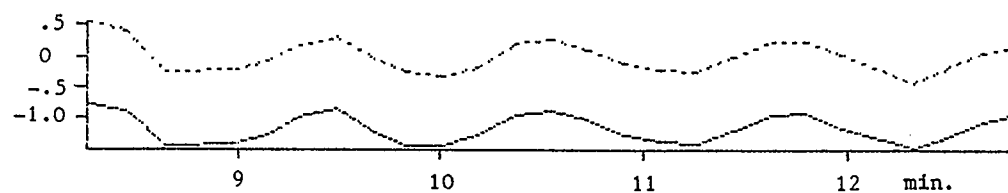


Fig. J.2: Range, Roll & Pitch as Functions of Time - Chron. Flight Line 1
Continuous Graph for Aux. - Broken Graph for Photo.

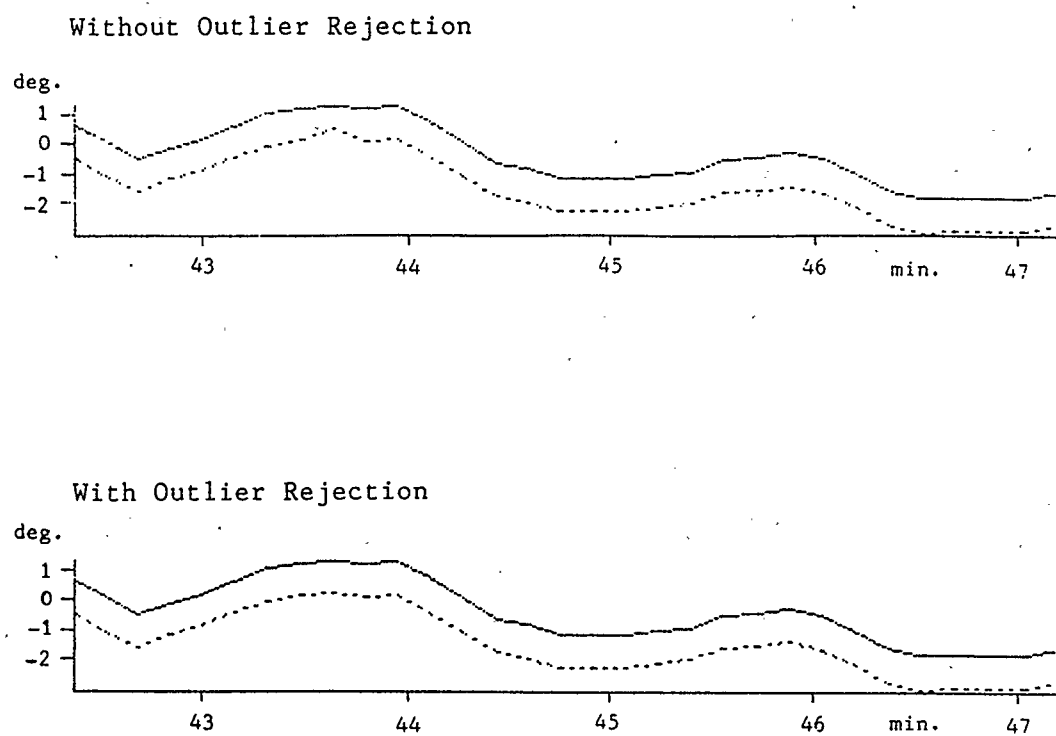
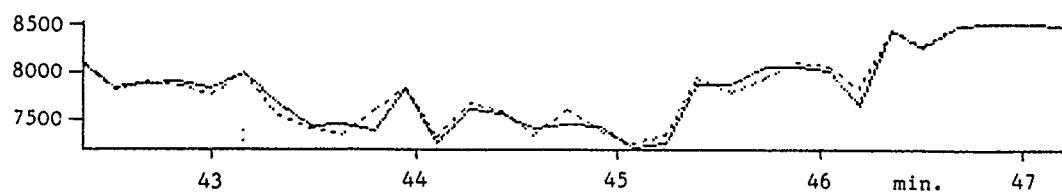


Fig. J.3: Heading Angle as a Function of Time - Chron. Flight Line 4
Continuous Graph for Aux. - Broken Graph for Photo.

Range (metres)



Roll Angle (deg)



Pitch Angle (deg)

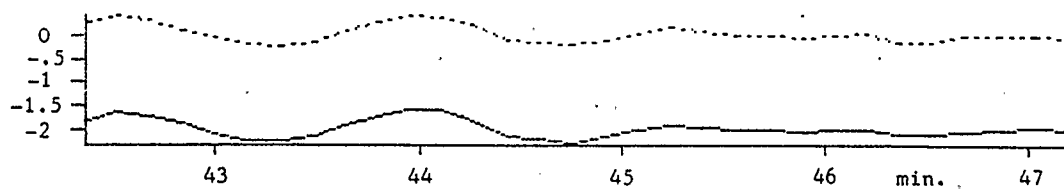


Fig. J.4: Range, Roll & Pitch as Functions of Time - Chron. Flight Line 4
Continuous Graph for Aux. - Broken Graph for Photo.

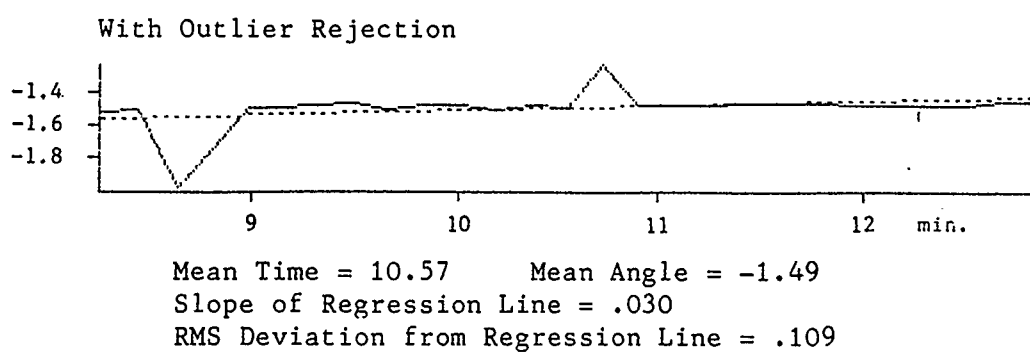
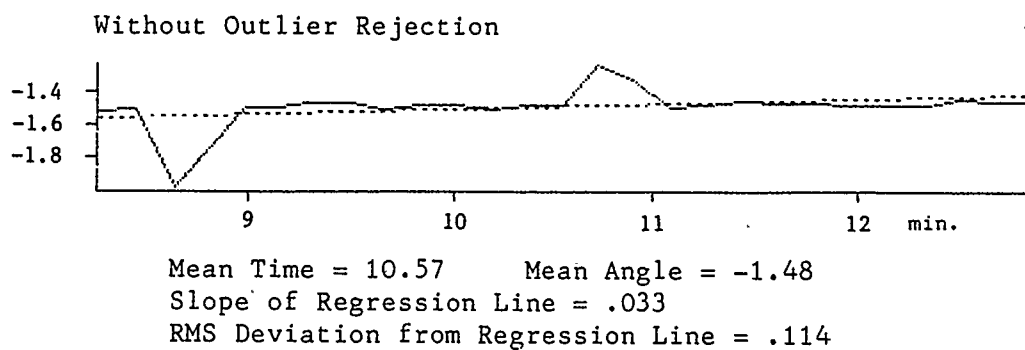
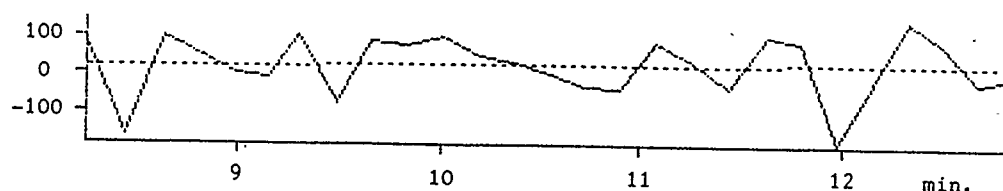


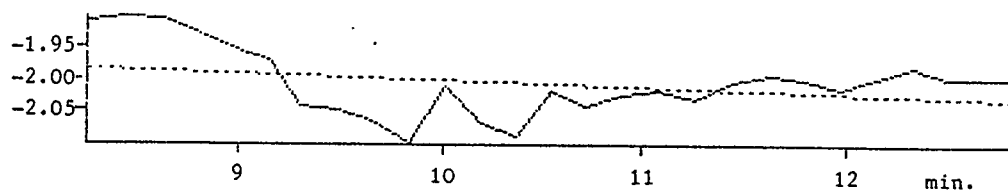
Fig. J.5: Photo. minus Aux. Values of Heading (deg) as Functions of Time
 Chron. Flight Line 1

Range (metres)



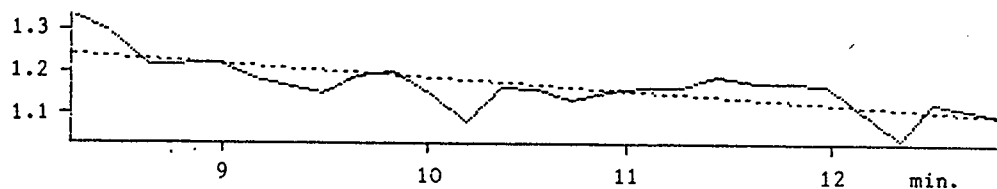
Mean Time = 10.57 Mean Range Diff. = 26.6
 Slope of Regression Line = 3.32
 RMS Deviation from Regression Line = 82.4

Roll Angle (deg)



Mean Time = 10.57 Mean Roll Angle Diff. = -2.01
 Slope of Regression Line = -0.010
 RMS Deviation from Regression Line = .05

Pitch Angle (deg)



Mean Time = 10.57 Mean Pitch Angle Diff. = 1.17
 Slope of Regression Line = -.031
 RMS Deviation from Regression Line = .043

Fig. J.6: Chron. Flight Line 1
 Photo. minus Aux. Values of Range,
 Roll & Pitch as Functions of Time
 with Outlier Rejection for kappa.

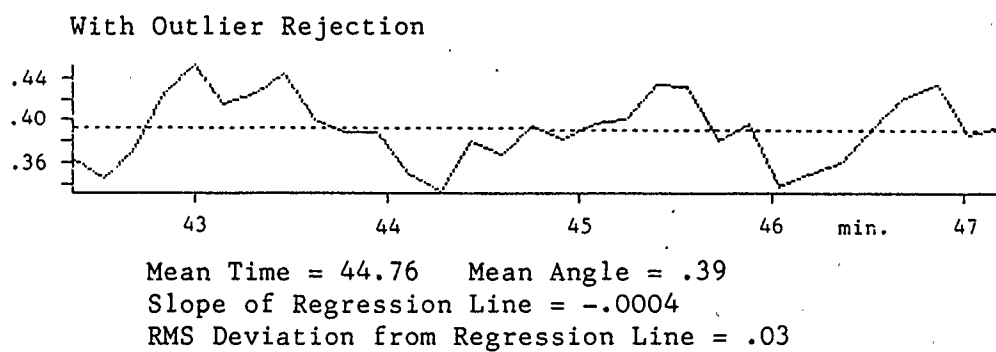
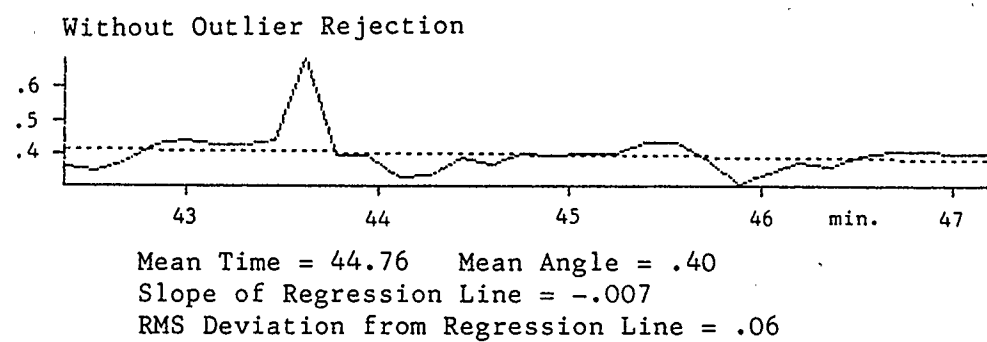
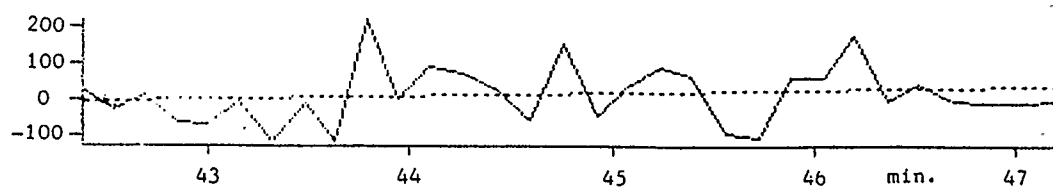


Fig. J.7: Photo. minus Aux. Values of Heading (deg) as Functions of Time
 Chron. Flight Line 1

Range (metres)



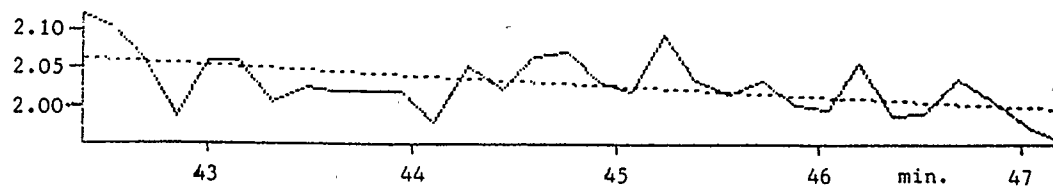
Mean Time = 44.76 Mean Range Diff. = 11.3
 Slope of Regression Line = 8.63
 RMS Deviation from Regression Line = 80.6

Roll Angle (deg)



Mean Time = 44.76 Mean Roll Angle Diff. = -1.63
 Slope of Regression Line = -.006
 RMS Deviation from Regression Line = .02

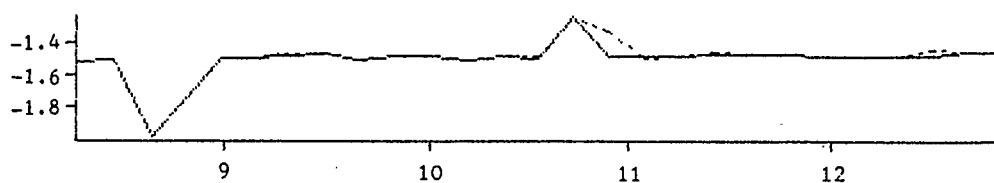
Pitch Angle (deg)



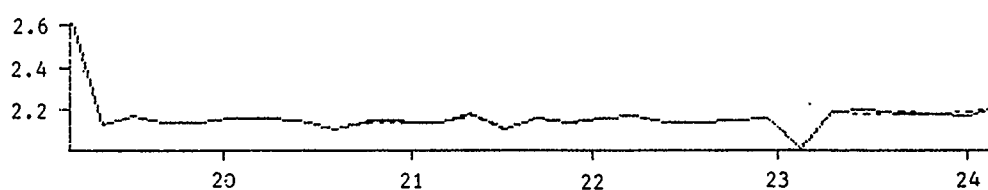
Mean Time = 44.76 Mean Pitch Angle Diff. = 2.03
 Slope of Regression Line = -.013
 RMS Deviation from Regression Line = .03

Fig. J.8: Chron. Flight Line 4
 Photo minus Aux. Values of Range,
 Roll & Pitch as Functions of Time
 with Outlier Rejection for kappa.

Chron. Flight Line 1



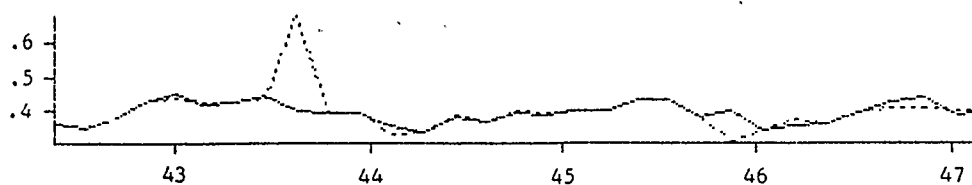
Chron. Flight Line 2



Chron. Flight Line 3



Chron. Flight Line 4



Chron. Flight Line 5

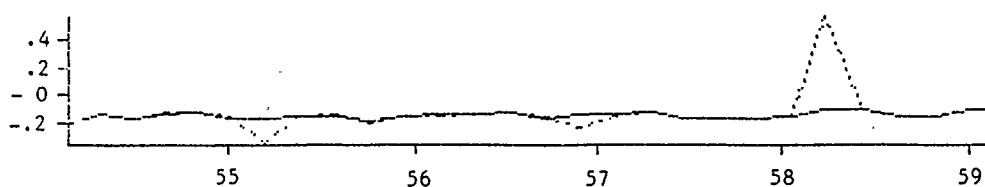


Fig. J.9: Photo. minus Values of Heading (deg)
 as Functions of Time (min.)
 Continuous Graph for Outliers Rejected
 Broken Graph for Outliers Not Rejected